IEEE GLOBECOM
IEEE Global Communications Conference
8–12 December 2024 // Cape Town, South Africa
Connecting the Intelligent World through Africa
IEEE ComSoc IEEE Communications Society
IEEE

Electromagnetic Information Theory:

Fundanentals, Modeling, Applications, and Open Problems

Linglong Dai (IEEE Fellow)
Tsinghua University,
Beijing, China
daill@tsinghua.edu.cn

Merouane Debbah (IEEE Fellow)
Khalifa University of Science and Technology,
Abu Dhabi, United Arab Emirates
merouane.debbah@ku.ac.ae

Starting from the Iceberg Effect

- **Different aspects of wireless communications**
  - **Classical communication theory: Research on the math-symbolized signal processing theory**
  - **Electromagnetic (EM) theory: EM waves carrying information as a physical process**

Iceberg

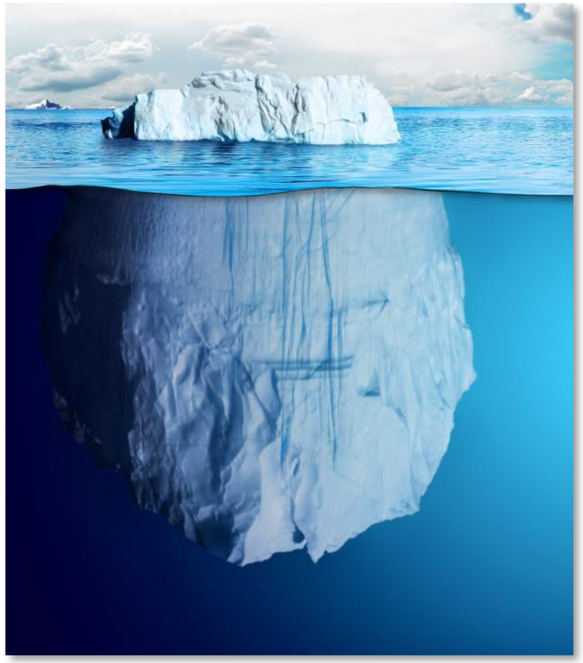

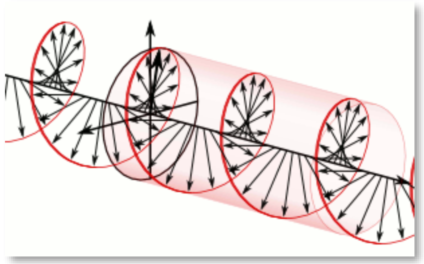

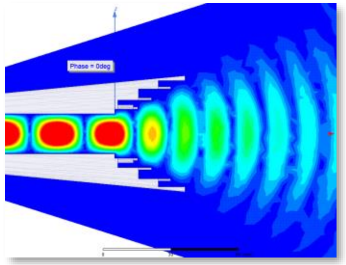

Communications

EM Theory

How can EM theory inspire future communication research?

Contents

Contents

1.1 EIT for 6G Novel Technologies

Extremely Large-Scale MIMO

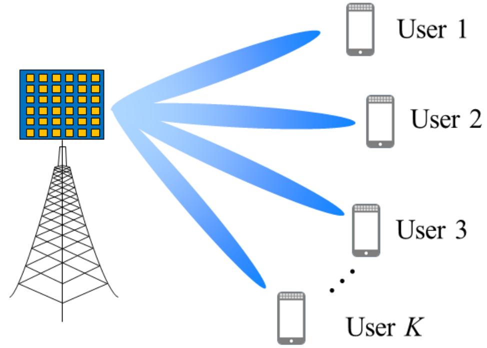

Increase Number of Antennas

Holographic MIMO

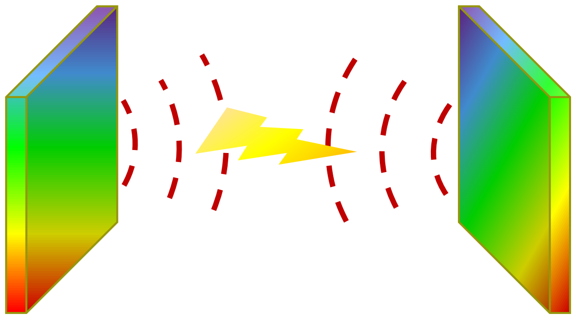

Increase Antenna Density

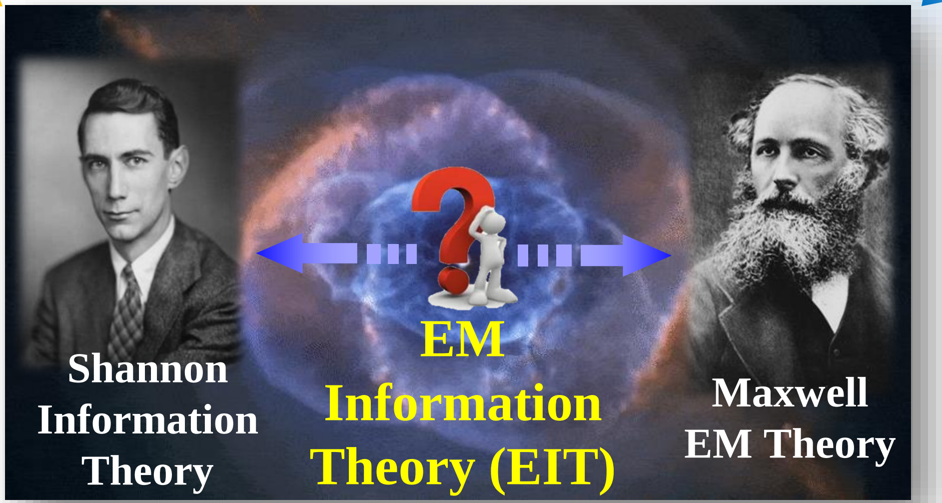

Unified theoretical limit?

RIS

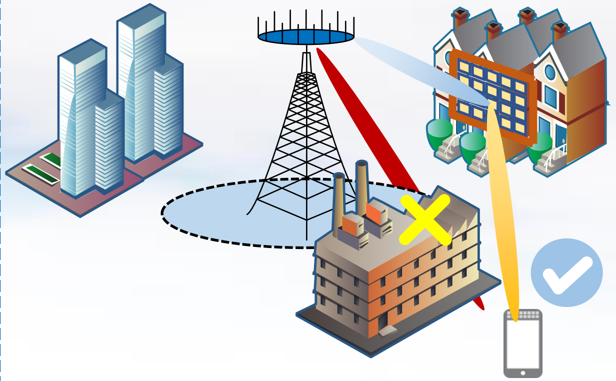

Control EM Channel

OAM

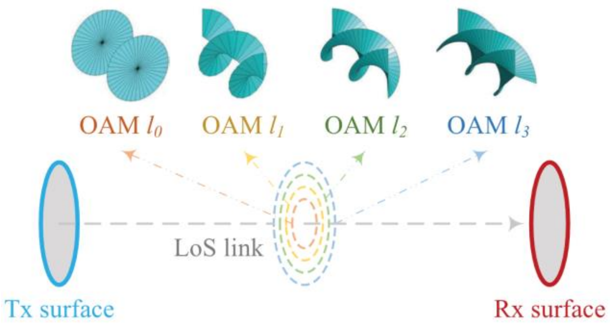

Control EM Modes

R. Li, D. Li, J. Ma, Z. Feng, L. Zhang, W. E. I. Sha, H. Chen, and E.-P. Li, "An electromagnetic information theory-based model for efficient characterization of MIMO systems in complex space," *IEEE Trans. Antennas Propagat.*, vol. 71, no. 4, pp. 3497-3508, Apr. 2023.

1.1 Theoretical Motivation of EIT

- **Transmit information with EM fields in a compact space-time region**
  - **MIMO IT: Apply discretization to EM channels for information-theoretic limits in the $T \to \infty$ regime**
  - **EIT: Treat EM channels as continuous operators for information-theoretic limits in the finite-spacetime regime**

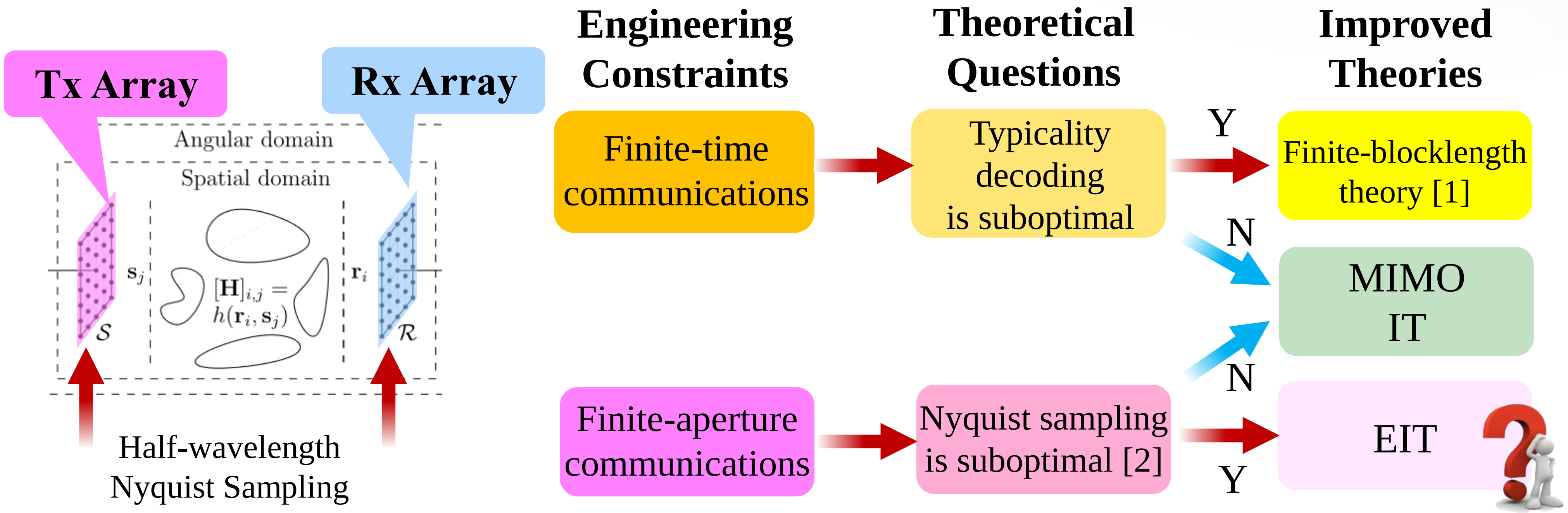

Yuri Polyanskiy
(IEEE Fellow)
MIT

[1] Y. Polyanskiy, H. V. Poor, and S. Verdu, "Channel coding rate in the finite blocklength regime," *IEEE Trans. Inf. Theory*, vol. 56, no. 5, pp. 2307-2359, May 2010.

[2] A. Pizzo, A. Torres, L. Sanguinetti, and T. L. Marzetta, "Nyquist sampling and degrees of freedom of electromagnetic fields," *IEEE Trans. Signal Process.*, vol. 70, pp. 1–12, Jun. 2022.

1.1 From Classical IT to Electromagnetic IT (EIT)

- **EM Information Theory (EIT): An interdisciplinary subject integrating deterministic physical theory and probabilistic mathematical theory to provide theoretical foundations for performance evaluation and optimization of wireless systems.**

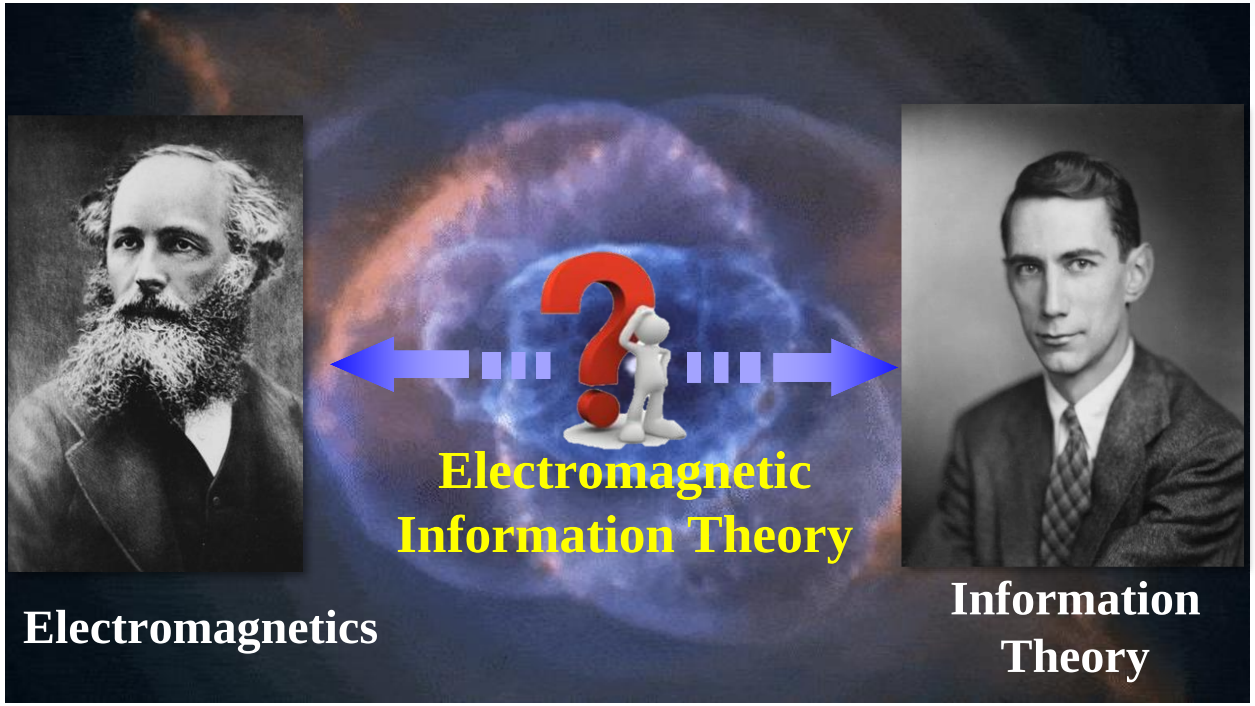

J. Zhu, Z. Wan, **L. Dai**, M. Debbah, and H. V. Poor, "Electromagnetic information theory: Fundamentals, modeling, applications, and open problems," *IEEE Wireless Commun.*, vol. 31, no. 3, pp. 156-162, Jun. 2023.

1.1 Academic and Industrial Interest

- **Studies of EIT has attracted widespread attention from academia and industry**

Academia

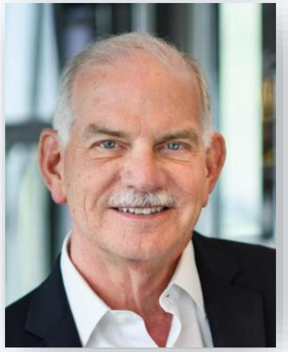

H. V. Poor
Member of National Academy of Sciences (US)

Lajos Hanzo
Fellow of the Royal Academy of Engineering (UK)

IEEE Globecom
2022 Industrial Panel

IEEE VTC-Spring
2023 Workshop

IEEE Globecom
2023 Workshop

IEEE ICC
2024 Workshop

Industry

Download:
https://www.chaspark.com/#/hotspots/857399644291072000

[1] Y. Yang, C.-X. Wang, J. Huang, J. Thompson, and H. V. Poor, "A 3D continuous-space electromagnetic channel model for 6G tri-polarized multi-user communications," *IEEE Trans. Wireless Commun.*, vol. 23, no. 11, pp. 17354-17367, Sep. 2024.

[2] C.-X. Wang, Y. Yang, J. Huang, X. Gao, T. J. Cui, and L. Hanzo, "Electromagnetic information theory: Fundamentals and applications for 6G wireless communication systems," *IEEE Wireless Commun.*, vol. 31, no. 5, pp. 279-286, Oct. 2024.

Contents

1.2 Shannon Information Theory

- **Shannon's Noisy Channel Coding Theorem**
  - **Theorem: Maximum error-free transmission rate = Channel capacity**
  - **Point-to-point information transmission without considering EM fields**

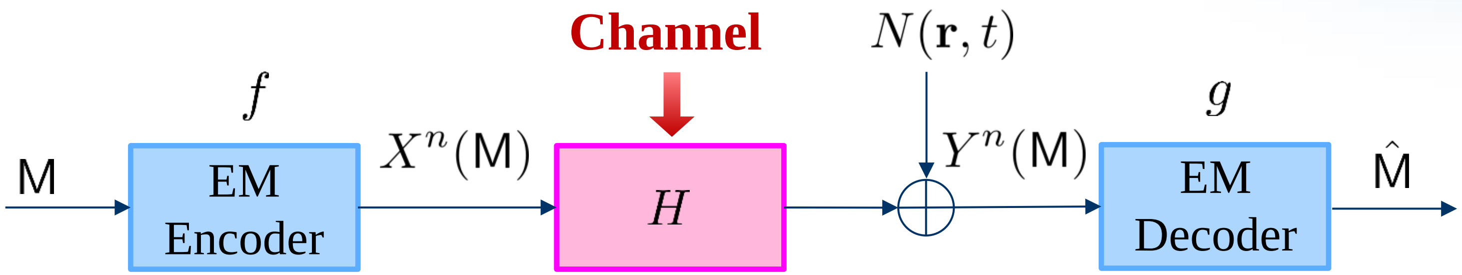

Channel codes

(n, P, M, ε)-code

Maximal codes

$M^*(n, P, \varepsilon) := \max\{M : \exists (n, P, M, \varepsilon)\text{-code}\}$

Shannon's theorem (modern form)

$$\lim_{\varepsilon \to 0} \liminf_{n \to \infty} \frac{1}{n} \log M^*(n, P, \varepsilon) \overset{1948}{=} C(P, H)$$

Error probability

$\varepsilon := \Pr[\mathsf{M} \neq \hat{\mathsf{M}}]$

Time constraint

$X^n \in \mathcal{X}^n, \quad Y^n \in \mathcal{Y}^n$

Bandwidth constraint

$H \in \mathcal{B}_W$

Energy constraint

$\mathbb{E}_{\mathsf{M}}[\|X^n(\mathsf{M})\|^2] \leq nP$

C. E. Shannon, "A mathematical theory of communication," *Bell Syst. Technical J.*, vol. 27, no. 3, pp. 379-423, Jul. 1948.

1.2 Shannon Information Theory

- **Information theory evolution**
  - **MIMO information theory: From point-to-point channel to MIMO channels**
  - **Network information theory: Network coding for uplink multiple access channel (MAC) and downlink broadcast channel (BC)**

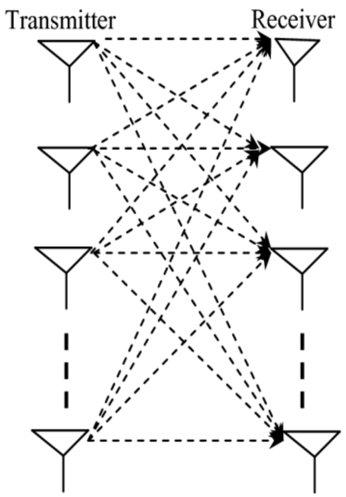

MIMO Channel
Point-to-point channel

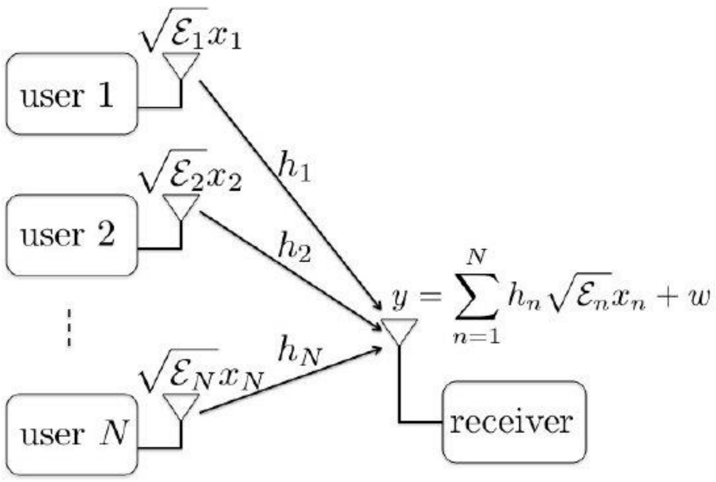

Multiple Access Channel
Network channel

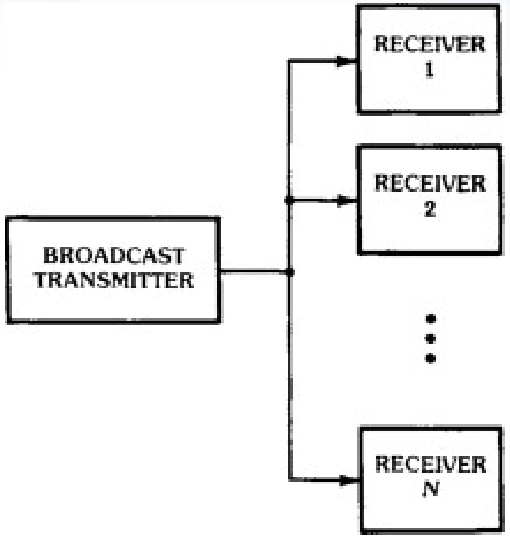

Broadcast Channel
Network channel

T. Cover and J. A. Thomas, *Elements of information theory*. Wiley-Interscience, 2006.

Contents

1.3 Maxwell Electromagnetic Theory

- **Maxwell's equations: A set of coupled partial differential equations that form the foundation of classical electromagnetism**
- **A unified mathematical model for electric, optical, and radio technologies**

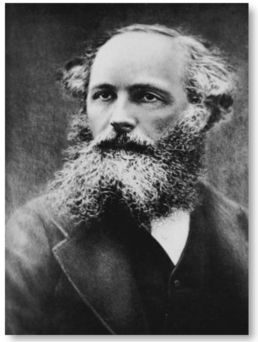

James Clerk Maxwell
（1831-1879）

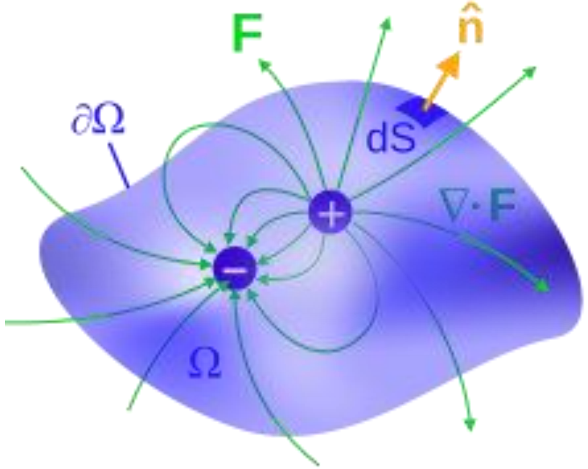

Gauss's law	$\nabla \cdot \mathbf{D} = \rho$
Gauss's law for magnetism	$\nabla \cdot \mathbf{B} = 0$
Ampère–Maxwell law	$\nabla \times \mathbf{H} = \mathbf{J} + \frac{\partial \mathbf{D}}{\partial t}$
Maxwell–Faraday equation	$\nabla \times \mathbf{E} = -\frac{\partial \mathbf{B}}{\partial t}$

J. C. Maxwell, "A dynamical theory of the electromagnetic field," *Philosophical transactions of the Royal Society of London*, 1865.

1.3 Maxwell Electromagnetic Theory

- **Lead to vector wave equation which depicts the relationship between source and generated fields**

Vector wave equation $\nabla \times \nabla \times \mathbf{E}(\mathbf{r}) - \omega^2 \epsilon \mu \mathbf{E}(\mathbf{r}) = \mathrm{j}\omega\mu \mathbf{J}(\mathbf{r})$

- **Green's function**

Green's function

$$\mathbf{E}(\mathbf{r}) = \mathrm{j}\omega \int_{V_s} \mathbf{G}(\mathbf{r}, \mathbf{r}')\mu_0 \mathbf{J}(\mathbf{r}')\mathrm{d}\mathbf{r}'$$

$$\mathbf{G}(\mathbf{r}, \mathbf{r}') = \frac{1}{4\pi} \boxed{\frac{e^{\mathrm{j}\kappa_0 \|\mathbf{r}-\mathbf{r}'\|}}{\|\mathbf{r}-\mathbf{r}'\|}} \left[\left(\mathbf{I} - \hat{\mathbf{p}}\hat{\mathbf{p}}^{\mathrm{H}}\right) + \boxed{\frac{\mathrm{j}}{2\pi \|\mathbf{r}-\mathbf{r}'\| / \lambda} \left(\mathbf{I} - 3\hat{\mathbf{p}}\hat{\mathbf{p}}^{\mathrm{H}}\right) - \frac{1}{(2\pi \|\mathbf{r}-\mathbf{r}'\| / \lambda)^2} \left(\mathbf{I} - 3\hat{\mathbf{p}}\hat{\mathbf{p}}^{\mathrm{H}}\right)} \right] [\mathrm{m}^{-1}]$$

Plane wave **Spherical wave** **Evanescent wave**

Far-field **Radiative Near-field** **Reactive Near-field**

Contents

1.4 Overview of EIT

- **Electromagnetic Information Theory (EIT) : An interdisciplinary subject integrating deterministic physics theory and statistical mathematical theory to provide theoretical foundations for performance evaluation and optimization of wireless systems**

Entropy of RVs:

$$H(X) = \sum_{x \in \mathcal{X}} p(x) \log_2 \left(\frac{1}{p(x)} \right)$$

Mutual information of RVs:

$$I(X;Y) = H(X) - H(X|Y)$$

Channel capacity of additive Gaussian noise:

$$C = \int_0^W \log \left(1 + \frac{P(f)}{N(f)} \right) \mathrm{d}f$$

Gauss's law:

$$\nabla \cdot \mathbf{D} = \rho$$

Gauss's law for magnetism:

$$\nabla \cdot \mathbf{B} = 0$$

Ampere-Maxwell law:

$$\nabla \times \mathbf{H} = \mathbf{j} + \frac{\partial \mathbf{D}}{\partial t}$$

Faraday's law:

$$\nabla \times \mathbf{E} = -\frac{\partial \mathbf{B}}{\partial t}$$

J. Zhu, Z. Wan, **L. Dai**, M. Debbah, and H. V. Poor, "Electromagnetic information theory: Fundamentals, modeling, applications, and open problems," *IEEE Wireless Commun.*, vol. 31, no. 3, pp. 156-162, Jun. 2023.

1.4 Discrete MIMO IT vs. Continuous EIT

	MIMO Information Theory	Electromagnetic Information Theory
Channel model	Mathematical channel	Physical channel
Channel characteristics	Discrete channel	Continuous channel
Channel form	Matrix	Operator (Green's function)
Channel Decomposition	SVD Matrix decomposition, Eigenvector	Spectrum decomposition of the operator, Eigenfunction
Signal model	Gaussian random vector	Gaussian random field
Noise model	i.i.d. Gaussian white noise	Electromagnetic colored noise
Capacity	Matrix determinant	Operator determinant (Fredholm determinant)

Transplant classical time-domain stochastic processes into spatial-domain random fields

1.4 Historical Evolution of EIT

James C. Maxwell
proposed Maxwell's equations, connecting the electric and magnetic fields

1865

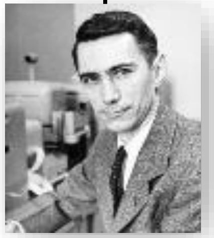

Claude E. Shannon
proposed information theory, the mathematical theory of communication

1949

Dennis Gabor
proposed that communication is the transmission of physical effects, connecting communication theory with physical effects

1950

Giorgio Franceschetti
proposed Bucci-Franceschetti diversity limits based on the analysis of scattering field

1987

Massimo Franceschetti
and his book "Wave Theory of Information" analyzed the capacity problems of MIMO

2008

Josef Nossek
proposed multiport communication theory by applying circuit theory to information theory

2014

Tapan K. Sarkar
applied the EM theory to channel capacity issues

2019

1.4 Functional Approximation of EM Fields

- **Approximating EM fields with bandlimited functions to get the EM degrees of freedom**
  - **A bandlimited EM field with $w \geq \beta a$ suffices to reconstruct arbitrary radiated EM fields [1]**
  - **Functional approximation techniques for EM fields are introduced in detail in [2]**

Giorgio Franceschetti
(IEEE Life Fellow)

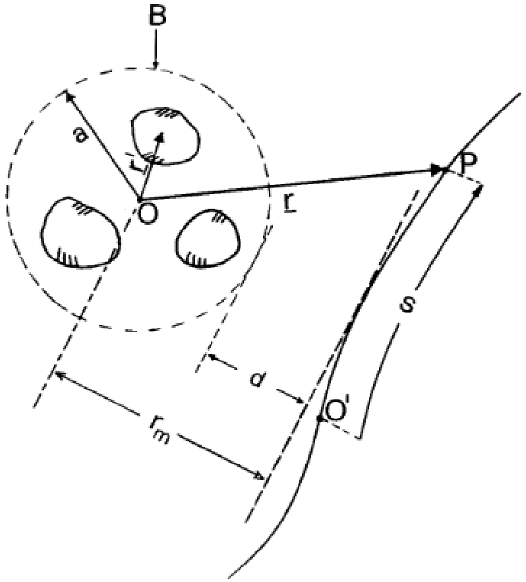

Spherical source (Tx) with linear observation (Rx)

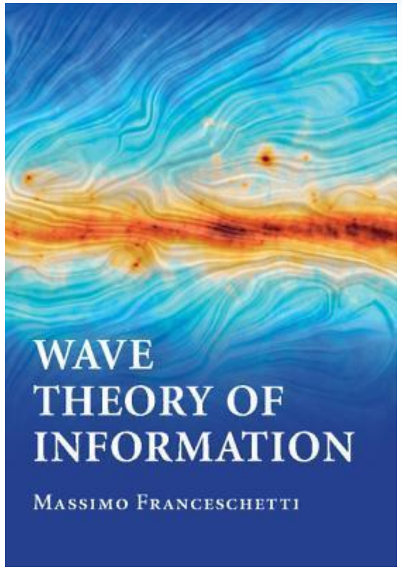

Functional approximation and DoF analysis for EM waves

Massimo Franceschetti
(IEEE Fellow)

[1] O. M. Bucci and G. Franceschetti, "On the spatial bandwidth of scattered fields," *IEEE Trans. Antennas Propagat.*, vol. 35, no. 12, pp. 1445-1455, Dec. 1987.
[2] M. Franceschetti, *Wave Theory of Information*. Cambridge University Press, 2017.

1.4 Information Contained in Electromagnetic Fields

- **Use Kolmogorov information theory which analyzes the number of distinguishable waveforms above an uncertainty level**

Marco Donald Migliore
(IEEE Fellow)

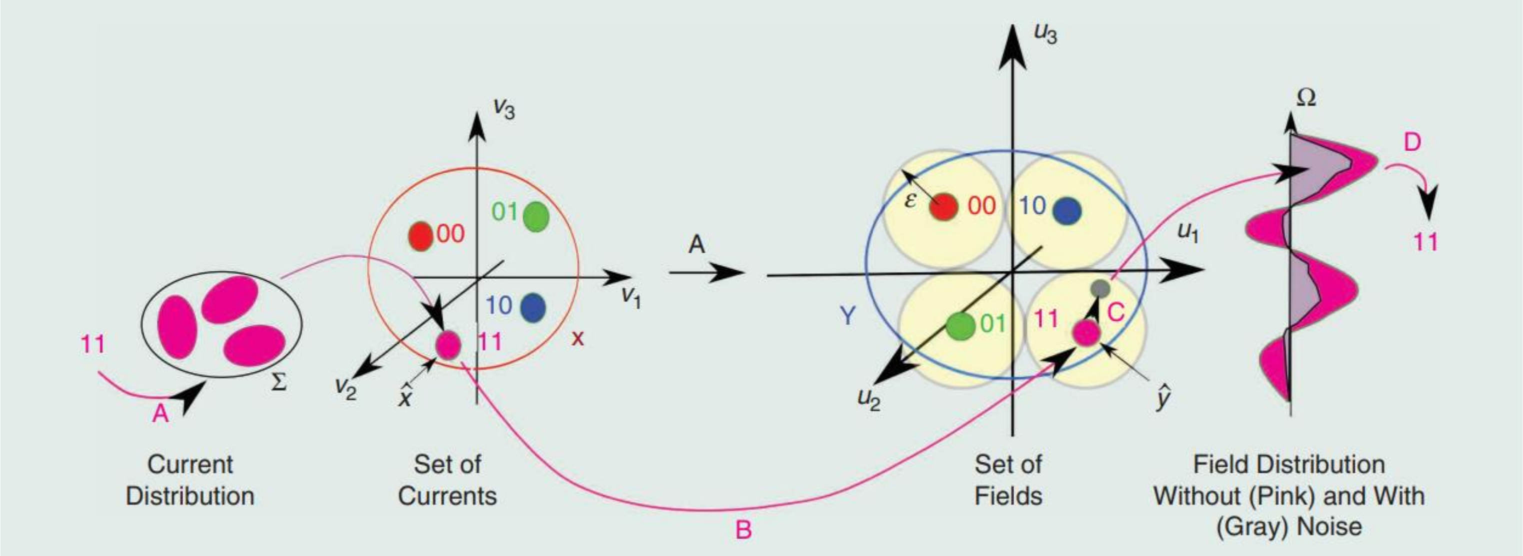

Distinguishable waveforms above an uncertainty level

[1] M. D. Migliore, "Horse (Electromagnetics) is more important than horseman (information) for wireless transmission," *IEEE Trans. Antennas Propagat.*, vol. 67, no. 4, pp. 2046–2055, Apr. 2019.
[2] M. D. Migliore, "Shannon and Kolmogorov in space communication channels," in *Proc. 14th EuCAP. Copenhagen, Denmark*, Mar. 2020, pp. 1–4.
[3] M. D. Migliore, "On electromagnetics and information theory," *IEEE Trans. Antennas Propagat.*, vol. 56, no. 10, pp. 3188–3200, Oct. 2008.

1.4 Channel Models for EIT

- **Various channel modeling schemes based on electromagnetic theory**
  - **Spatially-stationary scattering [1], smooth surface [2], resonant cavity [3], etc.**

Thomas Marzetta

Member of the National Academy of Engineering (US)

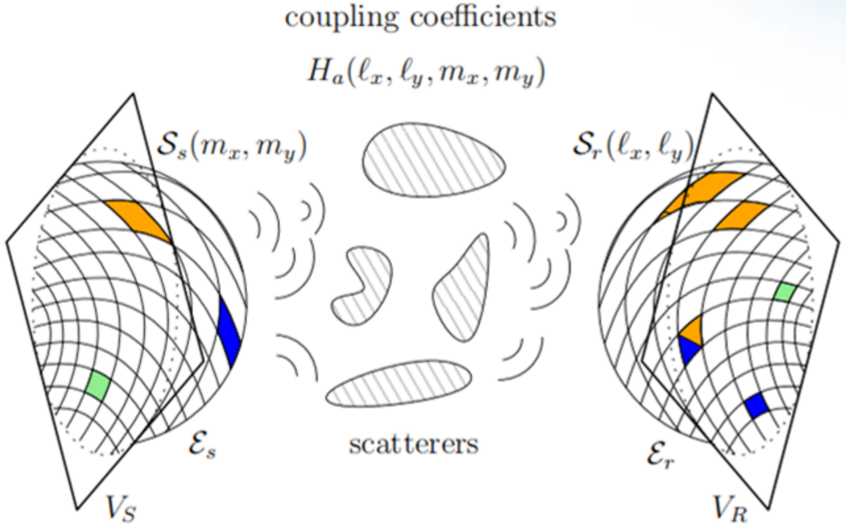

Spatially-stationary scattering

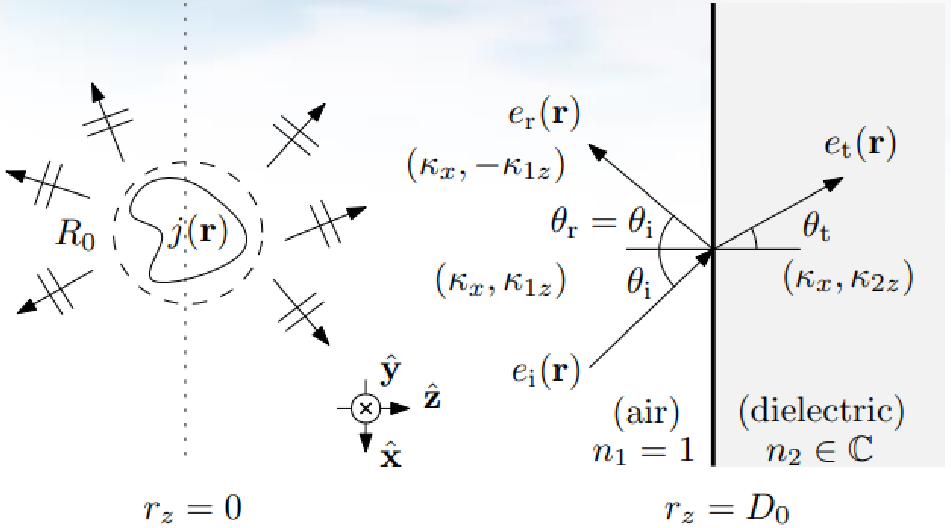

Smooth surface

[1] A. Pizzo, L. Sanguinetti, and T. L. Marzetta, “Fourier plane-wave series expansion for holographic MIMO communications,” *IEEE Trans. Wireless Commun.*, vol. 21, no. 9, pp. 6890–6905, Sep. 2022.

[2] A. Pizzo, A. Lozano, S. Rangan, and T. L. Marzetta, “Wide aperture MIMO via reflection off a smooth surface,” *IEEE Trans. Wireless Commun.*, vol. 22, no. 8, pp. 5229–5239, Aug. 2023.

[3] T. L. Marzetta and T. B. Hansen, “Rayleigh-jeans-clarke model for wireless noise in a resonant cavity: Scalar case,” *in Proc. IEEE Global Communications Conference*, Dec. 2022, pp. 4776–4781.

1.4 Information Capacity of Radiating Surfaces

- **Unified information-theoretic framework for arbitrary radiating systems**
  - **Surface or line sources are approximated by multiple discrete points**
  - **Shannon information capacity is computed with this discretized model**

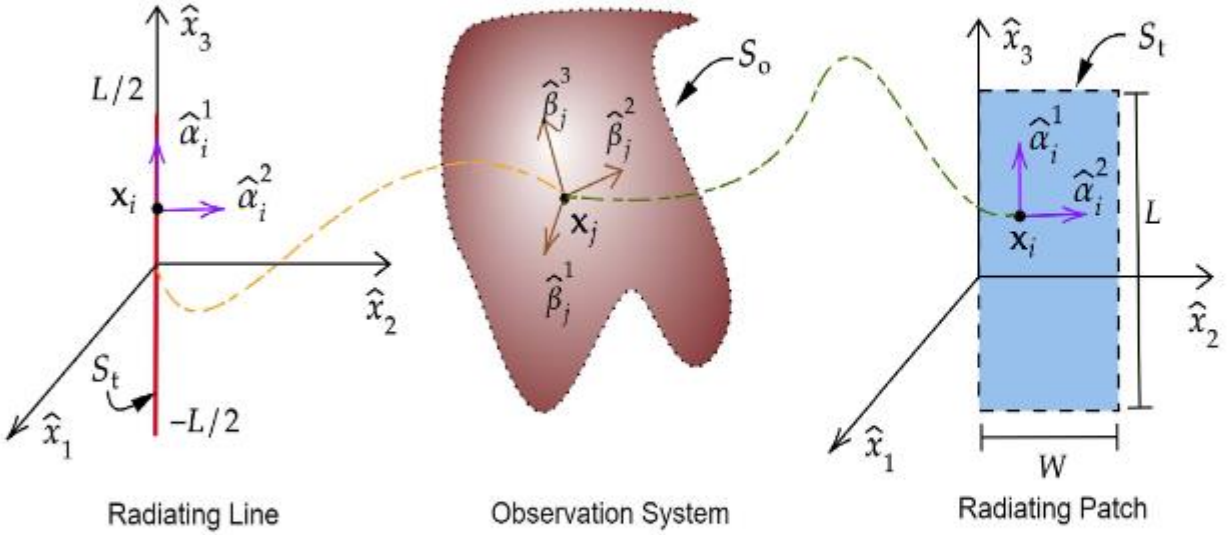

Channel capacity from a Tx line/patch to the Rx observation system

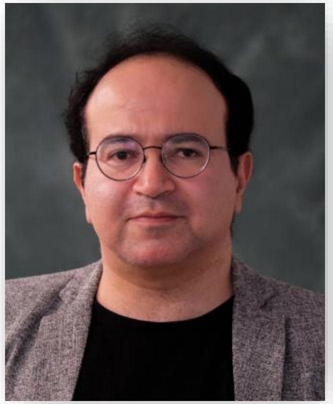

Said Mikki

S. Mikki, "The Shannon information capacity of an arbitrary radiating surface: An electromagnetic approach," *IEEE Trans. Antennas Propagat.*, vol. 71, no. 3, pp. 2556–2570, Mar. 2023. (**2023 IEEE AP-S Sergei A. Schelkonuff Transactions Prize Paper Award**)

Contents

2.1 EM Channel Model for EIT

- **Existing EM channel models**
  - **Tri-polarized LoS channel model [1]**
  - **Spatially-stationary scattering MIMO models with Fourier plane-wave expansion [2]**

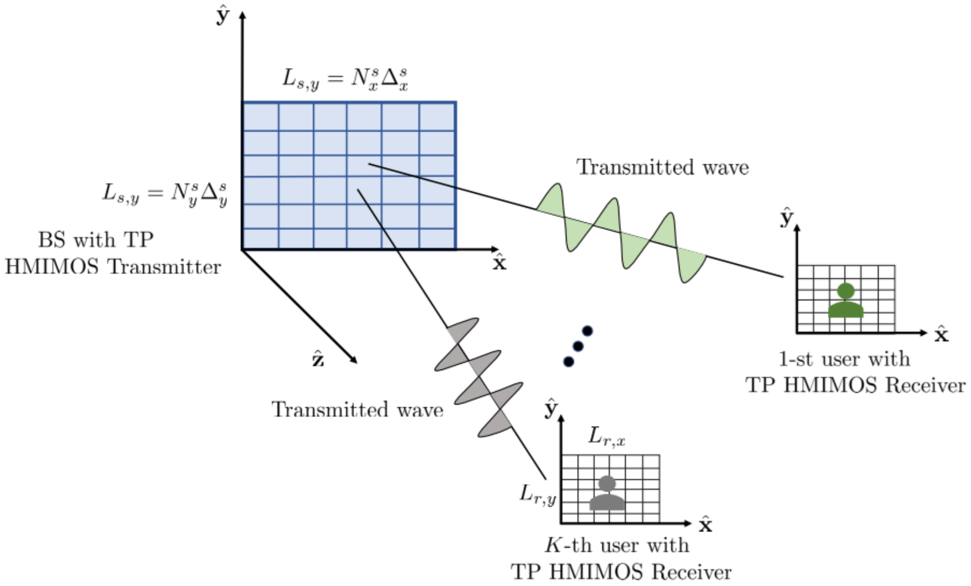

LoS channel model for EIT

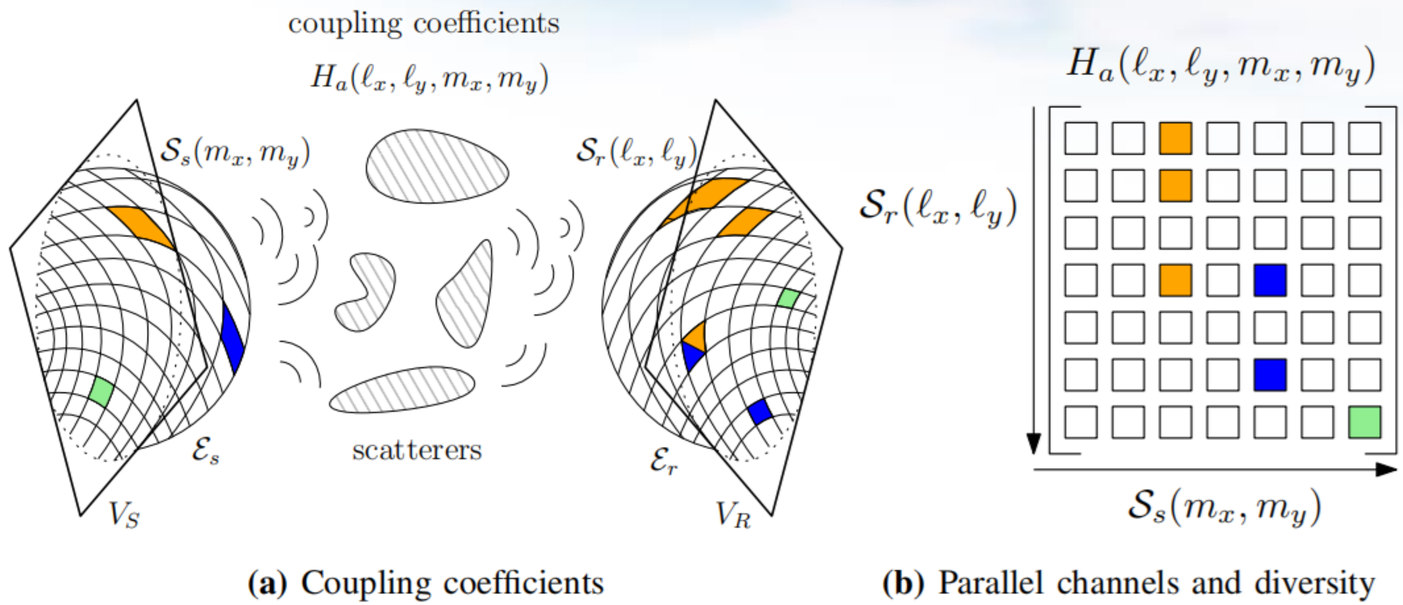

Spatially-stationary scattering

[1] L. Wei, C. Huang, G. C. Alexandropoulos, Z. Yang, J. Yang, E. Wei, Z. Zhang, M. Debbah, and C. Yuen, "Tri-polarized holographic MIMO surfaces for near-field communications: Channel modeling and precoding design," *IEEE Trans. Wireless Commun.*, vol. 22, no. 12, pp. 8828–8842, Dec. 2023.

[2] A. Pizzo, L. Sanguinetti, and T. L. Marzetta, "Fourier plane-wave series expansion for holographic MIMO communications," *IEEE Trans. Wireless Commun.*, vol. 21, no. 9, pp. 6890–6905, Sep. 2022.

2.1 EM Channel Model for EIT

- **Existing EM channel models**
  - **Wide aperture model with surface reflection [3]**
  - **Circuit-based model considering mutual coupling [4]**

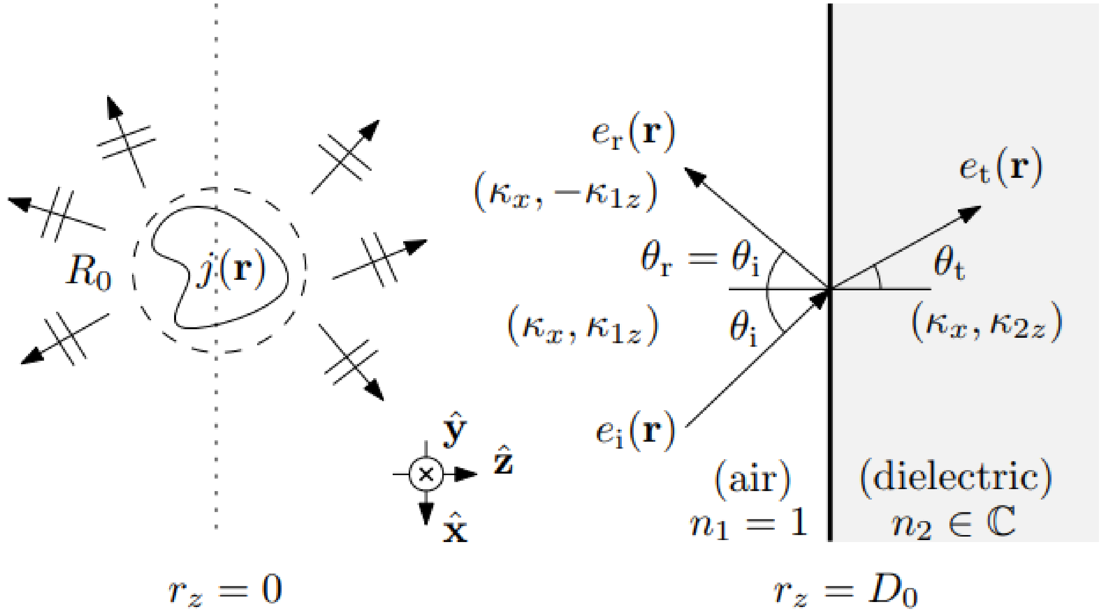

Reflection from a surface

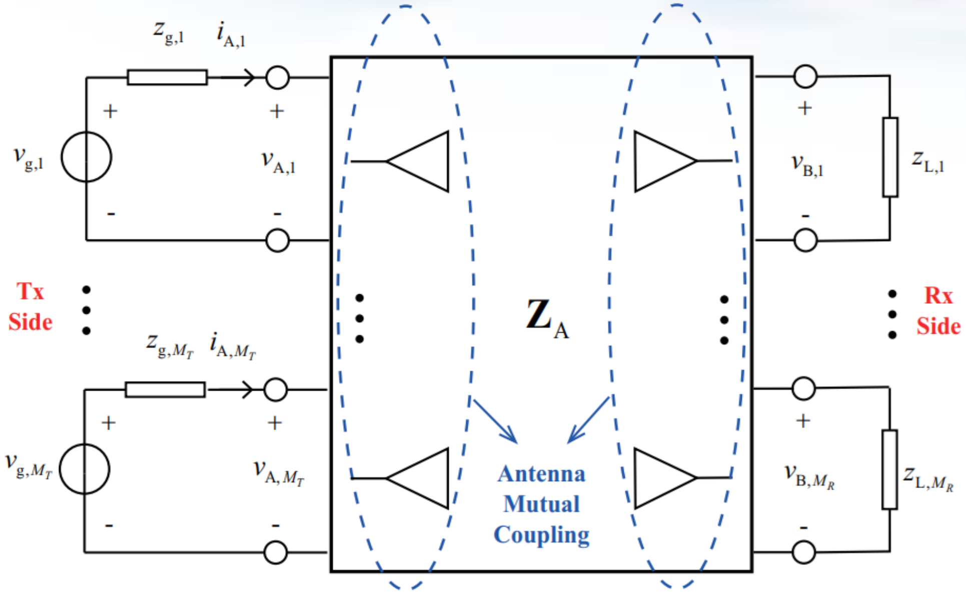

Circuit modeling

[3] A. Pizzo, A. Lozano, S. Rangan, and T. L. Marzetta, "Wide aperture MIMO via reflection off a smooth surface," *IEEE Trans. Wireless Commun.*, vol. 22, no. 8, pp. 5229–5239, Aug. 2023.
[4] J. Gao, C.-X. Wang, J. Huang, and Y. Yang, "A novel circuit-based MIMO channel model considering antenna size and mutual coupling," in *Proc. WCSP'21*, Changsha, China, Oct. 2021.

2.1 EIT-Enabled Near-Field Models

- **Existing near-field channel modeling scheme**
  - **Widely adopted schemes in wireless communication view scatterer as point: Simple but inaccurate**
  - **Schemes like full wave simulation based on electromagnetism: Accurate but complex, without analytical expression**

Single point assumption

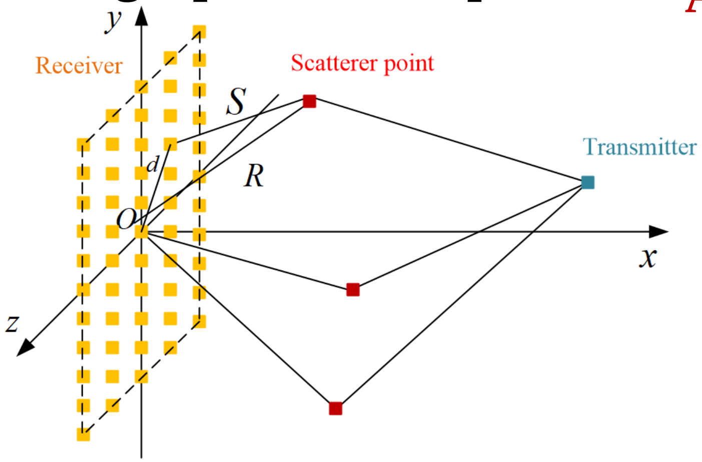

An analytical channel model that has enough accuracy

Full wave simulation

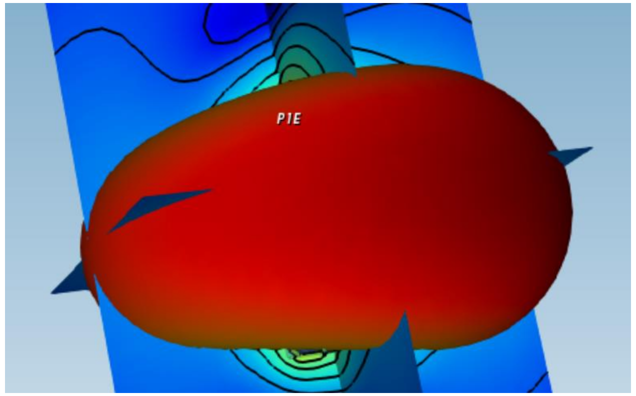

- **Problem: Construct an analytical channel model based on electromagnetism for wireless communication**

2.1 Channel Model Based on Electromagnetism

- **From electromagnetism, we view the scatterers as spatial inhomogeneity in the space**

Maxwell's equation in inhomogeneous space

$$\nabla \times \mathbf{E}(\mathbf{r}) = \mathrm{j}\omega\mu(\mathbf{r})\mathbf{H}(\mathbf{r}), \tag{1a}$$
$$\nabla \times \mathbf{H}(\mathbf{r}) = -\mathrm{j}\omega\epsilon(\mathbf{r})\mathbf{E}(\mathbf{r}) + \mathbf{J}(\mathbf{r}), \tag{1b}$$
$$\nabla \cdot (\epsilon(\mathbf{r})\mathbf{E}(\mathbf{r})) = \rho(\mathbf{r}), \tag{1c}$$
$$\nabla \cdot (\mu(\mathbf{r})\mathbf{H}(\mathbf{r})) = 0 \tag{1d}$$

$$\nabla \times \mu(\mathbf{r})^{-1} \times (1a) + \mathrm{j}\omega \times (1b)$$

Vector wave equation $\nabla \times \mu(\mathbf{r})^{-1}\nabla \times \mathbf{E}(\mathbf{r}) - \omega^2\epsilon(\mathbf{r})\mathbf{E}(\mathbf{r}) = \mathrm{j}\omega\mathbf{J}(\mathbf{r})$

Green's function $\mathbf{G}(\mathbf{r},\mathbf{r}') = \frac{1}{4\pi}\left(\mathbf{I} + \frac{\nabla_{\mathbf{r}}\nabla_{\mathbf{r}}^{\mathrm{H}}}{\kappa_0^2}\right)\frac{e^{\mathrm{j}\kappa_0\|\mathbf{r}-\mathbf{r}'\|}}{\|\mathbf{r}-\mathbf{r}'\|}$

Source-destination relationship $\mathbf{E}(\mathbf{r}) = \mathrm{j}\omega\int_{V_s}\mathbf{G}(\mathbf{r},\mathbf{r}')\mu_0\mathbf{J}(\mathbf{r}')\mathrm{d}\mathbf{r}' + \int_{V}\mathbf{G}(\mathbf{r},\mathbf{r}')(k^2(\mathbf{r}') - k_0^2)\mathbf{E}(\mathbf{r}')\mathrm{d}\mathbf{r}'$

A. F. Peterson, S. L. Ray, and R. Mittra, *Computational methods for electromagnetics*. Wiley-IEEE Press New York, 1998.

2.1 Channel Model Based on Electromagnetism

- **Based on electromagnetism, we can view the source current as the input signal and electric field at the destination as the output signal**
- **The received electric field is split into two parts: Incident and scattered fields**

Incident field **Scattered field**

$$\mathbf{E} = \mathbf{E}_{\text{inc}} + \mathbf{E}_{\text{sca}}$$

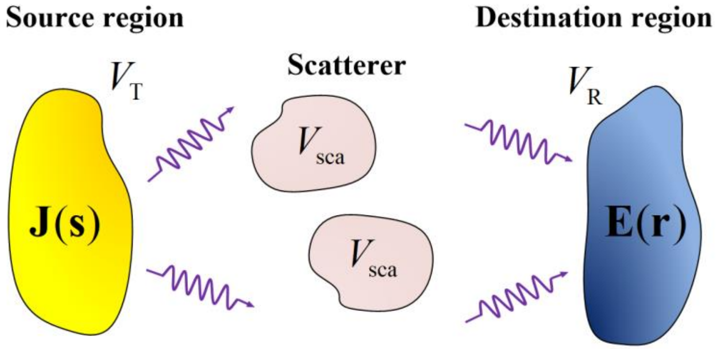

$$\mathbf{E}_{\text{inc}}(\mathbf{r}) = \mathrm{j}\omega \int_{V_s} \mathbf{G}(\mathbf{r},\mathbf{r}')\mu_0 \mathbf{J}(\mathbf{r}')\mathrm{d}\mathbf{r}'$$

Source current

$$\mathbf{E}_{\text{sca}} = \int_{V} \mathbf{G}(\mathbf{r},\mathbf{r}')(k^2(\mathbf{r}') - k_0^2)\mathbf{E}(\mathbf{r}')\mathrm{d}\mathbf{r}'$$

Electric field on the scatterer

The relationship between current and electric fields represent the channel characteristics

A. F. Peterson, S. L. Ray, and R. Mittra, *Computational methods for electromagnetics*. Wiley-IEEE Press New York, 1998.

2.1 Scalar Form Equation

- **For simplicity, we adopt scalar form of the wave and discard the evanescent waves**

$$\mathbf{G}(\mathbf{r},\mathbf{r}') = \frac{1}{4\pi}\frac{e^{\mathrm{j}\kappa_0\|\mathbf{r}-\mathbf{r}'\|}}{\|\mathbf{r}-\mathbf{r}'\|}\left[\boxed{(\mathbf{I}-\hat{\mathbf{p}}\hat{\mathbf{p}}^{\mathrm{H}})} + \boxed{\frac{\mathrm{j}}{2\pi\|\mathbf{r}-\mathbf{r}'\|/\lambda}(\mathbf{I}-3\hat{\mathbf{p}}\hat{\mathbf{p}}^{\mathrm{H}}) - \frac{1}{(2\pi\|\mathbf{r}-\mathbf{r}'\|/\lambda)^2}(\mathbf{I}-3\hat{\mathbf{p}}\hat{\mathbf{p}}^{\mathrm{H}})}\right][\mathrm{m}^{-1}]$$

Three polarization directions

Evanescent waves that can be ignored when the distance is far larger than wavelength

Discard evanescent waves

$$\mathbf{G}(\mathbf{r},\mathbf{r}') \approx \frac{1}{4\pi}\frac{e^{\mathrm{j}\kappa_0\|\mathbf{r}-\mathbf{r}'\|}}{\|\mathbf{r}-\mathbf{r}'\|}(\mathbf{I}-\hat{\mathbf{p}}\hat{\mathbf{p}}^{\mathrm{H}})$$

Take average on three directions

$$\mathrm{tr}(\mathbf{I}-\hat{\mathbf{p}}\hat{\mathbf{p}}^{\mathrm{H}})(\mathbf{I}-\hat{\mathbf{p}}\hat{\mathbf{p}}^{\mathrm{H}})^{\mathrm{H}} = 2$$

Incident field

Scatterer field

$$E(\mathbf{r}) = \mathrm{j}\omega\mu_0\int_{V_s} g(\mathbf{r},\mathbf{r}')J(\mathbf{r}')\mathrm{d}\mathbf{r}' + \int_V g(\mathbf{r},\mathbf{r}')(k^2(\mathbf{r}')-k_0^2)E(\mathbf{r}')\mathrm{d}\mathbf{r}'$$

$$g(\mathbf{r},\mathbf{r}') = \frac{1}{2\pi}\frac{e^{\mathrm{j}k_0\|\mathbf{r}-\mathbf{r}'\|}}{\|\mathbf{r}-\mathbf{r}'\|}$$

2.1 Incident Channel and Scattered Channel

- **Incident channel is fixed and simple**

$$E_{\mathrm{inc}}(\mathbf{r}) = \mathrm{j}\omega\mu_0 \int_{V_s} g(\mathbf{r},\mathbf{r}')J(\mathbf{r}')\mathrm{d}\mathbf{r}' \qquad g(\mathbf{r},\mathbf{r}') = \frac{1}{2\pi}\frac{e^{\mathrm{j}k_0\|\mathbf{r}-\mathbf{r}'\|}}{\|\mathbf{r}-\mathbf{r}'\|}$$

- **Scattered channel relies on complex scattering environment**

$$E_{\mathrm{sca}} = \int_{\boxed{V}} g(\mathbf{r},\mathbf{r}')\boxed{(k^2(\mathbf{r}') - k_0^2)}\boxed{E(\mathbf{r}')}\mathrm{d}\mathbf{r}'$$

Need proper assumption

Complex scattering environment

Scattering region V	**Solid circle**	$\mathrm{d}\mathbf{r} = \rho\mathrm{d}\rho\mathrm{d}\theta \begin{cases} 0 \leqslant \rho \leqslant r_0 \\ 0 \leqslant \theta \leqslant 2\pi \end{cases}$
$k^2(\mathbf{r}') - k_0^2$	**Parameterized function**	$f(\mathbf{r}) = \frac{a+1}{\pi r^{2a+2}}\rho(r^2-\rho^2)^a$
Electric field $\mathbf{E}(\mathbf{r}')$	**Statistical model**	$R_E(\mathbf{r},\mathbf{r}')$

2.1 Decouple Integral Variables

- **Depict the scattering field's characteristics using the statistical model**

$$R_E(\mathbf{d}_1, \mathbf{d}_2) = \sum_k \beta_k \int_{\mathbf{r}} \frac{S_k^2(\mathbf{r}, 0)}{S_k(\mathbf{r}, \mathbf{d}_1) S_k(\mathbf{r}, \mathbf{d}_2)} e^{-\mathrm{j}\frac{2\pi}{\lambda}(S_k(\mathbf{r},\mathbf{d}_1) - S_k(\mathbf{r},\mathbf{d}_2))} f(\mathbf{r}) \mathrm{d}\mathbf{r}$$

$$S_k = \sqrt{(\mathbf{R}_k \cdot \hat{\boldsymbol{\mu}}_k - \mathbf{d}_1 \cdot \hat{\boldsymbol{\mu}}_k)^2 + (\mathbf{R}_k \cdot \hat{\boldsymbol{\mu}}_{k1} + \rho \cos\theta - \mathbf{d}_1 \cdot \hat{\boldsymbol{\mu}}_{k1})^2 + (\mathbf{R}_k \cdot \hat{\boldsymbol{\mu}}_{k2} + \rho \sin\theta - \mathbf{d}_1 \cdot \hat{\boldsymbol{\mu}}_{k2})^2}$$

Distance from one point on the scatterer to the destination

Lemma 1: **Assume a circle-shaped scattering region centered at R, its radius is r, its direction is μ, its concentration parameter is a. Assume that the radius is far smaller than the distance between the scattering region and the receiver, then the received electric field at position d_1 and d_2 has the following correlation function:**

$$\tilde{R}(\mathbf{d}_1, \mathbf{d}_2) = \beta_0 \frac{A(\mathbf{d}_0)}{\sqrt{A(\mathbf{d}_1) A(\mathbf{d}_2)}} e^{-\mathrm{j}\frac{2\pi}{\lambda} R\left(\sqrt{A(\mathbf{d}_1)} - \sqrt{A(\mathbf{d}_2)}\right)} 2(a+1) 2^a \Gamma(a+1) (\sqrt{C} r)^{-(a+1)} J_{a+1}(\sqrt{C} r)$$

Channel can be generated by $\mathbf{h} = \mathbf{L}\mathbf{w}$ **where** $\mathbf{R} = \mathbf{L}\mathbf{L}^{\mathrm{H}}$ $\mathbf{w} \sim \mathcal{CN}(0, \mathbf{I})$

Z. Wan, J. Zhu, and **L. Dai**, "Near-field channel modeling for electromagnetic information theory," *IEEE Trans. Wireless Commun.*, Sep. 2024.

2.1 Scatterer parameters and channel DoF

- **Eigenvalue analysis based on the proposed correlation function of the channel**
- **The slower the eigenvalue decay, the larger the channel DoF**

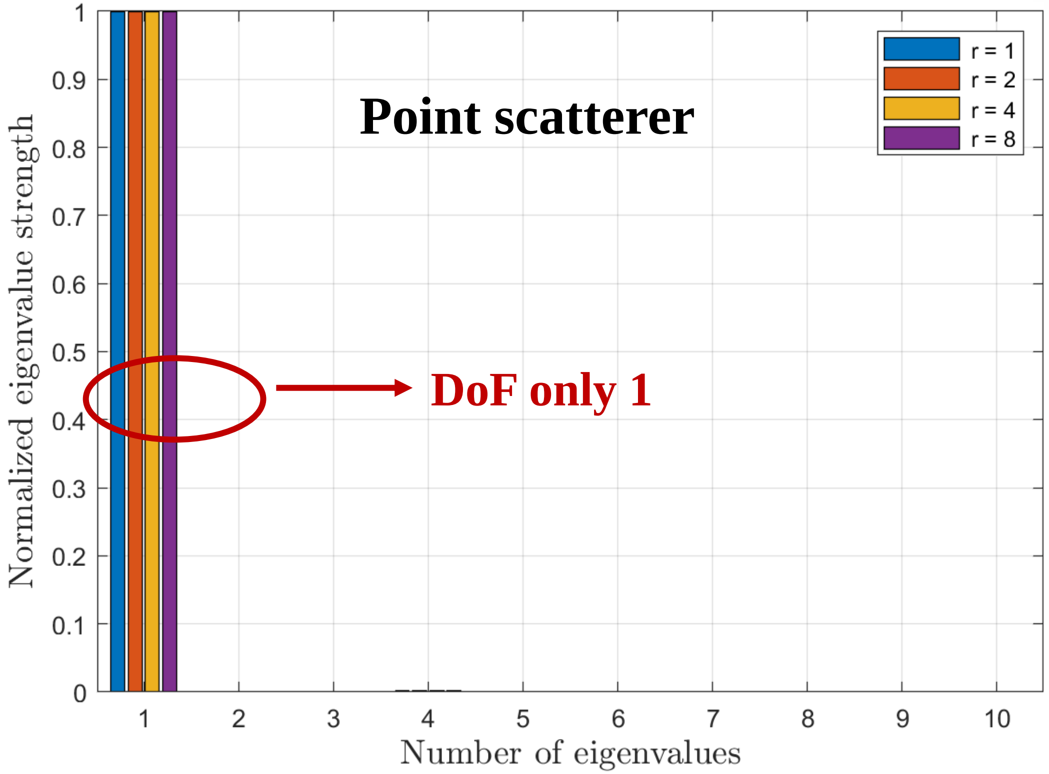

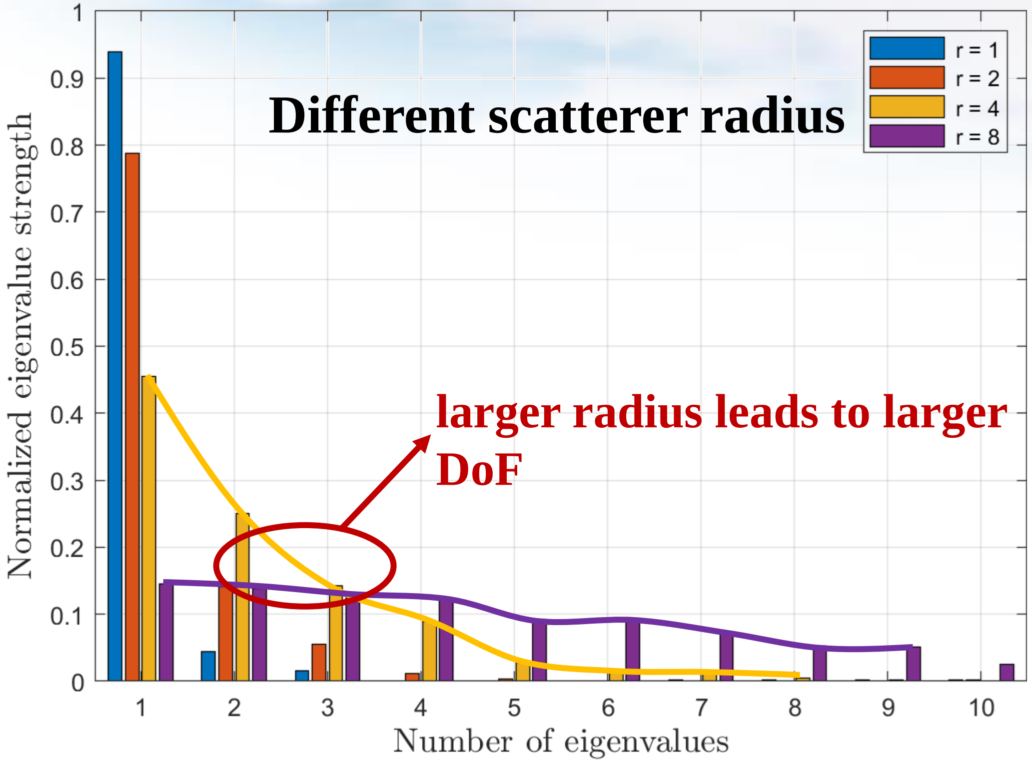

The near-field channel model for EIT provides more accurate description of DoF

Z. Wan, J. Zhu, and **L. Dai**, "Near-field channel modeling for electromagnetic information theory," *IEEE Trans. Wireless Commun.*, Sep. 2024

Contents

2.2 Introduction to EM DoF Analysis

- **Evaluation of EM degrees-of-freedom (DoF)**

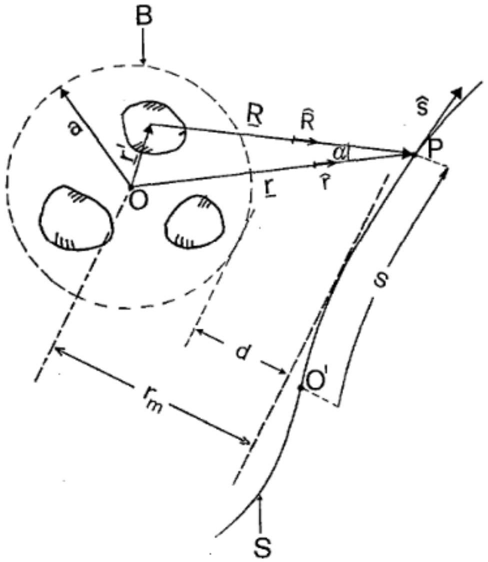

DoF analysis via spatial bandwidth [1]

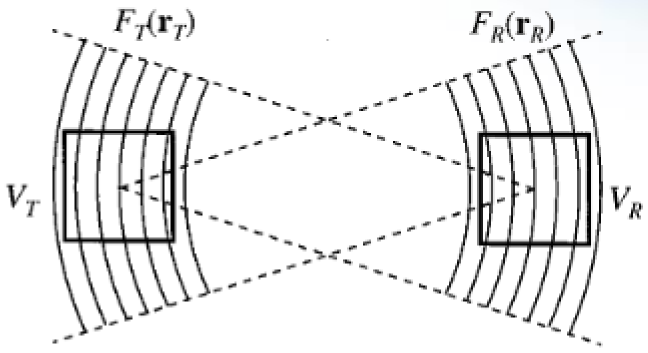

DoF analysis of a LoS volume communication system [2]

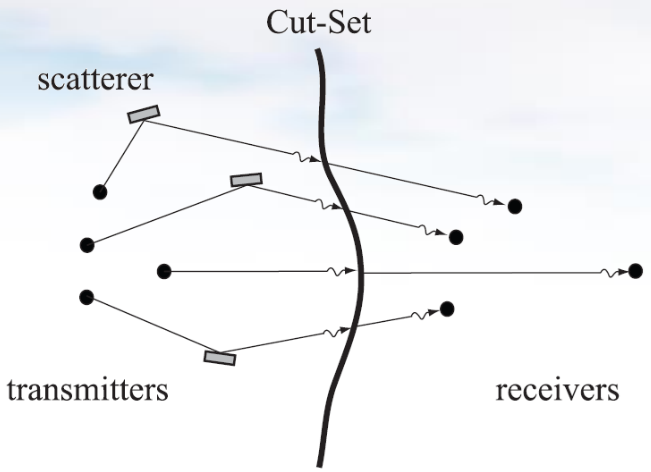

DoF analysis via information cut-set theory [3]

DoF analysis is based on continuous EM fields

[1] O. M. Bucci and G. Franceschetti, "On the spatial bandwidth of scattered fields," *IEEE Trans. Antennas Propagat.*, vol. 35, no. 12, pp. 1445-1455, Dec. 1987.

[2] D. A. B. Miller, "Communicating with waves between volmes: Evaluating orthogonal spatial channels and limits on coupling strengths," *Applied Optics*, vol. 39, no. 11, pp. 1681-1699, Nov. 2000.

[3] M. Franceschetti, "On Landau's eigenvalue theorem and information cut-sets," *IEEE Trans. Inf. Theory*, vol. 61, no. 9, pp. 5042–5051, Sep. 2015.

2.2 Continuous EM Transmission Model

- **Transmission model: From discrete matrices to continuous operators**
  - **Discrete MIMO model: Based on matrix theory, while neglecting continuous EM distribution**
  - **EM operator model: Based on operator theory for nearly-continuous transceiver regions**

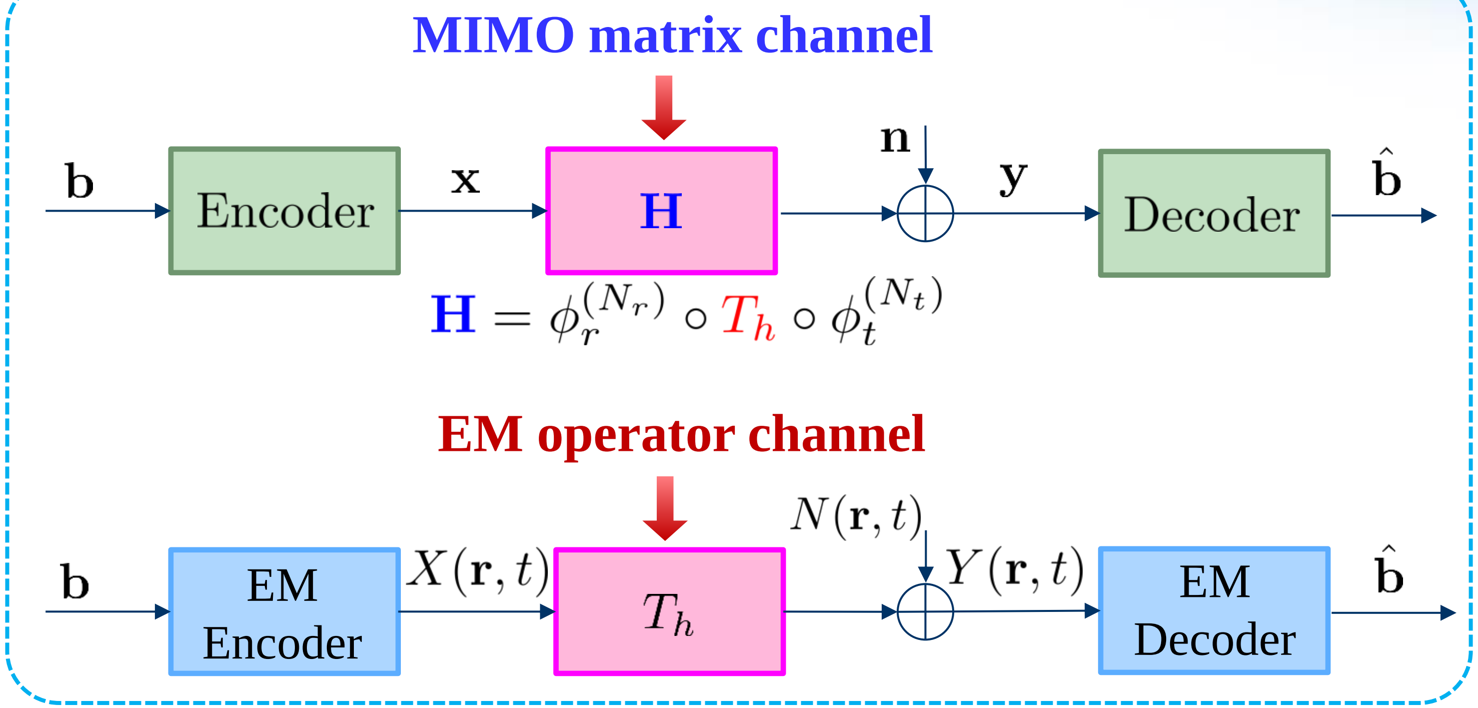

MIMO matrix model

$$\mathbf{y} = \mathbf{H}\mathbf{x} + \mathbf{n}$$

EM operator model

$$Y = T_h X + N$$

[1] D. Dardari, "Communicating with large intelligent surfaces: Fundamental limits and models," *IEEE J. Sel. Areas Commun.*, vol. 38, no. 11, pp. 2526–2537, Nov. 2020.

[2] Z. Wan, J. Zhu, Z. Zhang, **L. Dai**, and C.-B. Chae, "Mutual information for electromagnetic information theory based on random fields," *IEEE Trans. Commun.*, vol. 71, no. 4, pp. 1982-1996, Apr. 2023.

2.2 EIT Degrees of Freedom (DoFs)

- **The discrete-continuous comparison lemma for evaluating EM Degrees of Freedom**
  - **Definition: Discrete system = Continuous system cascaded with antenna system**
  - **Remark: Enabling continuous analysis to be applied to discrete systems, obtaining EIT upper bounds for arbitrary MIMO systems**

Rx Antenna **Tx Antenna**

$$\mathbf{H} = \phi_r^{(N_r)} \circ T_h \circ \phi_t^{(N_t)}$$

Data processing inequality (dpi)

$$\mathbb{E}[C_{\mathrm{MIMO}}] \leq \mathbb{E}[C_{\mathrm{EIT}}]$$

Theorem 2.2.1 Let the Tx/Rx region be $V_{\mathrm{T}},\ V_{\mathrm{R}} \subset \mathbb{R}^3$, $T_h:\ \mathcal{L}^2(V_{\mathrm{T}}) \to \mathcal{L}^2(V_{\mathrm{R}})$ **is the channel operator,** $\phi_t^{(N_t)}:\ \mathbb{C}^{N_t} \to \mathcal{L}^2(V_{\mathrm{T}}),\ \phi_r^{(N_r)}:\ \mathcal{L}^2(V_{\mathrm{R}}) \to \mathbb{C}^{N_r}$ **are energy-conservative Tx/Rx antenna operators, then for any** $\varepsilon > 0$ **, the following inequality holds:**

$$\mathrm{DoF}(\mathbf{H}, \varepsilon) \leq \mathrm{DoF}(T_h, \varepsilon),$$

where $\mathbf{H} = \phi_r^{(N_r)} \circ T_h \circ \phi_t^{(N_t)}$ **is the discrete channel matrix,** $\mathrm{DoF}(T, \varepsilon)$ **is the operator** T**'s** ε**-DoF.**

J. Zhu, V. Y. F. Tan, and **L. Dai**, "MIMO capacity analysis and channel estimation for electromagnetic information theory," submitted to *IEEE Trans. Inf. Theory*, Jun. 2024.

2.2 Dual-bandlimited Property of the EM Channel

- **Basic properties of the EM channel: Dual-bandlimited property**
  - **Spatially bandlimited [1]: The spatial FT of the channel $h(q,p)$ is bandlimited on $\mathcal{A}_r \times \mathcal{A}_t \subset [-1,1]^2$**
  - **Angularly bandlimited [2]: The angular channel $\tilde{h}(\beta,\alpha)$ is Γ-bandlimited with colored scattering**

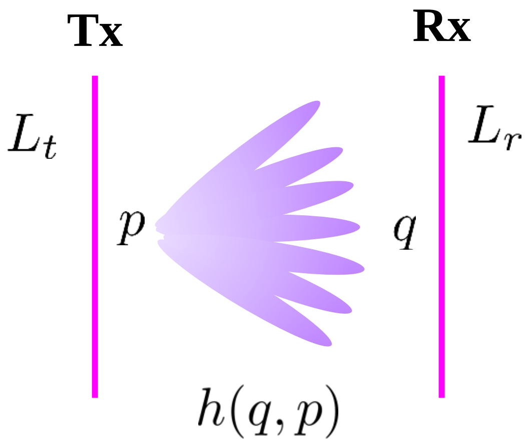

EM Channel

From Helmholtz equation, we have the spatially bandlimited channel

$$\tilde{h}(\beta,\alpha) = \int_{-L_r/2}^{L_r/2} \mathrm{d}q \int_{-L_t/2}^{L_t/2} \mathrm{d}p\, h(q,p) e^{-\mathrm{i}2\pi q\beta} e^{-\mathrm{i}2\pi p\alpha}.$$

For colored scattering, [2] assumes an angularly bandlimited channel

$$\mathbb{E}\left[\tilde{h}(\beta,\alpha)\tilde{h}^*(\beta',\alpha')\right] = \frac{\sigma_{\tilde{h}}^2}{\Gamma_t\Gamma_r}\mathrm{sinc}\left(\frac{\alpha-\alpha'}{\Gamma_t}\right)\cdot \mathrm{sinc}\left(\frac{\beta-\beta'}{\Gamma_r}\right).$$

David Tse
Shannon Award Recipient (2017)
Member of the National Academy of Engineering (US)

[1] A. S. Poon, D. N. Tse, and R. W. Brodersen, "Impact of scattering on the capacity, diversity, and propagation range of multiple-antenna channels," *IEEE Trans. Inf. Theory*, vol. 52, no. 3, pp. 1087–1100, Mar. 2006.

[2] W. Nam, D. Bai, J. Lee, and I. Kang, "On the capacity limit of wireless channels under colored scattering," *IEEE Trans. Inf. Theory*, vol. 60, no. 6, pp. 3529–3543, Apr. 2014.

2.2 Ergodic Capacity Analysis: Upper Bound

- **Dual bandlimited property leads to a special eigen problem**
  - **PSWF eigen problem: Find a $\mathcal{B}$ -bandlimited function that is most concentrated in $\mathcal{A}$**
  - **Solution to the above eigenproblem is called $(\mathcal{A}, \mathcal{B})$-prolate spheroidal wave function (PSWF)**

Truncation $\Pi_{\mathcal{A}}: f \to f 1_{\mathcal{A}}$

Bandpass filtering $\Pi_{\mathcal{B}}: f \to \mathcal{F}^{-1}[\mathcal{F}(f) 1_{\mathcal{B}}]$

PSWF eigenproblem $\gamma_\ell \psi_\ell = \Pi_{\mathcal{B}} \Pi_{\mathcal{A}} \psi_\ell$

- **Upper bound of the ergodic capacity is given by the PSWF eigenvalues $\{\gamma_\ell\}_{\ell=0}^{\infty}$ [1]**

Thm 2.2.2[1] Assume the channel operator $T_h: \mathcal{L}^2(V_{\mathrm{T}}) \to \mathcal{L}^2(V_{\mathrm{R}})$ is spatially bandlimited in $\mathcal{A}_t = \mathcal{A}_r = \mathcal{A}$ with colored scattering bandwidth Γ. Then, the ergodic capacity $\mathbb{E}[C_{\mathrm{EIT}}(T_h, P_{\mathrm{T}}/\sigma_z^2)]$ is upper-bounded by the eigenvalues of $(\mathcal{A}, \mathcal{B}_\Omega)$ -PSWF through

$$\mathbb{E}\left[C_{\mathrm{EIT}}\left(T_h, \frac{P_{\mathrm{T}}}{\sigma_z^2}\right)\right] \le \sum_{\ell=0}^{\infty} \log\left(1 + \frac{P_{\mathrm{T}}}{\sigma_z^2}\gamma_\ell\right),$$ **where** $\Omega = \min\left\{\frac{L}{\lambda}, \frac{1}{\Gamma}\right\}$, L [m] **is the receiver aperture**

[1] W. Nam, D. Bai, J. Lee, and I. Kang, "On the capacity limit of wireless channels under colored scattering," *IEEE Trans. Inf. Theory*, vol. 60, no. 6, pp. 3529–3543, Apr. 2014.

2.2 Apply Continuous Upper Bound to Discrete Systems

- **Discrete-continuous comparison (Thm 2.2.1) applied to novel MIMO architectures**
  - **Holographic MIMO (H-MIMO): Aperture limited, but antenna spacing unlimited**
  - **Extremely large-scale MIMO (XL-MIMO): Aperture unlimited, but antenna spacing limited**

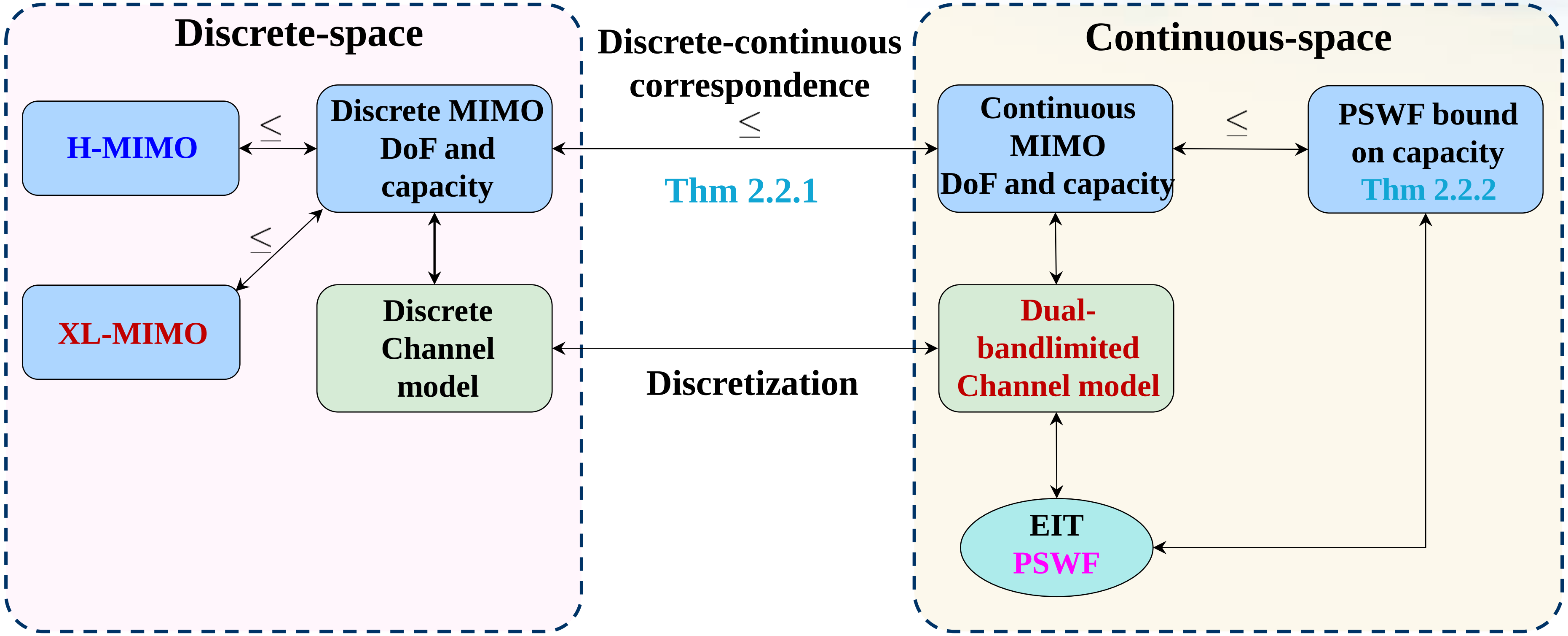

J. Zhu, V. Y. F. Tan, and **L. Dai**, "MIMO capacity analysis and channel estimation for electromagnetic information theory," submitted to *IEEE Trans. Inf. Theory*, Jun. 2024.

2.2 Ergodic Capacity Upper Bound Algorithm

- **Legendre spectral method for PSWF eigenvalues** $\{\gamma_\ell\}_{\ell=0}^{\infty}$

PSWF eigen-problem $\gamma_\ell \psi_\ell = \Pi_{\mathcal{B}} \Pi_{\mathcal{A}} \psi_\ell$

Spatial representation

Integral operator eigen-problem

$$\lambda_n \psi_n(x) = [\mathcal{M}_c \psi_n](x) := \int_{-1}^{1} \frac{\sin(c(x-y))}{\pi(x-y)} \psi_n(y) \mathrm{d}y$$

Operator commutes $\mathcal{M}_c \mathcal{L}_c = \mathcal{L}_c \mathcal{M}_c$

Differential operator eigen-problem

$$\chi_n(c)\psi_n(x) = [\mathcal{L}_c \psi_n](x) := \left(\frac{\mathrm{d}}{\mathrm{d}x}(1-x^2)\frac{\mathrm{d}}{\mathrm{d}x} - c^2 x^2 \right) \psi_n(x)$$

Legendre series expansion

$$\psi_n(x) = \sum_{k=0}^{\infty} \beta_{nk}(c) \bar{P}_k(x)$$

Matrix eigen-problem $(\mathbf{A} - \chi_n(c)\mathbf{I})\boldsymbol{\beta}_n(c) = \mathbf{0}$

Algorithm 1 Modified Bouwkamp Algorithm

Input: Bandwidth parameter Ω; interval $\mathcal{A} = [a, b]$; maximum spectral order $n_{\max}$.

Output: Approximated PSWFs $\{\phi_\ell(x)\}_{\ell=0}^{n_{\max}}$; approximated prolate spheroidal eigenvalues $\{\gamma_\ell\}_{\ell=0}^{n_{\max}}$.

```
c ← πΩ(b − a)/2.
Construct the normalized Legendre polynomials up to order n_max by (34), and gather the polynomial coefficients in the matrix P ∈ ℝ^((n_max+1)×(n_max+1)).
Compute [V, D] = eig(A) of (36) with eigenvalues sorted in descending order.
Let β_nk(c) ← [V]_k,n to determine ψ_n via (35).
Compute the coefficient matrix P′ of P̄′_n(x) from P.
μ_0 ← Numerical(⟨ψ_0, F_c ψ_0⟩).
y_prev ← Numerical(ψ_0), y′_prev ← Numerical(ψ′_0).
for ℓ = 1, 2, ..., n_max do
    y_cur ← Numerical(ψ_ℓ) by β_ℓk(c) and P.
    y′_cur ← Numerical(ψ′_ℓ) by β_ℓk(c) and P′.
    a ← Numerical(⟨y_cur, y′_prev⟩).
    b ← Numerical(⟨y′_cur, y_prev⟩).
    μ_ℓ ← iμ_(ℓ−1) · sqrt(|a/b|).
    y_prev ← y_cur, y′_prev ← y′_cur.
end for
γ_ℓ ← c|λ_ℓ|^2/(2π), ∀ℓ ∈ [n_max + 1].
Get φ_ℓ: rescale ψ_ℓ from [−1, 1] to [a, b] by (29) and applying a re-normalization factor sqrt(2/(b − a)).
return {γ_ℓ}_(ℓ=0)^(n_max), {φ_ℓ}_(ℓ=0)^(n_max).
```

A. Karoui and T. Moumni, "New efficient methods of computing the prolate spheroidal wave functions and their corresponding eigenvalues," *Applied and Comput. Harmon.*, Jul. 2008.

2.2 Numerical Results

- **EIT upper bound applied to H-MIMO and XL-MIMO architecture**

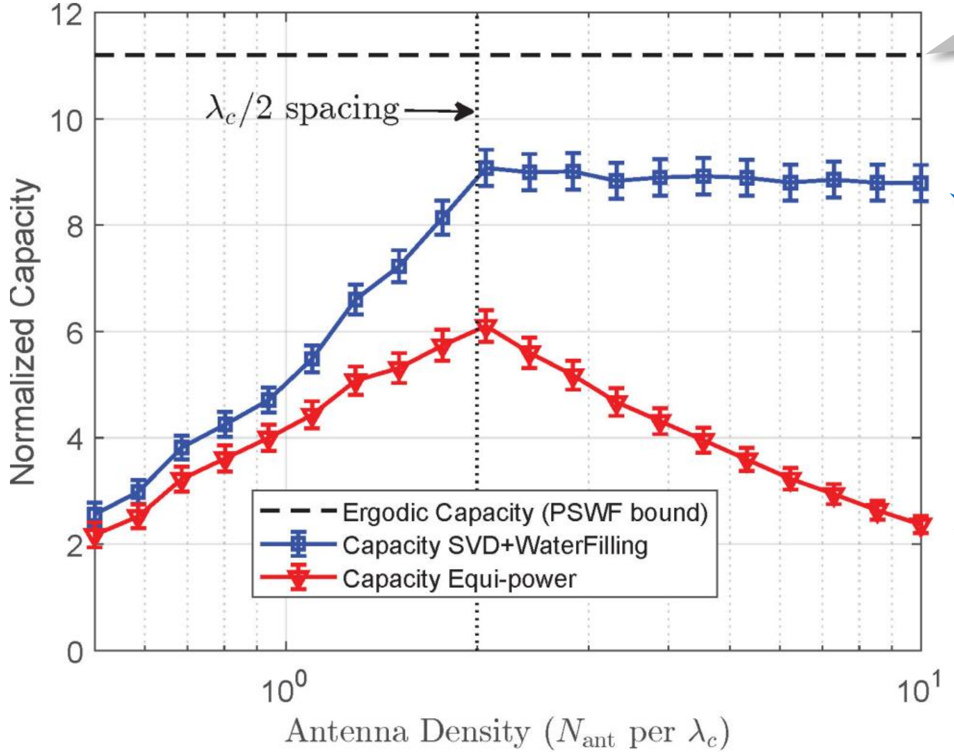

H-MIMO (unlimited antenna spacing)

EIT Upper Bound

Achievable Rate (SVD)

Achievable Rate (Eq power)

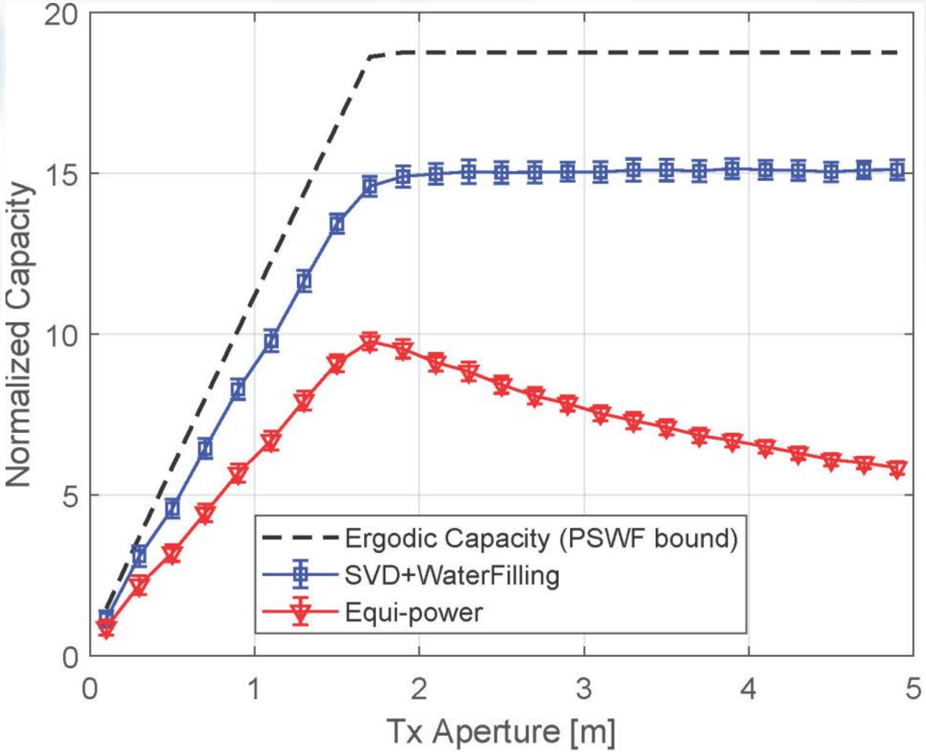

XL-MIMO (unlimited aperture size)

Capacity growth of H-MIMO and XL-MIMO is limited by EM dual-bandlimited property

J. Zhu, V. Y. F. Tan, and **L. Dai**, "MIMO capacity analysis and channel estimation for electromagnetic information theory," submitted to *IEEE Trans. Inf. Theory*, Jun. 2024.

Contents

2.3 Mutual Information & Capacity Analysis

- Use classical MIMO information theory based on spatial discretization of EM model [1]
- Use spherical harmonic functions to decompose continuous fields [2]
- Kolmogorov's ε-capacity considering distinguishable waveforms above an uncertainty level [3]

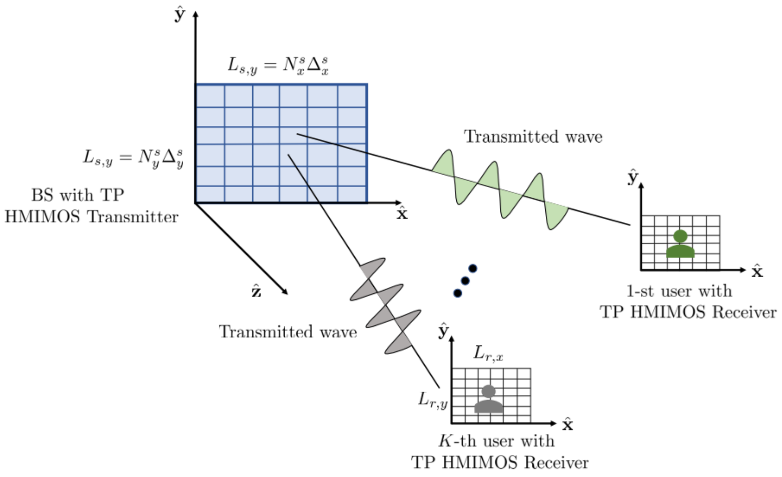

Discretized EM model

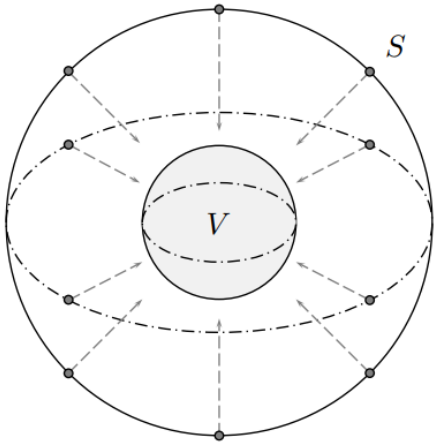

Concentric spherical transceivers

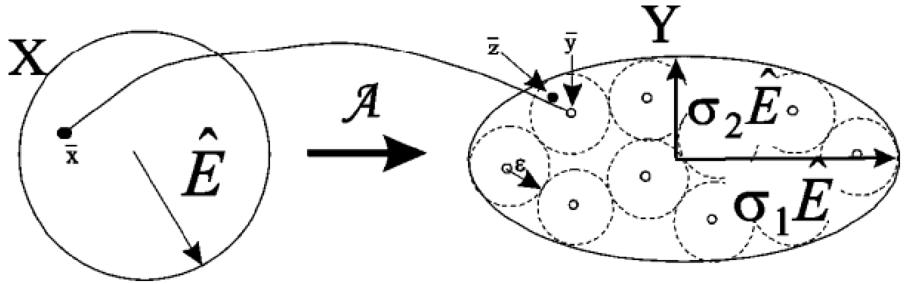

Sphere packing of radiation operator

[1] L. Wei, C. Huang, G. C. Alexandropoulos, Z. Yang, J. Yang, E. Wei, Z. Zhang, M. Debbah, and C. Yuen, "Tri-polarized holographic MIMO surfaces for near-field communications: Channel modeling and precoding design," *IEEE Trans. Wireless Commun.*, vol. 22, no. 12, pp. 8828–8842, Dec. 2023.
[2] W. Jeon and S.-Y. Chung, "Capacity of continuous-space electromagnetic channels with lossy transceivers," *IEEE Trans. Inf. Theory*, vol. 64, no. 3, pp. 1977–1991, Mar. 2018.
[3] M. D. Migliore, "On electromagnetics and information theory," *IEEE Trans. Antennas Propag.*, vol. 56, no. 10, pp. 3188–3200, Oct. 2008.

2.3 Mutual Information Analysis of EIT

- **Input-output relationship of continuous EM model**

Electric field

Green's function

From current density at transmitter
To electric field at receiver

$$\mathbf{E}(\mathbf{r}) = \int_{V_s} \mathbf{G}(\mathbf{r},\mathbf{s})\mathbf{J}(\mathbf{s})\mathrm{d}\mathbf{s}, \quad \mathbf{r} \in V_r$$

Current density

Received electric field with noise

$$\mathbf{Y}(\mathbf{r}) = \mathbf{E}(\mathbf{r}) + \mathbf{N}(\mathbf{r}) \quad \mathbf{r} \in V_r$$

- **Green's function (Spatial impulse response)**

Green's function

$$\mathbf{G}(\mathbf{r},\mathbf{s}) = \frac{\mathrm{j}\kappa Z_0}{4\pi}\frac{e^{\mathrm{j}\kappa\|\mathbf{r}-\mathbf{s}\|}}{\|\mathbf{r}-\mathbf{s}\|}\left(\mathbf{I} + \frac{\nabla_{\mathbf{r}}\nabla_{\mathbf{r}}^{\mathrm{H}}}{\kappa^2}\right) \approx \frac{\mathrm{j}\kappa Z_0}{4\pi}\frac{e^{\mathrm{j}\kappa\|\mathbf{r}-\mathbf{s}\|}}{\|\mathbf{r}-\mathbf{s}\|}\left(\mathbf{I} - \hat{\mathbf{p}}\hat{\mathbf{p}}^{\mathrm{H}}\right)$$

$$\hat{\mathbf{p}} = \frac{\mathbf{p}}{\|\mathbf{p}\|} \qquad \mathbf{p} = \mathbf{r} - \mathbf{s}$$

Conditions: infinite boundary, homogeneous dielectric, time-harmonic field

From spatially discrete model to spatially continuous model

2.3 Mutual Information Analysis of EIT

- **Convey information by continuous electromagnetic fields**
- **Mutual information: Eliminate the uncertainty of the current J from the observed electric field Y**
  - **Model current and electric field by Gaussian random fields**

Current density

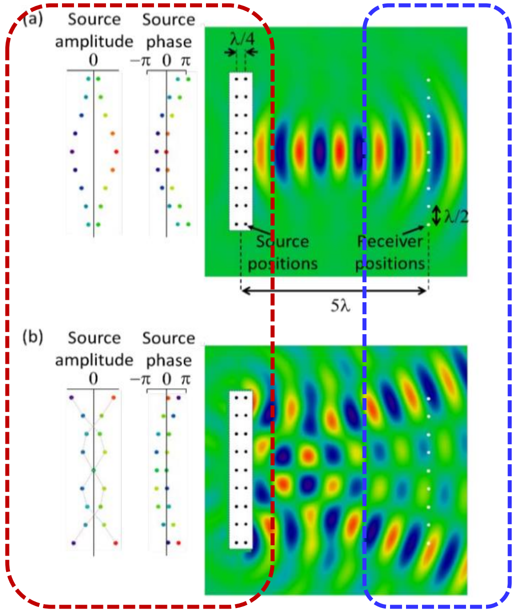

Electric field

Electromagnetic channel $\mathbf{E}(\mathbf{r}) = \int_{V_s} \mathbf{G}(\mathbf{r}, \mathbf{s})\mathbf{J}(\mathbf{s})\mathrm{d}\mathbf{s}$

Noisy received field $\mathbf{Y}(\mathbf{r}) = \mathbf{E}(\mathbf{r}) + \mathbf{N}(\mathbf{r})$

Mutual information $I(\mathbf{J}; \mathbf{Y}) = \sup\{I(\mathbf{J}(\phi_1, \cdots, \phi_m), \mathbf{Y}(\psi_1, \cdots, \psi_n))\}$

Challeng: How to drive the mutual information?

2.3 Mutual Information Analysis of EIT

- **Use KL expansion to derive the mutual information**

Random field and Correlation function

$$E(\mathbf{r}) = \sum_{k=1}^{+\infty} \xi_k \phi_k(\mathbf{r}), \quad R_E(\mathbf{r}, \mathbf{r}') = \sum_{k=1}^{+\infty} \lambda_k \phi_k(\mathbf{r}) \phi_k^*(\mathbf{r}')$$

Integral equation

$$\lambda_k \phi_k(\mathbf{r}') = \int_0^l R_E(\mathbf{r}, \mathbf{r}') \phi_k(\mathbf{r}) \mathrm{d}\mathbf{r}; k > 0, k \in \mathbb{N}$$

Eigenvalue: gain → **Eigenfunction: base**

Orthogonal basis, independent coefficients

$$\int \phi_{k_1}(\mathbf{r}) \phi_{k_2}(\mathbf{r}) \mathrm{d}\mathbf{r} = \delta_{k_1 k_2}, \quad \mathbb{E}[\xi_{k_1} \xi_{k_2}] = \mathbb{1}_{k_1 = k_2} \lambda_{k_1}$$

Electric field

$$E(\mathbf{r}) = \sum_{k=1}^{+\infty} \xi_k \phi_k(\mathbf{r}) \quad \lambda_k \phi_k(\mathbf{r}') = \int_0^l R_E(\mathbf{r}, \mathbf{r}') \phi_k(\mathbf{r}) \mathrm{d}\mathbf{r}; k > 0, k \in \mathbb{N}$$

Noise field

$$N(\mathbf{r}) = \sum_{k=1}^{+\infty} \xi_k' \phi_k(\mathbf{r}) \quad \frac{n_0}{2} \phi_k(\mathbf{r}') = \int_0^l \frac{n_0}{2} \delta(\mathbf{r}' - \mathbf{r}) \phi_k(\mathbf{r}) \mathrm{d}\mathbf{r}; k > 0, k \in \mathbb{N}$$

→ **MI for continuous field**

$$I = \sum_{k=1}^{\infty} \log\left(1 + \frac{\lambda_k}{n_0/2}\right)$$

Z. Wan, J. Zhu, Z. Zhang, **L. Dai**, and C.-B. Chae, "Mutual information for electromagnetic information theory based on random fields," *IEEE Trans. Commun.*, vol. 71, no. 4, pp. 1982-1996, Feb. 2023.

2.3 Mutual Information Analysis of EIT

- **Expression of the mutual information in operator determinant form (Fredholm determinant)**

	Matrix H	Operator T
Equation	$\mathbf{H}\mathbf{x}_k = \lambda \mathbf{x}_k$	$\mathrm{T}\phi_k(r) = \lambda_k \phi_k(r)$
Base	Eigenvector $\mathbf{x}_k$	Eigenfunction $\phi_k(r)$
Trace	$\sum_{k=1}^{N} \lambda_k = \sum_{i=1}^{N} H_{i,i}$	$\sum_{k=1}^{+\infty} \lambda_k = \int_0^l K(r,r)\mathrm{d}r$
Determinant	$\prod_{k=1}^{N} \lambda_k = \det(\mathrm{H})$	$\prod_{k=1}^{+\infty} \lambda_k = \det(\mathrm{T})$

$$
\begin{aligned}
I &= \sum_{k=1}^{+\infty} \log\left(1 + \frac{\lambda_k}{n_0/2}\right) \\
&= \log \prod \left(1 + \frac{\lambda_k}{n_0/2}\right) \\
&= \log\left(\det(\mathbf{1} + \frac{\mathrm{T}_E}{n_0/2})\right)
\end{aligned}
$$

Operator determinant

New tool to analyze the properties of mutual information between continuous fields

Z. Wan, J. Zhu, Z. Zhang, **L. Dai**, and C.-B. Chae, "Mutual information for electromagnetic information theory based on random fields," *IEEE Trans. Commun.*, vol. 71, no. 4, pp. 1982-1996, Feb. 2023.

2.3 CAP-MIMO Based Wireless Communications

- **Continuous-aperture MIMO (CAP-MIMO), holographic MIMO, large intelligent surface**
- **The current density (pattern) is generated on the aperture of CAP-MIMO transmitter which induces the information-carrying electromagnetic waves**

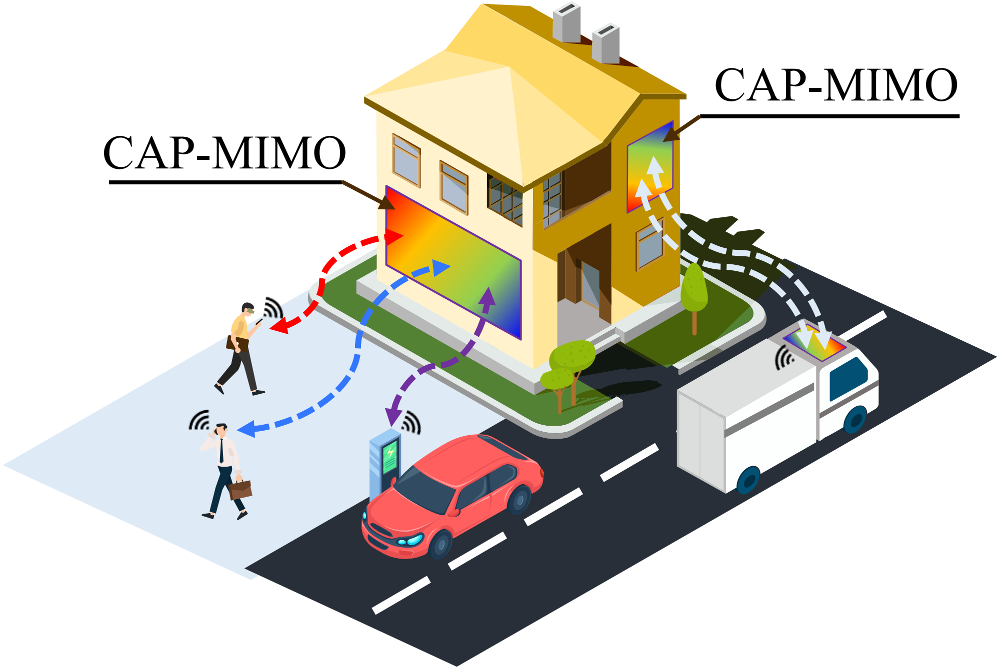

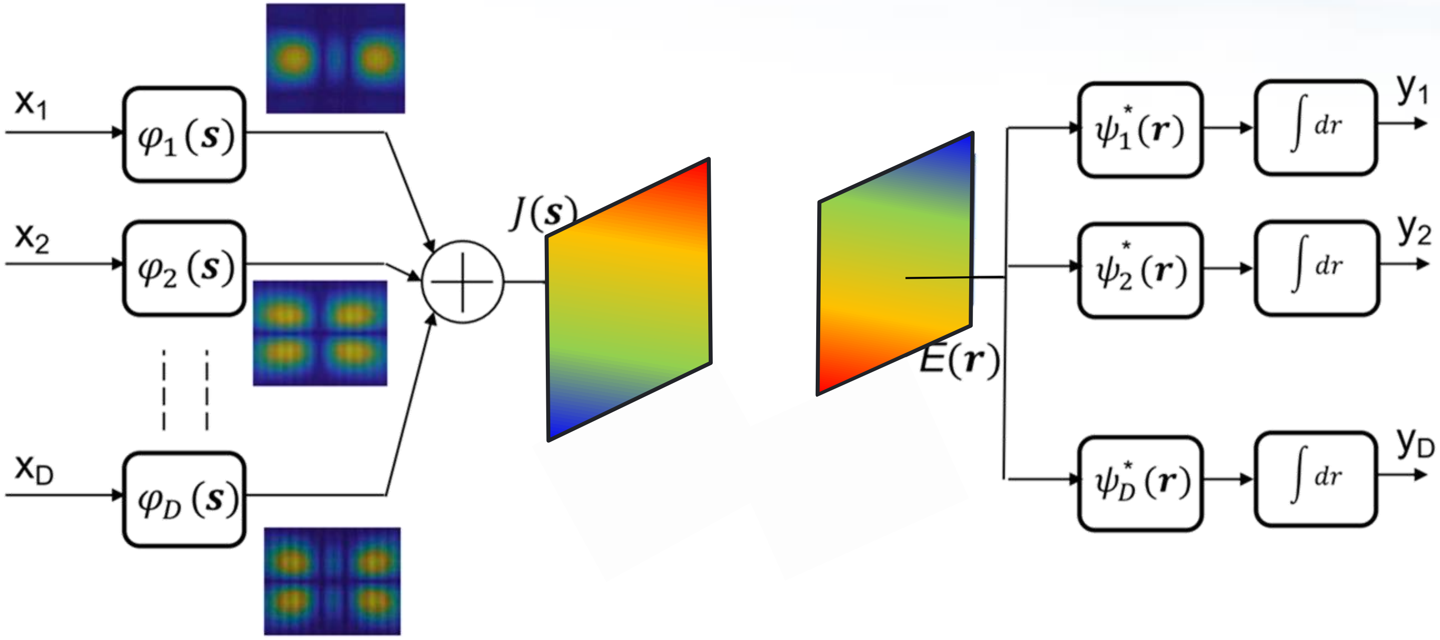

A. Pizzo, T. L. Marzetta and L. Sanguinetti, "Spatially-stationary model for holographic MIMO small-scale fading," *IEEE J. Sel. Areas Commun.*, vol. 38, no. 9, pp. 1964-1979, Sep. 2020.

2.3 CAP-MIMO and Discrete MIMO

- **Can CAP-MIMO achieve infinite performance gain by deploying infinitely dense antennas?**
- **If not, what is the relationship between the performance of CAP-MIMO and discrete MIMO?**

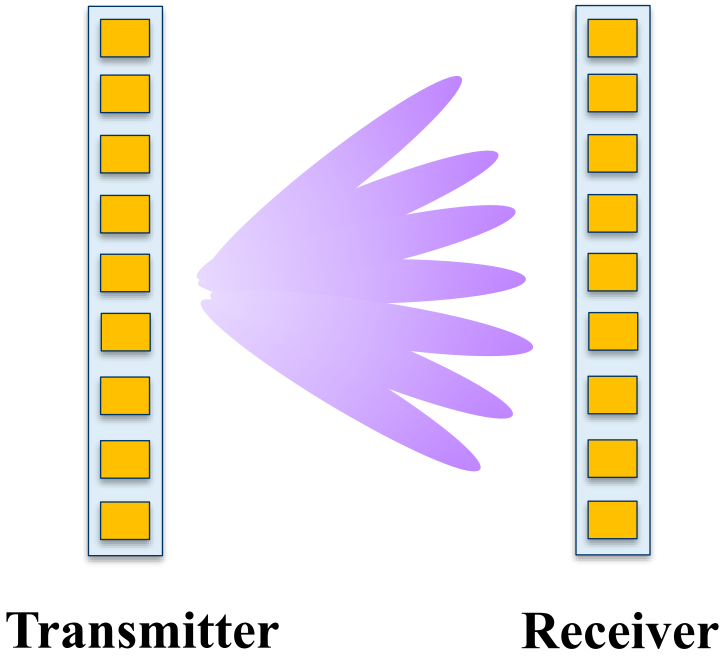

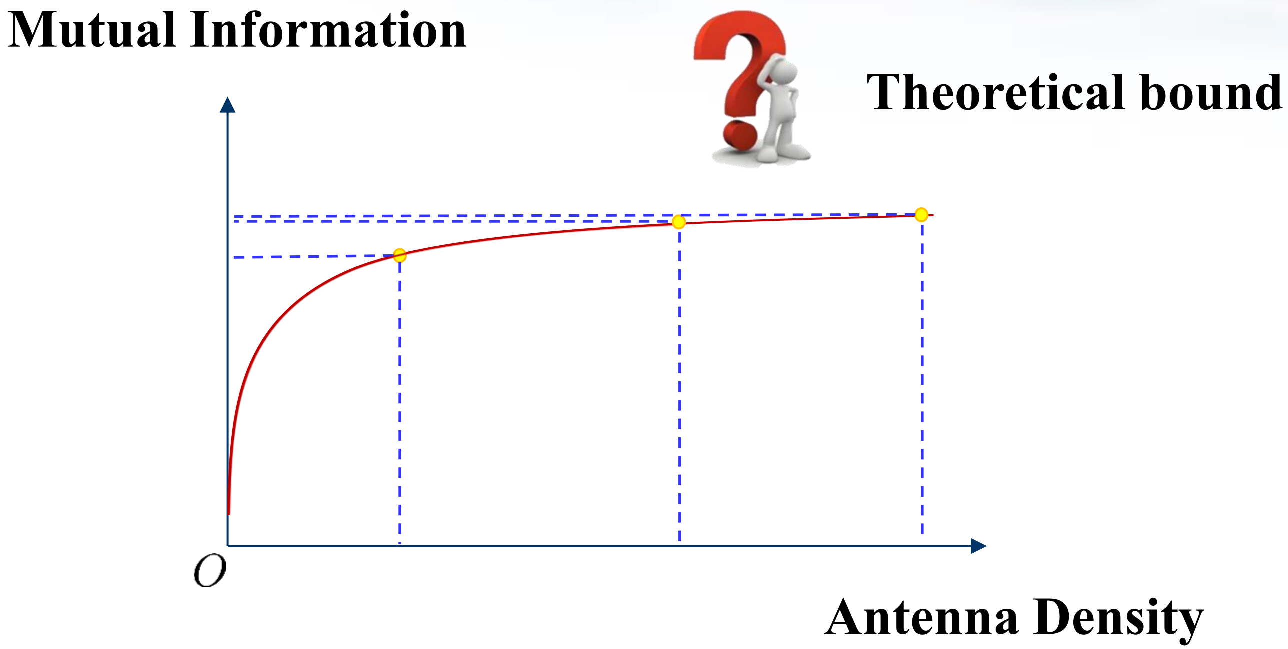

Z. Wan, J. Zhu, and **L. Dai**, "Can continuous aperture MIMO achieve much better performance than discrete MIMO?," *IEEE Commun. Lett.*, vol. 27, no. 12, pp. 3185-3189, Dec. 2023.

2.3 Modeling

- The **distances** between transceivers are **equal** for CAP-MIMO and discrete MIMO
- **CAP-MIMO**: Length-l transmitter and length-l receiver
- **Discrete MIMO**: m_1 antennas in length-l transmitting region and m_2 antennas in length-l receiving region

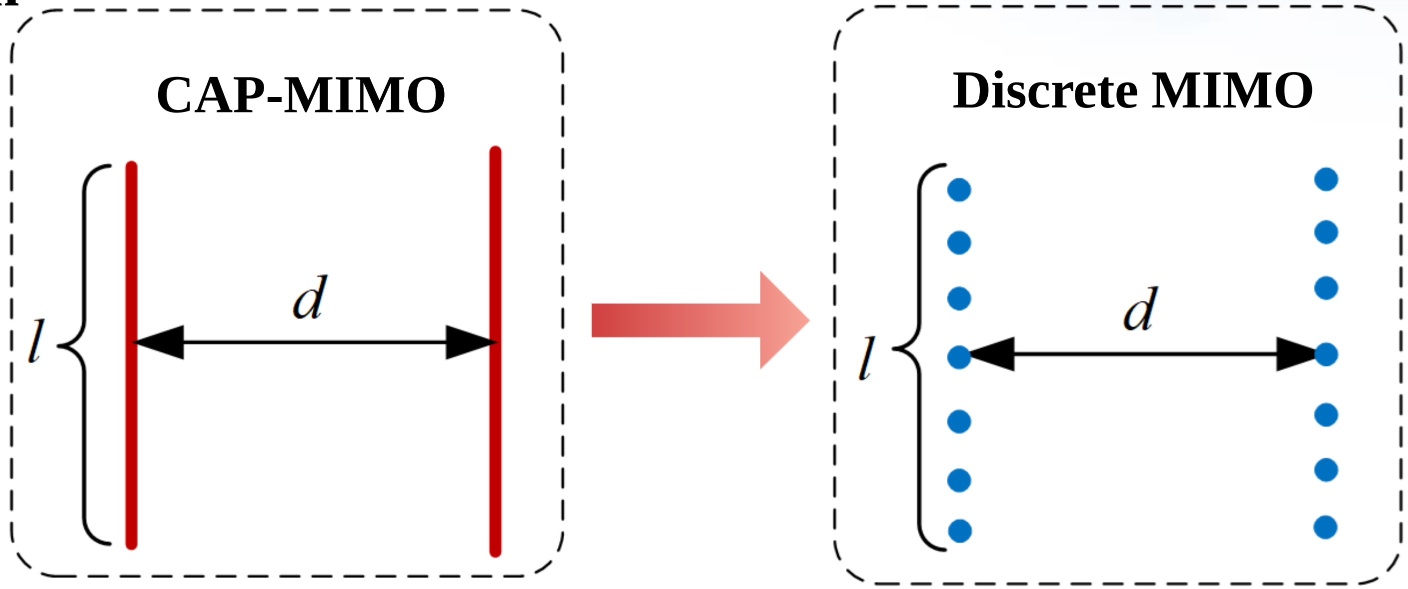

Signal	Noise	Signal	Noise
$R_J(s, s') = P_1 \delta(s - s')$	$R_N(r, r') = \frac{n_1}{2} \delta(r - r')$	$R_{\mathbf{J}} = P_2 \mathbf{I}_{m_1}$	$R_{\mathbf{N}} = \frac{n_2}{2} \mathbf{I}_{m_2}$

Z. Wan, J. Zhu, and **L. Dai**, "Can continuous aperture MIMO achieve much better performance than discrete MIMO?," *IEEE Commun. Lett.*, vol. 27, no. 12, pp. 3185-3189, Dec. 2023.

2.3 Performance Comparison

- **Mutual information (MI) difference between CAP-MIMO and discrete MIMO**

Theorem 1: The MI difference can be bounded by

$$|I_1 - I_2| \leqslant \frac{C_1}{(\min(\boxed{m_1, m_2}))^2}$$

Antenna number/density

Constant C_1 is determined by various parameters including channel characteristics and transmitter sizes and distances

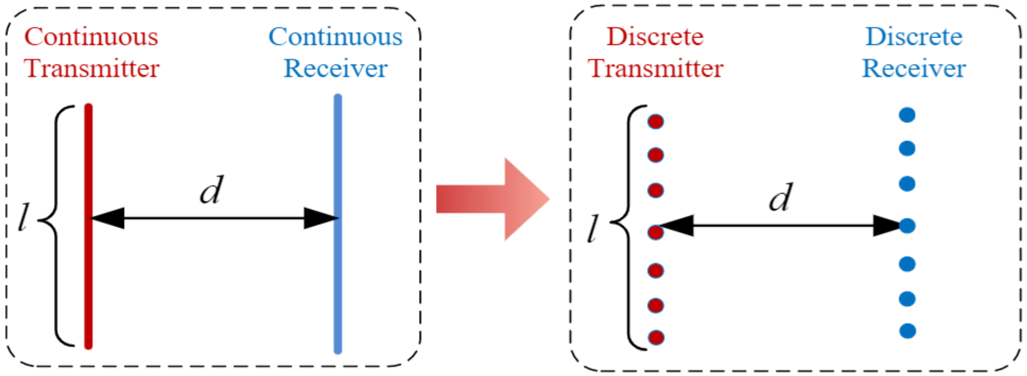

$$C_1 \propto \boxed{x}^2 e^{cx^2}$$

$$\boxed{\max \left\| \frac{\partial_x^i \partial_y^j \partial_z^k g(x, y, z)}{\partial x^i \partial y^j \partial z^k} \right\|_{L^\infty((0,l)^3)}}$$

The MI difference is at most inverse proportional to square of number of antennas

Z. Wan, J. Zhu, and **L. Dai**, "Can continuous aperture MIMO achieve much better performance than discrete MIMO?," *IEEE Commun. Lett.*, vol. 27, no. 12, pp. 3185-3189, Dec. 2023.

2.3 Numerical Verification: Symmetric Sampling

- **Comparison of mutual information**

Deduction 1: When the discrete array is viewed as a compact discretization of the continuous aperture, the mutual information of discrete MIMO converges to that of CAP-MIMO

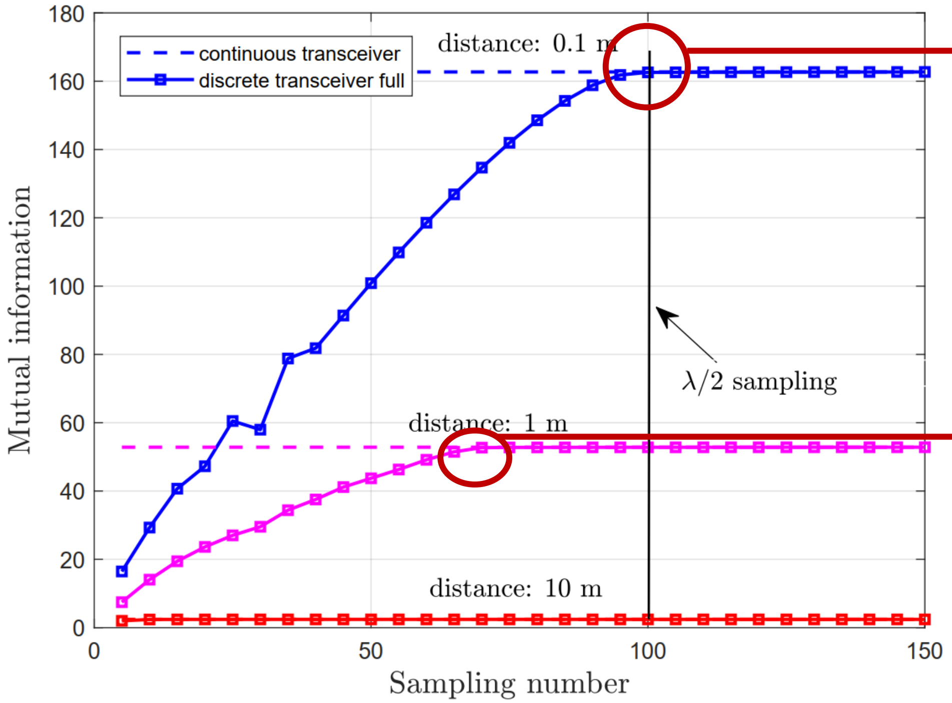

0.5λ achieves nearly all mutual information

0.7λ achieves nearly all mutual information

Z. Wan, J. Zhu, and **L. Dai**, "Can continuous aperture MIMO achieve much better performance than discrete MIMO?," *IEEE Commun. Lett.*, vol. 27, no. 12, pp. 3185-3189, Dec. 2023.

2.3 Numerical Verification: Asymmetric Sampling

- **Comparison of mutual information**

Deduction 2: The number of antennas m_1 and m_2 has duality. Moreover, their effect on the mutual information has a short-board effect.

Discrete MIMO:

$$C \propto \boxed{\min(m_1, m_2)} \log(1 + SNR)$$

Also has duality and short-board effect

CAP-MIMO:

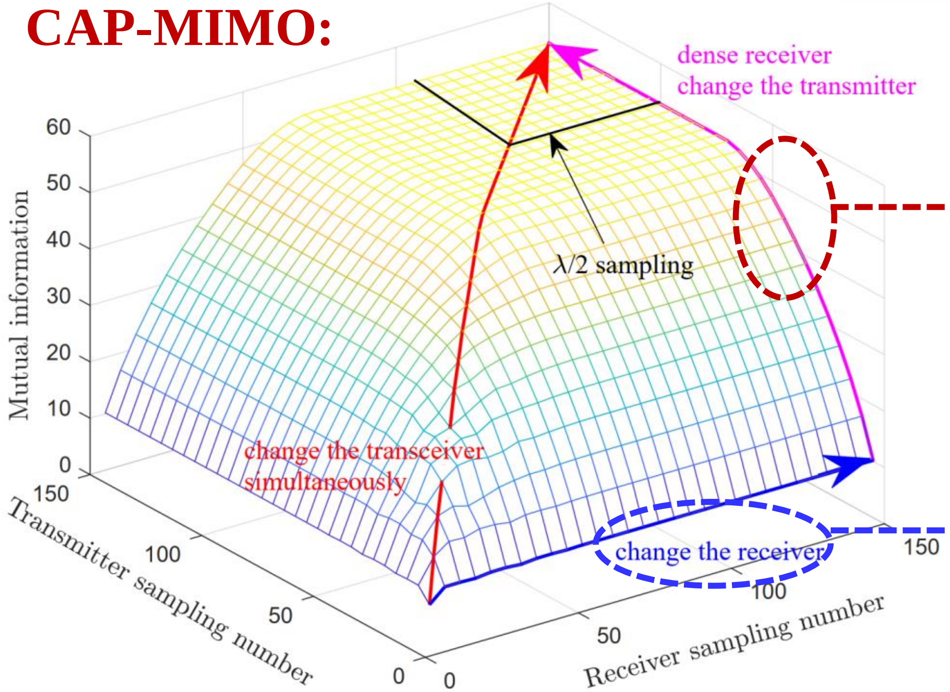

Lare receiver array, when increasing transmitter sampling number, mutual information increases rapidly

Fixed small transmitter array, when increasing receiver sampling number, mutual information nearly keeps the same

Z. Wan, J. Zhu, and **L. Dai**, "Can continuous aperture MIMO achieve much better performance than discrete MIMO?," *IEEE Commun. Lett.*, vol. 27, no. 12, pp. 3185-3189, Dec. 2023.

Contents

3.1 Concept of Holographic MIMO (H-MIMO)

- **Holographic MIMO (H-MIMO), continuous-aperture MIMO (CAP-MIMO): Densely deploy massive antennas in a compact space to form a fully adjustable EM surface**
- **The current density (pattern) is generated on the aperture of H-MIMO transmitter and the information-carrying electromagnetic wave is induced at the receiver**

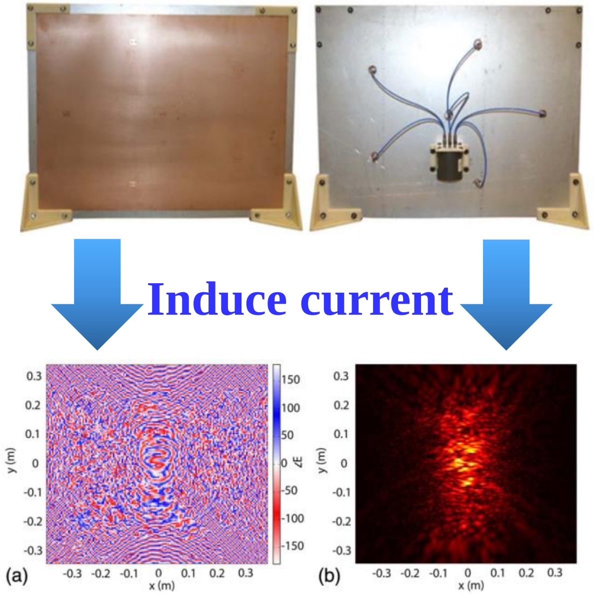

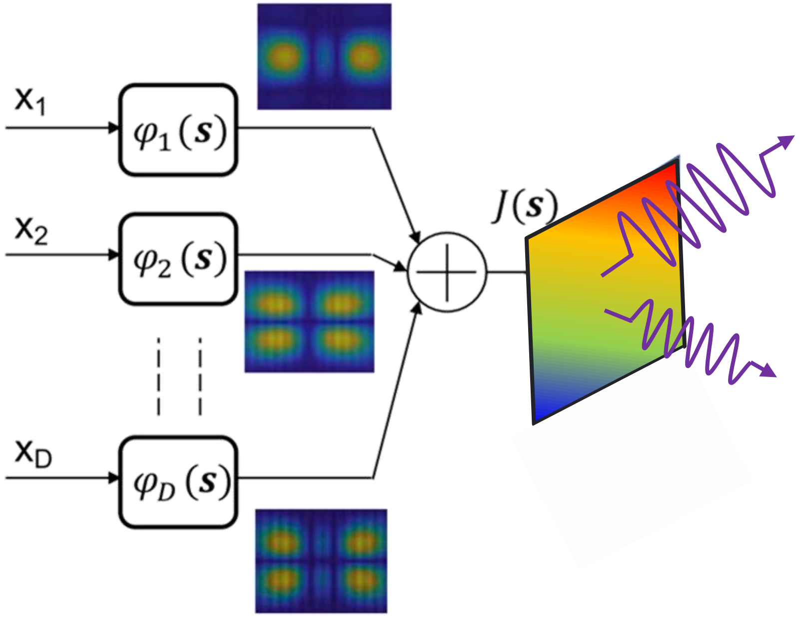

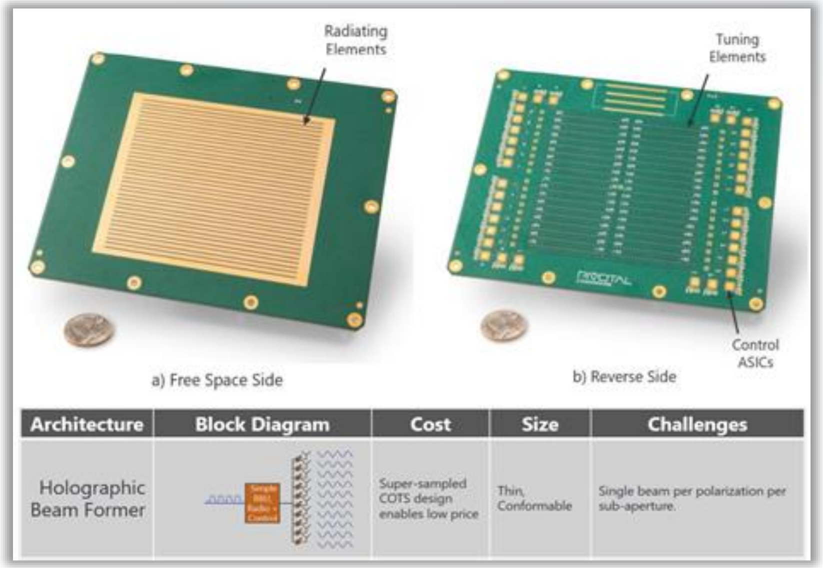

Holographic MIMO by Pivotal

A. Pizzo, T. L. Marzetta and L. Sanguinetti, "Spatially-stationary model for holographic MIMO small-scale fading," *IEEE J. Sel. Areas Commun.*, vol. 38, no. 9, pp. 1964-1979, Sep. 2020.

3.1 Hardware Implementations of H-MIMO

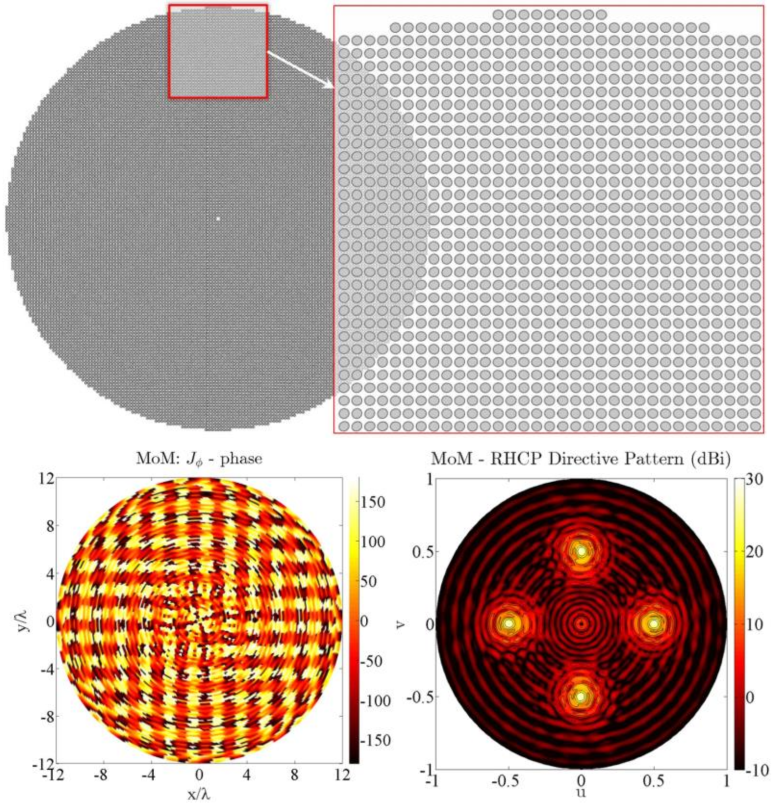

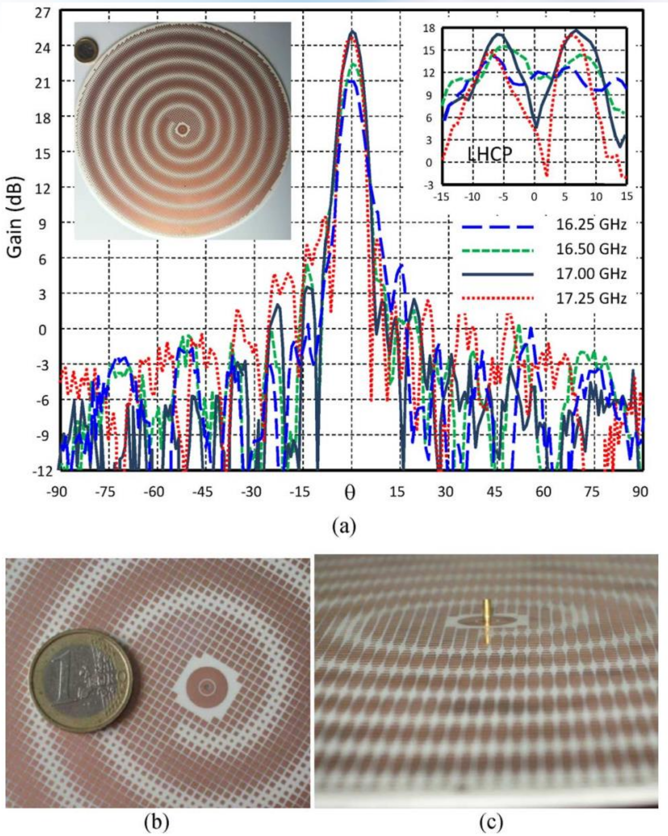

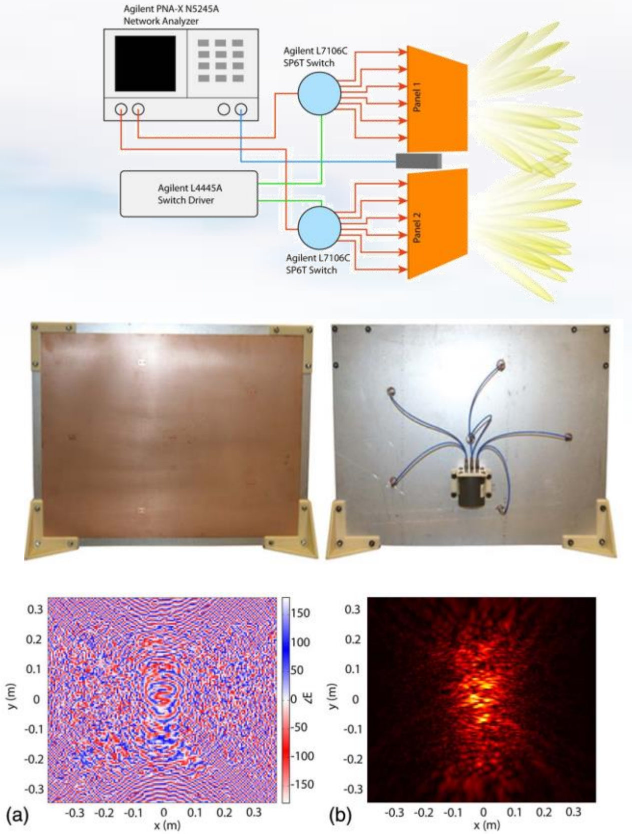

[1] D. Gonzalez-Ovejero, G. Minatti, G. Chattopadhyay, and S. Maci, "Multibeam by metasurface antennas," *IEEE Trans. Antennas Propag.*, vol. 65, no. 6, pp. 2923-2930, Jun. 2017.

[2] S. Maci, G. Minatti, M. Casaletti, and M. Bosiljevac, "Metasurfing: Addressing waves on impenetrable metasurfaces," *IEEE Antennas Wireless Propag. Lett.*, vol. 10, pp. 1499-1502, 2011.

[3] J. Hunt, J. Gollub, T. Driscoll, et al., "Metamaterial microwave holographic imaging system," *J. Opt. Soc. Am. A.*, vol. 31, no. 10, pp. 2109-2119, 2014.

3.1 Existing Typical Works of H-MIMO

- **Channel modeling**: **Modeling small-scale fading of electromagnetic channel with Gaussian random field in wavenumber domain [1]**
- **DoF analysis**: **Degrees of freedom of communication between two H-MIMO is analyzed [2]**
- **Transmission design: Wavenumber-division multiplexing (WDM) is proposed to modulate symbols on different wavenumbers for sum-rate maximization [3]**

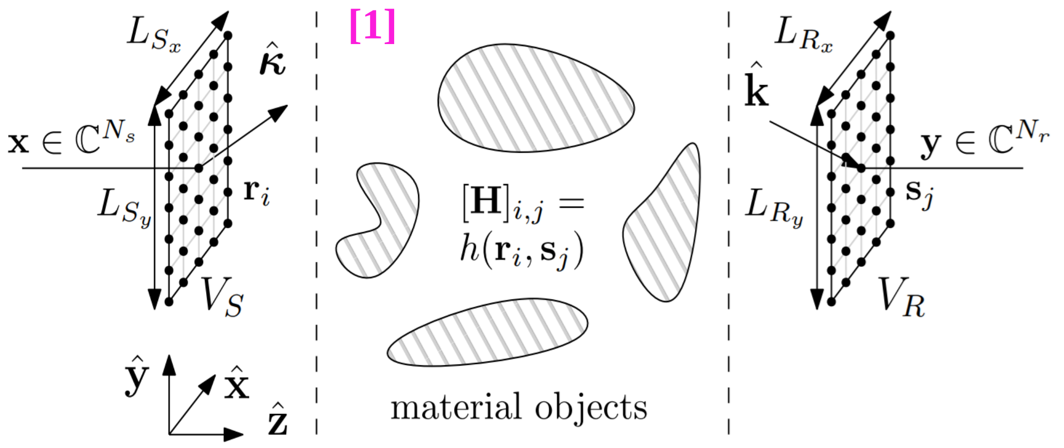

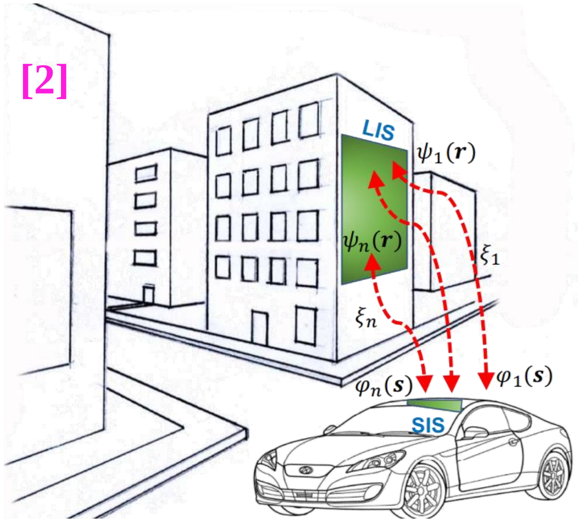

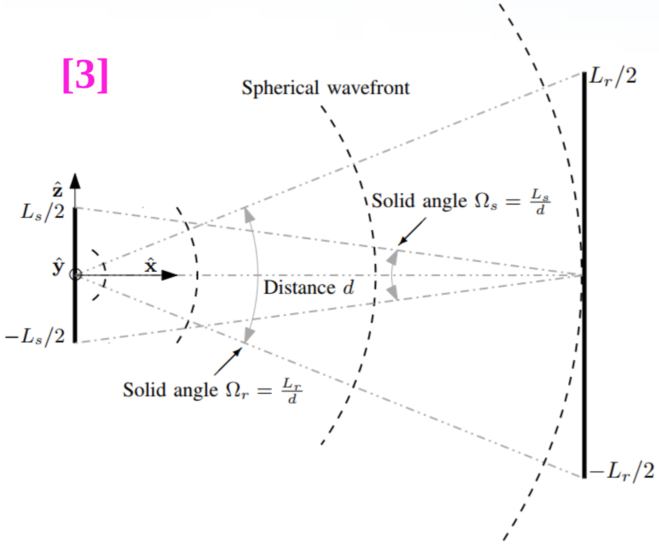

[1] A. Pizzo, T. L. Marzetta, and L. Sanguinetti, "Spatially-stationary model for holographic MIMO small-scale fading," *IEEE J. Sel. Areas Commun.*, vol. 38, no. 9, pp. 1964-1979, Sep. 2020.
[2] D. Dardari, "Communicating with large intelligent surfaces: Fundamental limits and models," *IEEE J. Sel. Areas Commun.*, vol. 38, no. 11, pp. 2526-2537, Nov. 2020.
[3] L. Sanguinetti, A. A. D'Amico, and M. Debbah, "Wavenumber-division multiplexing in line-of-sight holographic MIMO communications," *IEEE Trans. Wireless Commun.*, vol. 22, no. 4, pp. 2186-2201, Apr. 2023.

3.1 Proposed Pattern Design for H-MIMO

- **Existing methods: Use the conjugate of channel functions as the pattern**
- **Proposed method: Transform the optimization of pattern functions into their projection lengths (vector-form) in the wavenumber domain for sum-rate maximization**

Continuous-discrete transform:

$$\int_{\mathcal{S}_{\mathrm{T}}} \mathbf{G}_k(\mathbf{s})\boldsymbol{\theta}_j(\mathbf{s})\mathrm{d}\mathbf{s} = \sum_{\mathbf{n}}^{\infty} \boldsymbol{\Omega}_{k,\mathbf{n}}\mathbf{w}_{j,\mathbf{n}}$$

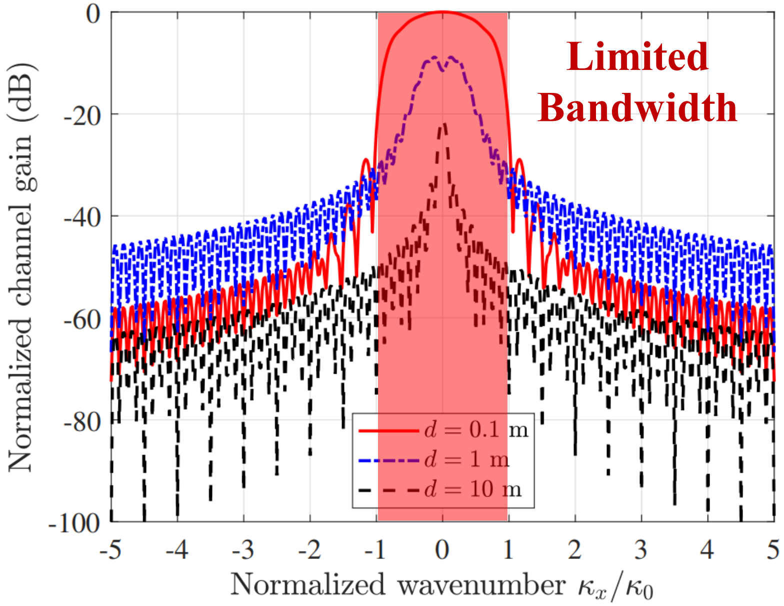

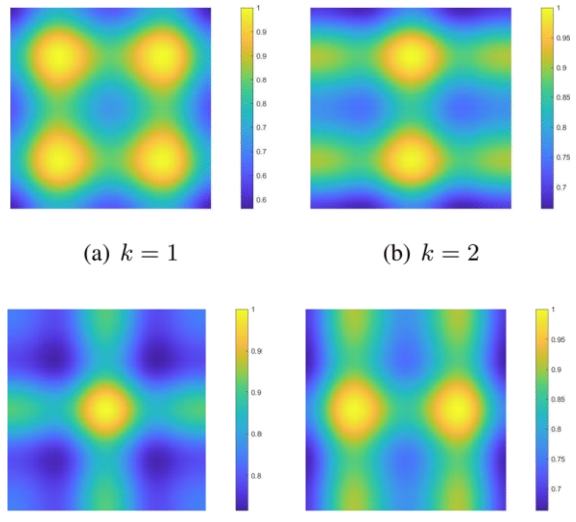
(a) $k = 1$ (b) $k = 2$ (c) $k = 3$ (d) $k = 4$

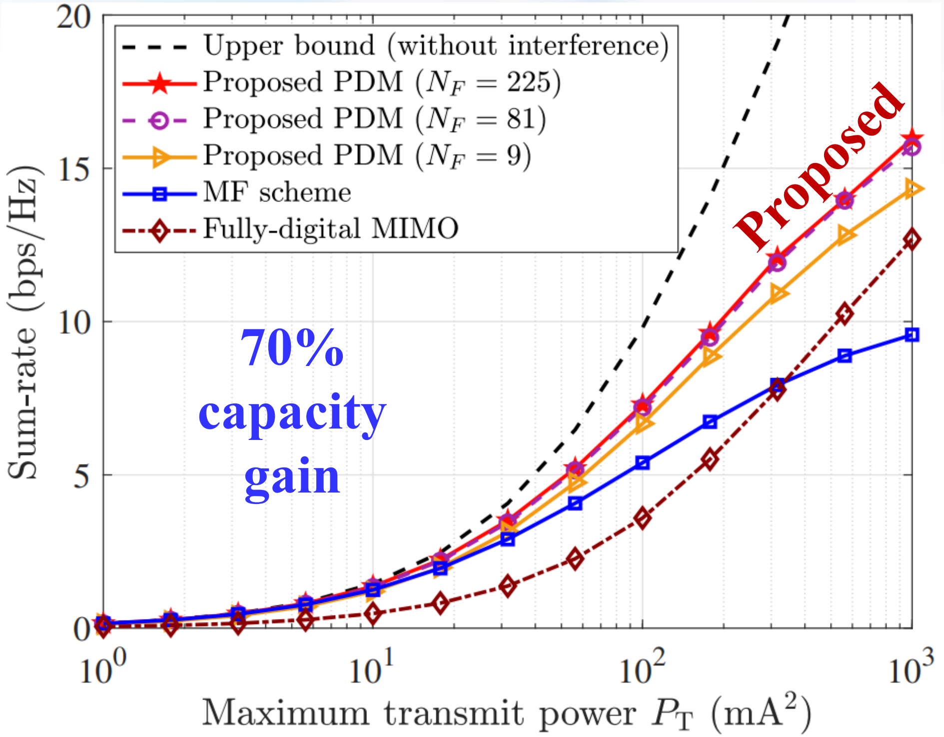

Z. Zhang and **L. Dai**, "Pattern-division multiplexing for multi-user continuous-aperture MIMO," *IEEE J. Sel. Areas Commun.*, vol. 41, no. 8, pp. 2350-2366, Aug. 2023.

Contents

3.2 Near-Field Communications for 6G

- **EM propagation can be divided into far-field and near-field regions**

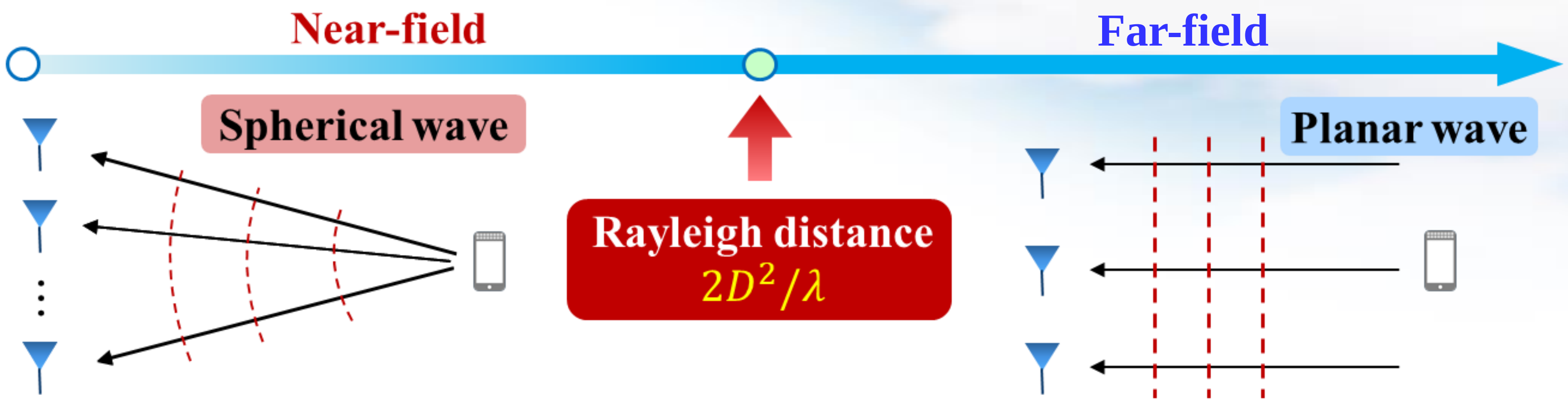

$$\phi_n^{\text{near}} = \frac{2\pi}{\lambda}\left(\sqrt{r^2 - 2ndr\theta + n^2d^2} - r\right)$$

$$\phi_n^{\text{far}} = -\frac{2\pi}{\lambda} nd\theta$$

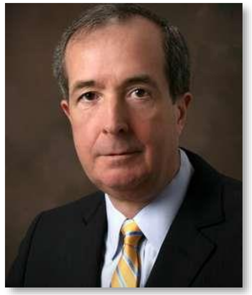

T. L. Marzetta

Table I. Rayleigh distance [m] (data from [1])

f \ D	0.1 m	0.5 m	1 m	3 m
3 GHz	0.21	5	20	180
28 GHz	1.9	47	187	/
142 GHz	9.0	237	/	/

2304 array

Evolution from massive MIMO to ELAA results in the near-field propagation

A. Pizzo, L. Sanguinetti, and T. L. Marzetta, "Fourier plane-wave series expansion for holographic MIMO communications," *IEEE Trans. Wireless Commun.*, Mar. 2022.

3.2 Far-Field Beamsteering v.s. Near-Field Beamfocusing

- **Channel model**

Far-field: $$\mathbf{h}^{\text{far}} = g^{\text{far}}\left[1, e^{-j\frac{2\pi}{\lambda}\boxed{d\theta}}, \cdots, e^{-j\frac{2\pi}{\lambda}(2N+1)d\theta}\right]^T$$

Linear phase item

Near-field: $$\mathbf{h}^{\text{near}} = \boxed{g}\left[e^{-j\frac{2\pi}{\lambda}\boxed{\phi_{-N}^{\text{near}}}}, \cdots, e^{-j\frac{2\pi}{\lambda}\phi_{N}^{\text{near}}}\right]^T$$

Non-linear phase item

Channel Gain

$$\phi_n^{\text{near}} = \frac{2\pi}{\lambda}\left(\sqrt{r^2 - 2ndr\theta + n^2d^2} - r\right)$$

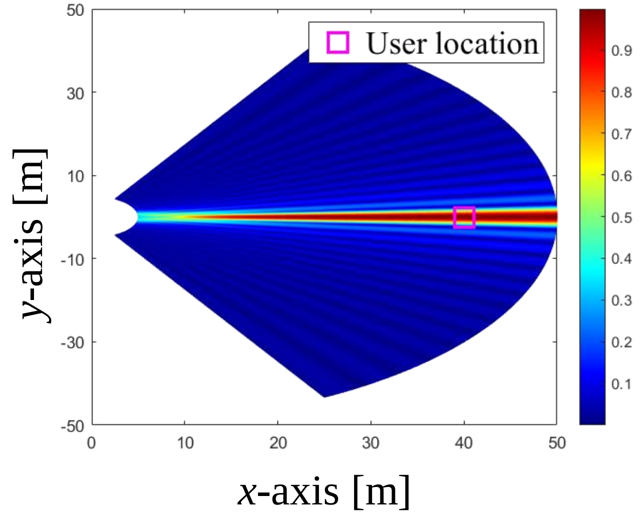

Far-field beamsteering

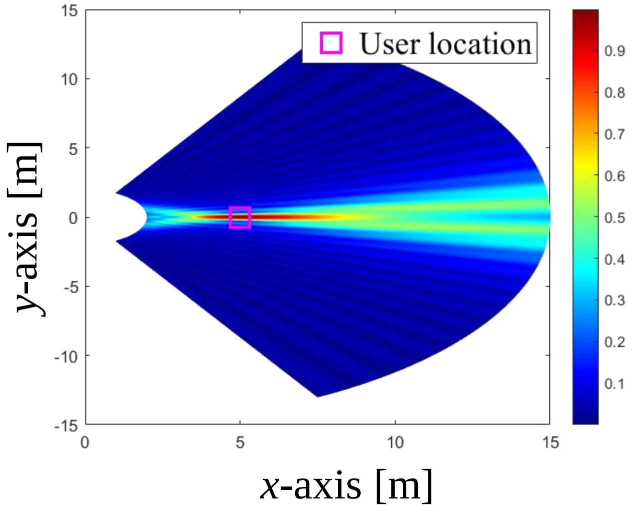

Near-field beamfocusing

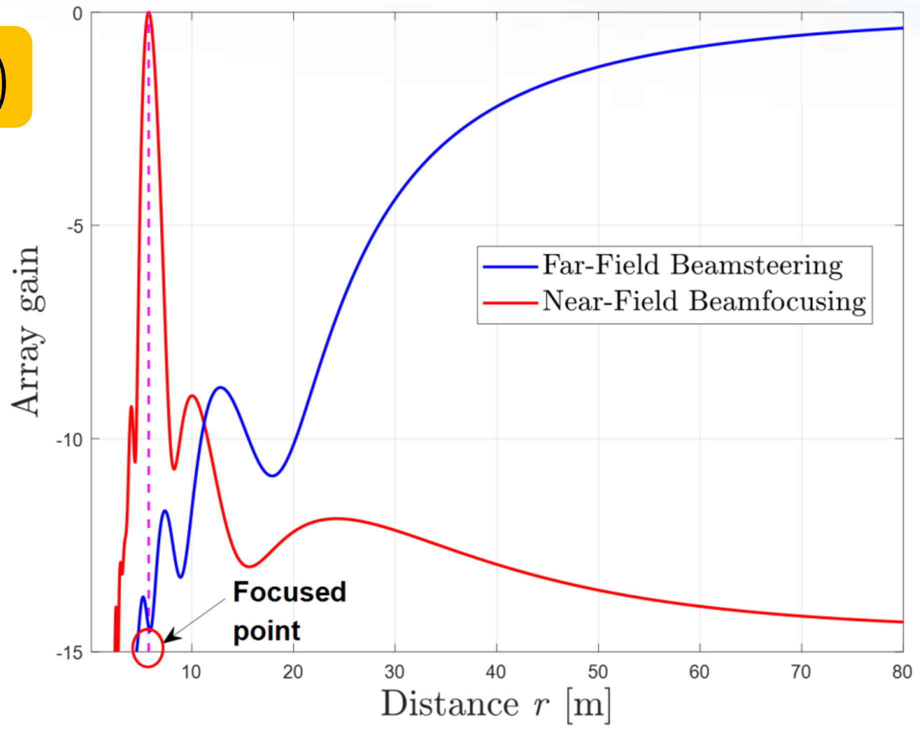

M. Cui and **L. Dai**, "Channel estimation for extremely large-scale MIMO: Far-field or near-field?," *IEEE Trans. Commun.*, vol. 70, no. 4, pp. 2663-2677, Apr. 2022.

3.2 Applications of Near-Field Communications

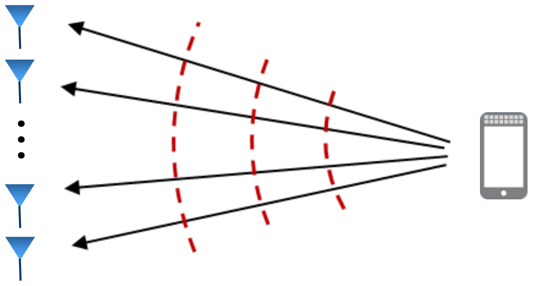

Near-Field Beamfocusing

Communications

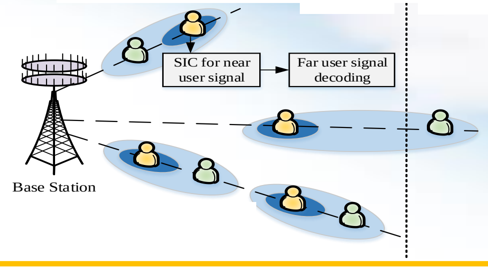

Increased capacity through signal focusing

Sensing and Localization

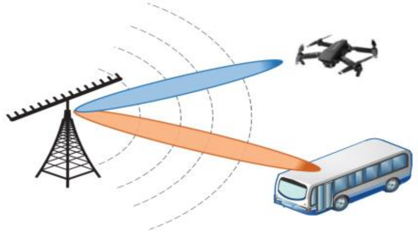

Higher accuracy through distance sensing

Wireless Power Transfer

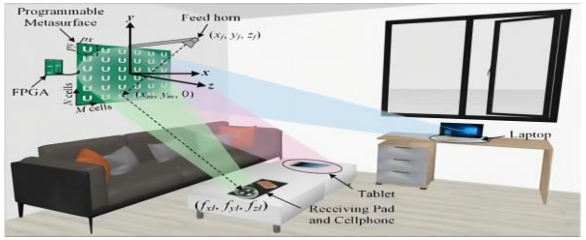

Improved efficiency through energy focusing

M. Cui, Z. Wu, Y. Lu, X. Wei, and **L. Dai**, "Near-field MIMO communications for 6G: Fundamentals, challenges, potentials, and future directions," *IEEE Commun. Mag.*, vol. 61, no. 1, pp. 40-46, Jan. 2023.

3.2 Challenge of SDMA for Far-Field Communication

- **Spatial division multiple access (SDMA) is employed by massive MIMO to multiplex data streams to different users for improving spectral efficiency**
- **In massive MIMO systems, far-field beamsteering vectors only focus on specific angles, which enables the multiple access for users at different angles**

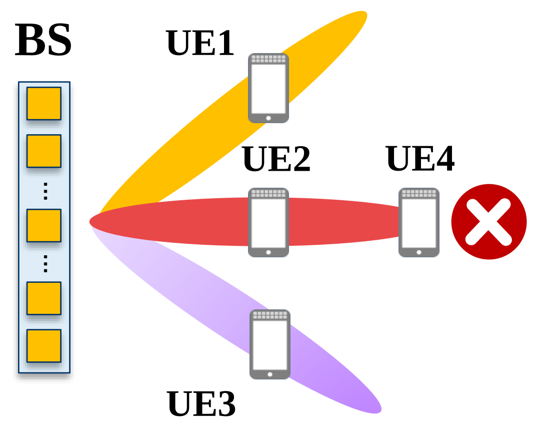

SDMA for far-field communications

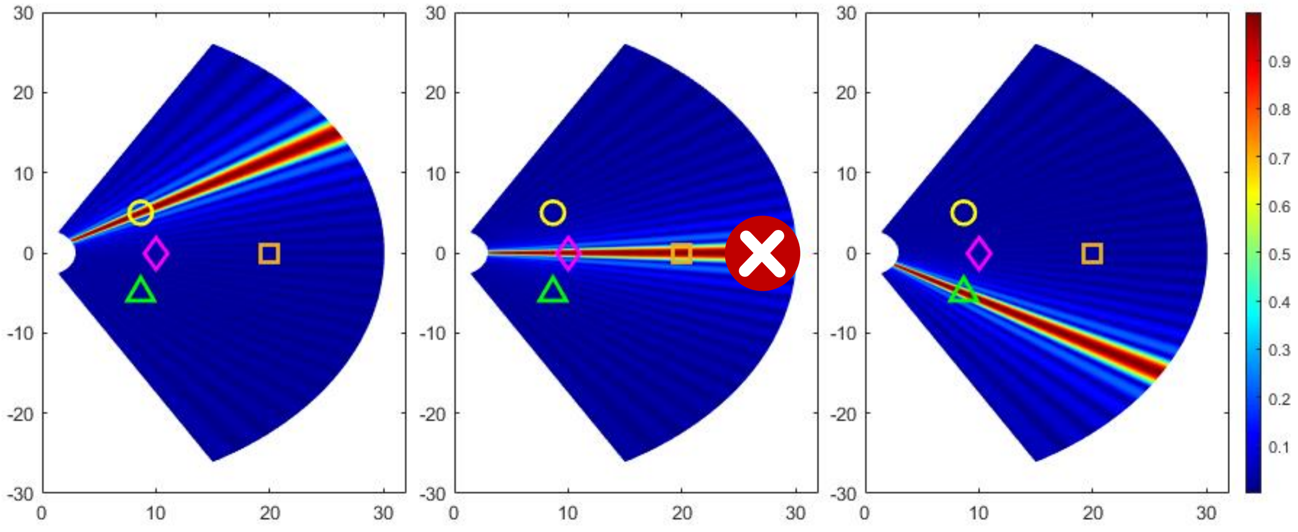

Users at the same angle cannot be simultaneously served by massive MIMO with SDMA

3.2 Mitigated Interference with Near-Field Beamfocusing

- **Far-field beamsteering vectors focus on specific spatial angle**
- **Near-field beamfocusing is capable to focus on specific location, which could be leveraged to mitigate inter-user interferences**

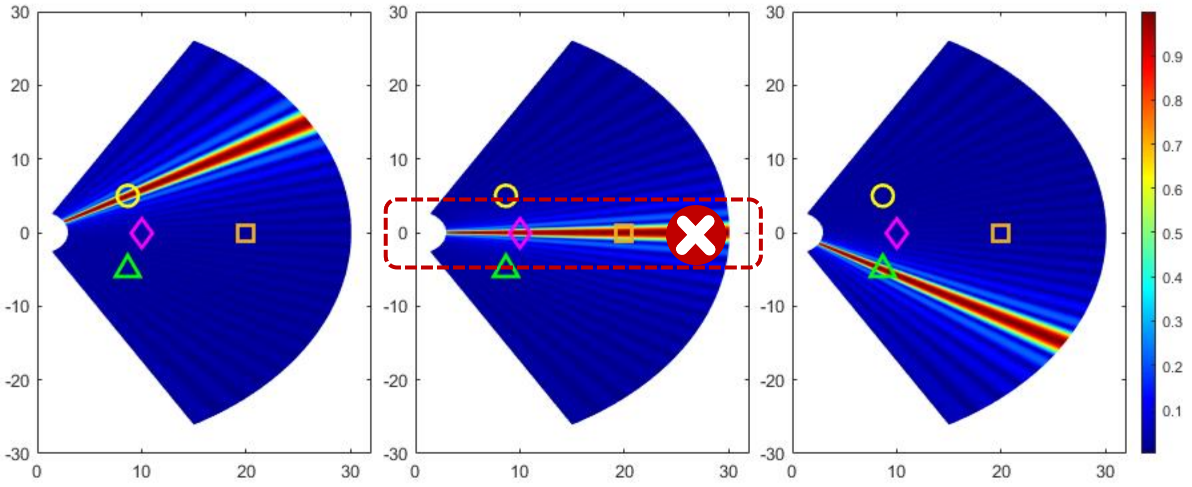

Far-field beamsteering

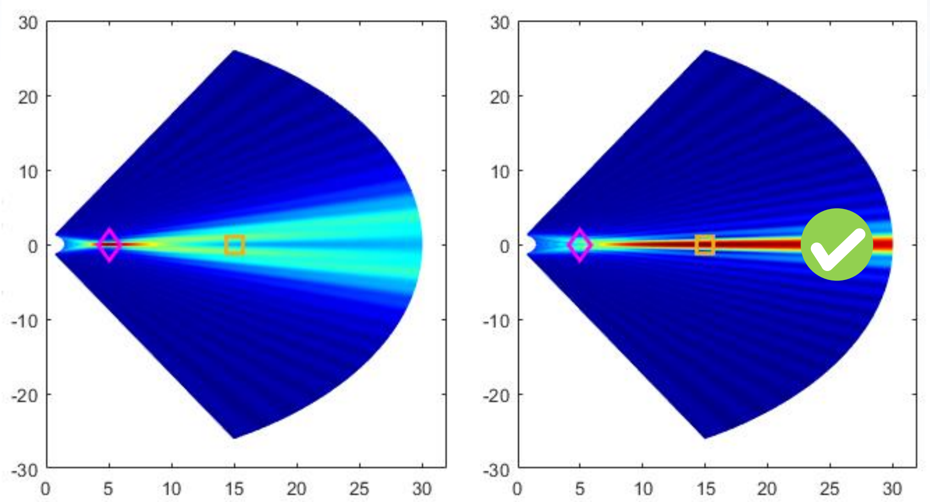

Near-field beamfocusing

Near-field beamfocusing has the potential to serve users at the same spatial angle

H. Zhang, N. Shlezinger, F. Guidi, D. Dardari, and Y. C. Eldar, "6G wireless communications: From far-field beam steering to near-field beam focusing," *IEEE Commun. Mag.*, vol. 61, no. 4, pp. 72-77, Apr. 2023.

3.2 Multiple Access for Near-Field Communications: SDMA or LDMA?

- **Far-field SDMA: Users at different angles can be served by orthogonal far-field beams**
- **Near-field location division multiple access (LDMA): Users at different locations can be simultaneously served due to property of near-field beam focusing**

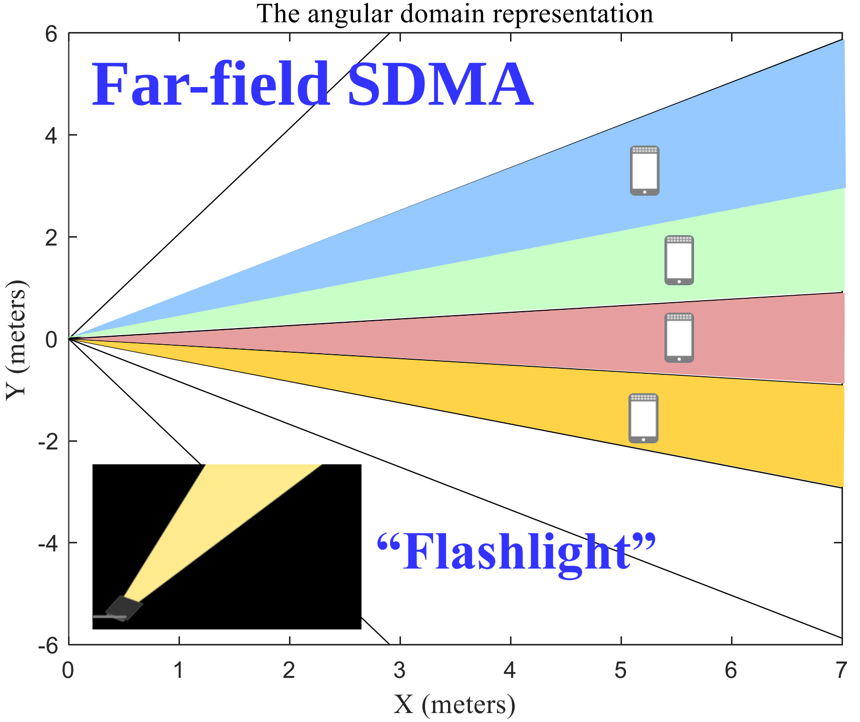

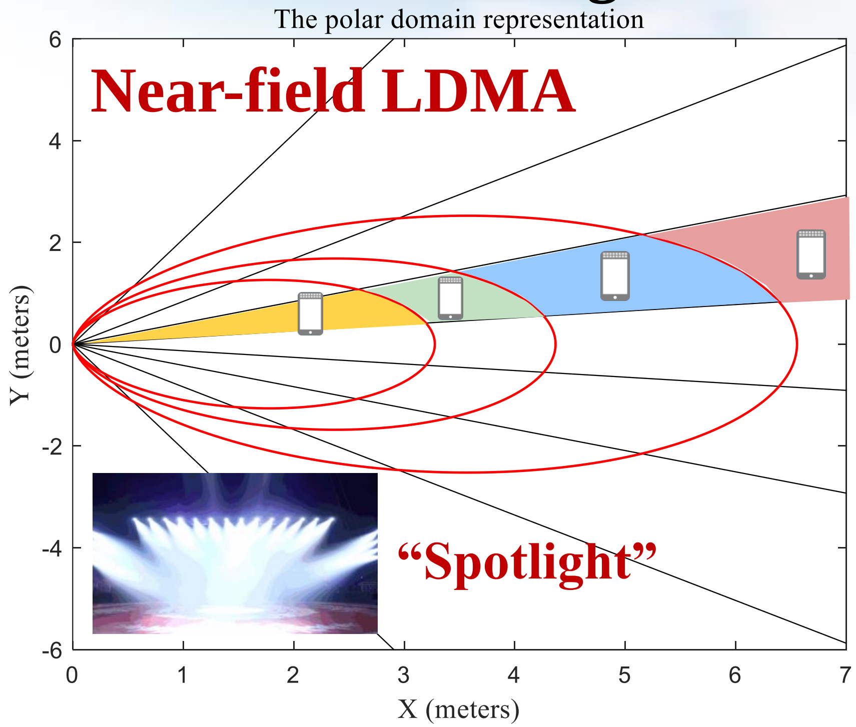

Compared with far-field SDMA, near-field LDMA provides a new possibility for capacity improvement

Z. Wu and **L. Dai**, "Multiple access for near-field communications: SDMA or LDMA? " *IEEE J. Sel. Areas Commun.*, vol. 41, no. 6, pp. 1918-1935, Jun. 2023.

3.2 Distance Domain Asymptotic Orthogonality

- **Far-field orthogonality in angular domain**

  Phase: $\phi_n^{\text{far}}(\theta) = -\frac{2\pi}{\lambda} n d\theta$

  Correlation: $f^{\text{far}} = |\mathbf{a}^H(\theta_1)\mathbf{a}(\theta_2)| = \frac{1}{N}\left|\frac{\sin(\frac{1}{2}Nkd(\sin\theta_1 - \sin\theta_2))}{\sin(\frac{1}{2}kd(\sin\theta_1 - \sin\theta_2))}\right|$

  As $N \to \infty$, interference from different angles $I^{\text{far}} \to 0$ $(\theta_1 \neq \theta_2)$

- **Lemma 2: Near-field orthogonality in distance domain**

  Phase: $\phi_n^{\text{near}}(\theta) = -\frac{2\pi}{\lambda} n d\theta + \frac{1-\theta^2}{\lambda r}\pi n^2 d^2$

  Correlation: $f^{\text{near}} = |\mathbf{a}^H(\theta, r_1)\mathbf{a}(\theta, r_2)| \approx |G(\beta)| = \left|\frac{C(\beta)+jS(\beta)}{\beta}\right|$

  where $\beta = \sqrt{\frac{N^2 d^2(1-\theta^2)}{2\lambda}\left|\frac{1}{r} - \frac{1}{\bar{r}}\right|}$

  As $N \to \infty$, interference from different distances $I^{\text{near}} \to 0$ $(\forall\theta, r_1 \neq r_2)$

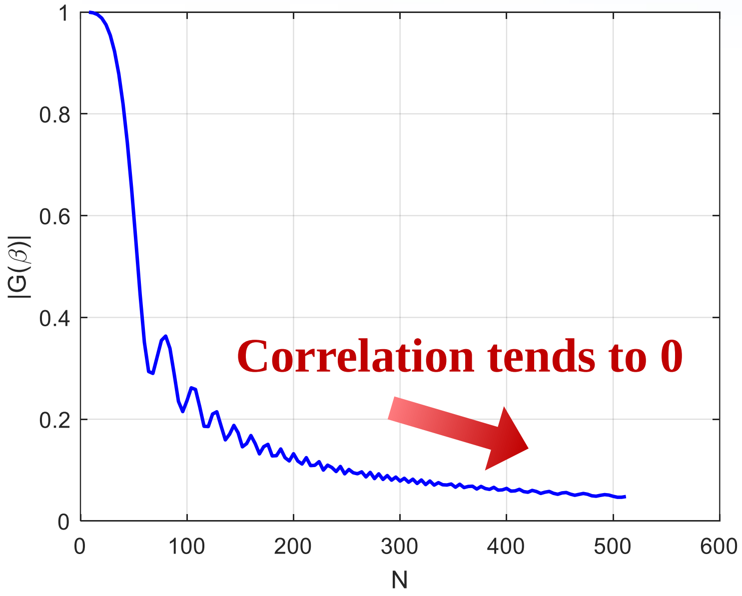

Correlation with increasing antennas

Z. Wu and **L. Dai**, "Multiple access for near-field communications: SDMA or LDMA?" *IEEE J. Sel. Areas Commun.*, vol. 41, no. 6, pp. 1918-1935, Jun. 2023.

3.2 Simulation Results for LDMA

- **Scenario 1: Users are linearly distributed along the same direction**
- **Scenario 2: Users are uniformly distributed within a cell**

BS Antennas	UE Antennas	Frequency	UE Numbers	Elevation/ Azimuth Angle Range	Distance Range
256	1	30 GHz	20	$[-\pi/2, \pi/2]$	[4m, 100m]

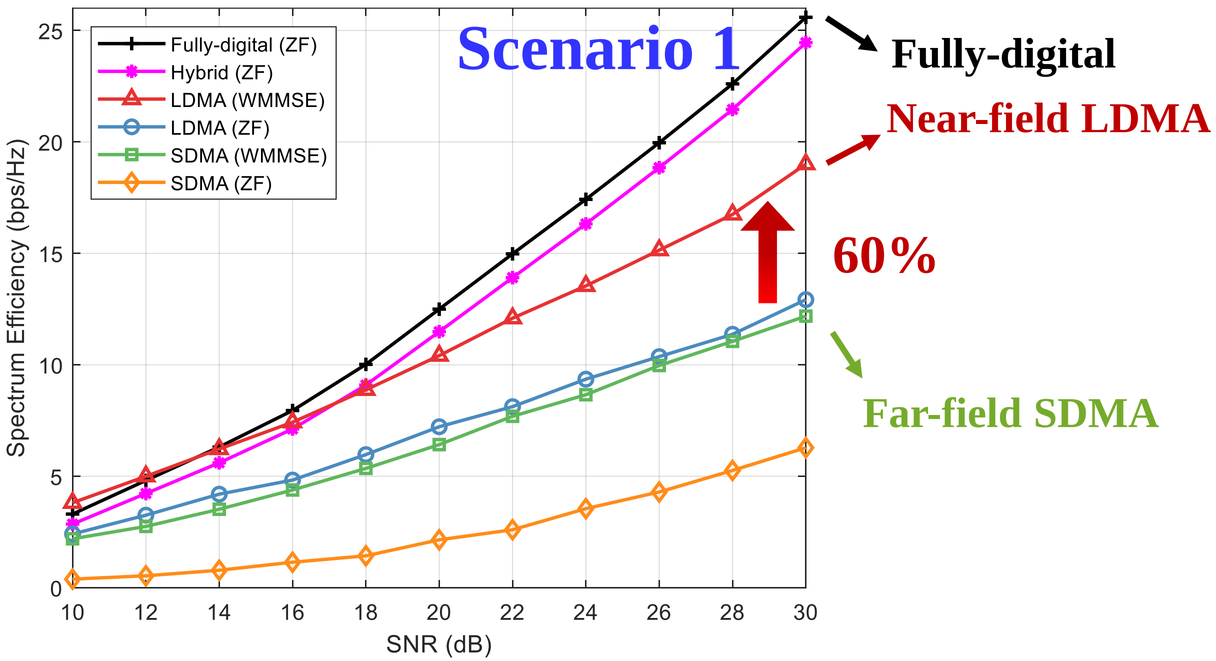

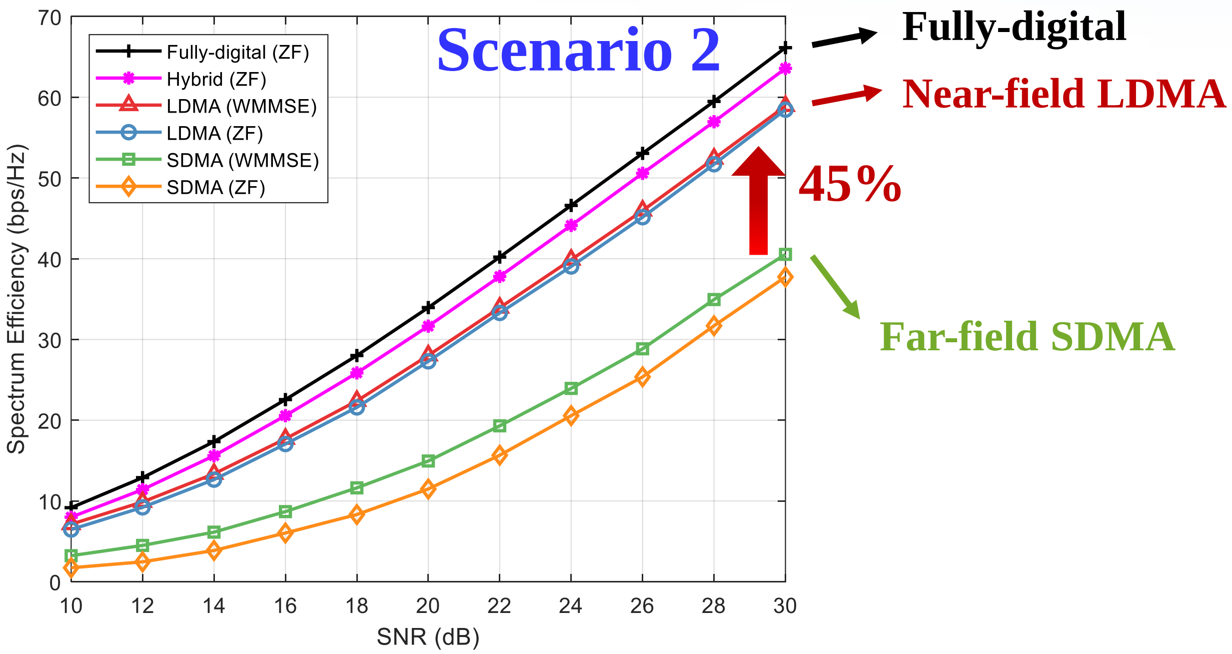

Z. Wu and **L. Dai**, "Multiple access for near-field communications: SDMA or LDMA? " *IEEE J. Sel. Areas Commun.*, vol. 41, no. 6, pp. 1918-1935, Jun. 2023.

Contents

3.3 Mutual Coupling and Superdirective Antennas

- **From avoiding mutual coupling to utilizing mutual coupling**
  - **Mutual coupling between closely-placed antennas (especially for antenna spacing less than $\lambda/2$)**
  - **Directivity of linear array can be greatly improved when antenna spacing tends to 0**
  - **Challenge: The radiation efficiency will be decreased**

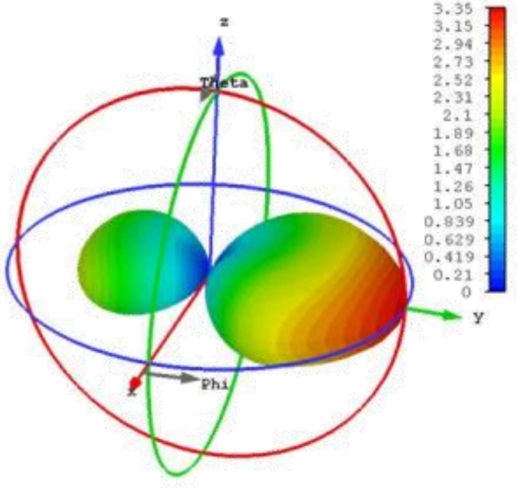

(a) Directivity based on traditional model

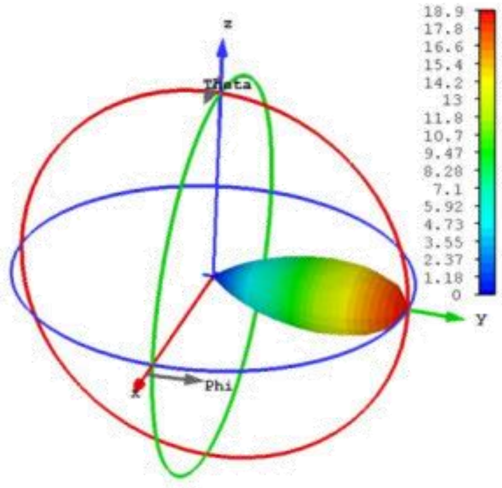

(b) Directivity based on coupling matrix model

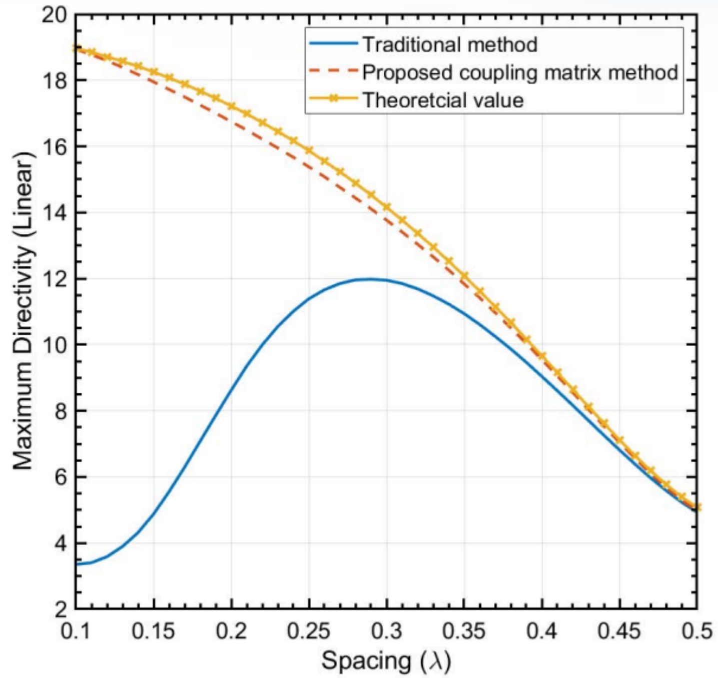

[1] T. L. Marzetta, "Super-directive antenna arrays: Fundamentals and new perspectives," in *Proc. 53rd Asilomar Conference on Signals, Systems, and Computers*, 2019, pp. 1–4
[2] L. Han, H. Yin, and T. L. Marzetta, "Coupling matrix-based beamforming for superdirective antenna arrays," in *Proc. IEEE Int. Conf. Commun. (ICC),* May 2022, pp. 5159–5164.

3.4 Orbital Angular Momentum

- **From massive MIMO to massive modes**
  - **Orbital angular momentum (OAM) has infinite number of modes (states) theoretically**
  - **Holographic MIMO surfaces are powerful in transferring the OAM property**

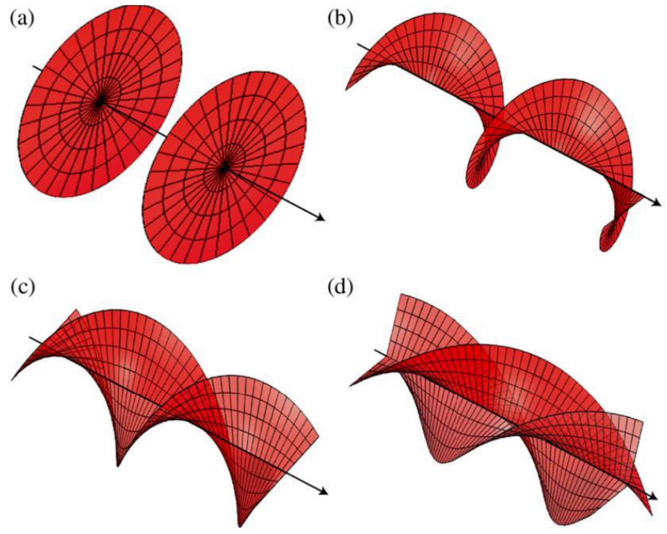

Helical phase fronts for (a) $\ell = 0$, (b) $\ell = 1$, (c) $\ell = 2$, and (d) $\ell = 3$.

OAM modes

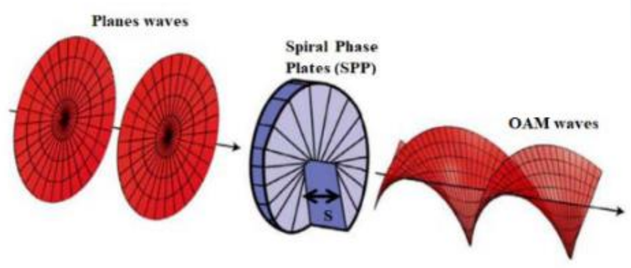

OAM wave generation with Spiral phase plate (SPP)

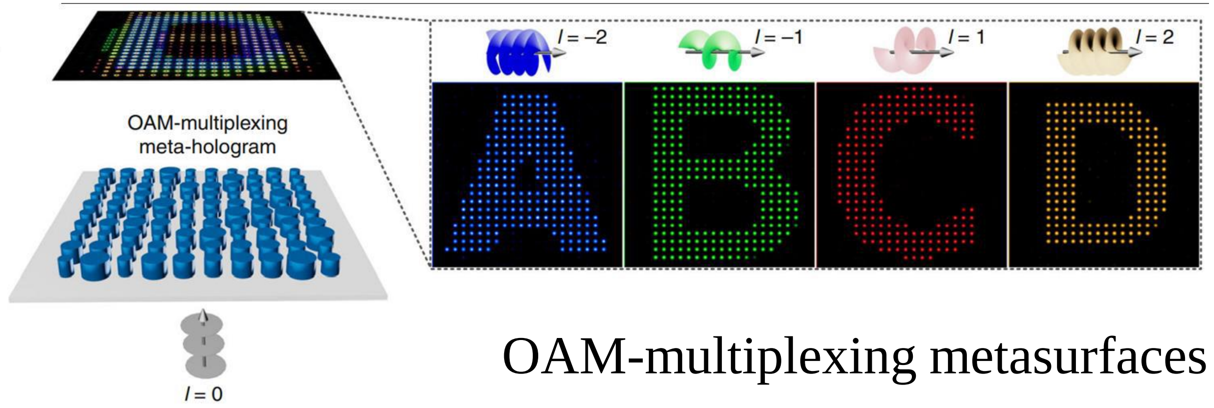

OAM-multiplexing metasurfaces

[1] Y. Yan, G. Xie, M. Lavery, H. Huang, et. al, "High-capacity millimetre-wave communications with orbital angular momentum multiplexing," *Nature Communications*, vol. 5, Sep. 2014.
[2] A. E. Willner, H. Huang, Y. Yan, Y. Ren, N. Ahmed, et. al., "Optical communications using orbital angular momentum beams," *Adv. Optics and Photonics,* vol. 7, no. 1, pp. 66-106, Jan. 2015.

3.5 3D Antenna Array

- **Deploy multiple antenna array layers to explore the third spatial dimension**
  - **The DoF and capacity constraints of traditional holographic MIMO systems can be surpassed by adopting such a 3D antenna array**

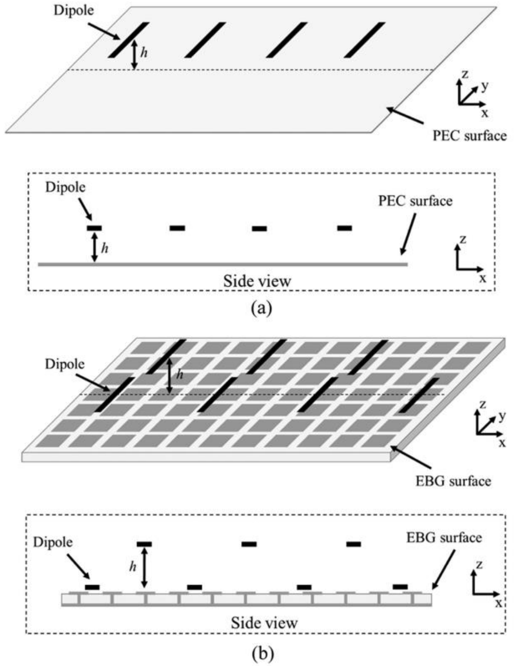

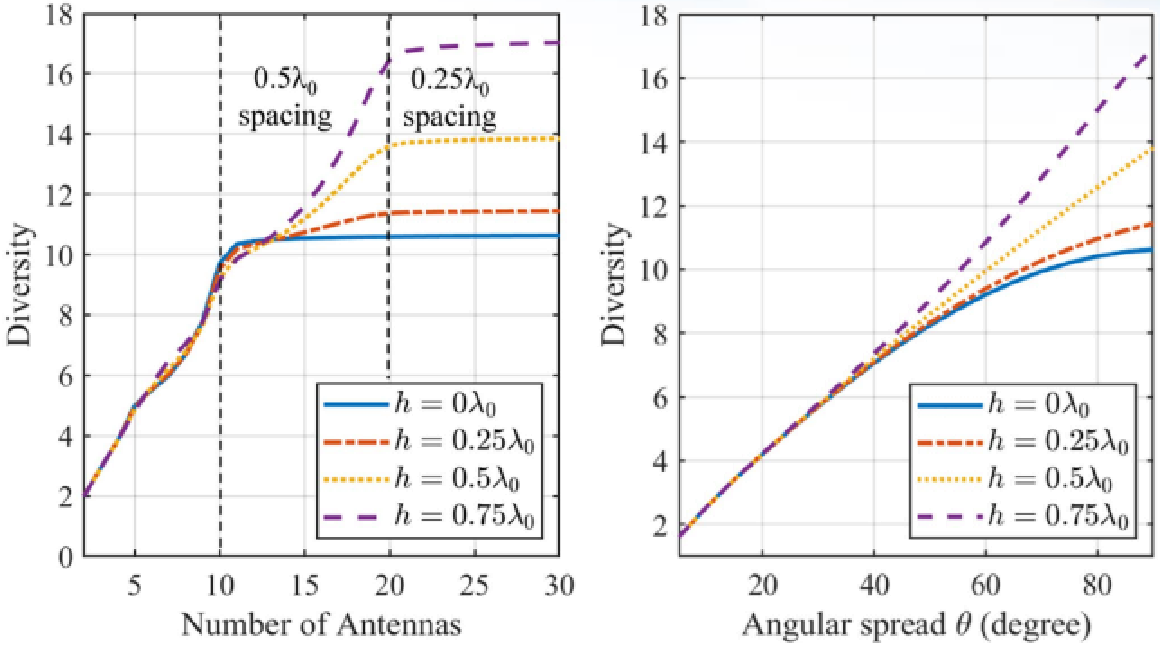

(a) (b)

[1] S. S. A. Yuan, J. Wu, H. Xu, T. Wang, D. Li, X. Chen, C. Huang, S. Sun, S. Zheng, X. Zhang, E. Li, and W. E. I. Sha, "Breaking the degrees-of-freedom limit of holographic MIMO communications: A 3-D antenna array topology," *IEEE Trans. Veh. Technol.*, vol. 73, no. 8, pp. 11276-11288, Aug. 2024.
[2] R. Ji, C. Huang, X. Chen, W. Sha, Z. Zhang, J. Yang, K. Yang, C. Yuen, and M. Debbah. "Exploring Hannan limitation for 3D antenna array," *arXiv preprint arXiv:2409.01566*, Sep. 2024.

Contents

4.1 Channel Estimation

- **Signal recovery: Get transmitted X from received y by knowing channel h**
- **Channel estimation: Get channel h from received pilots y by knowing X**

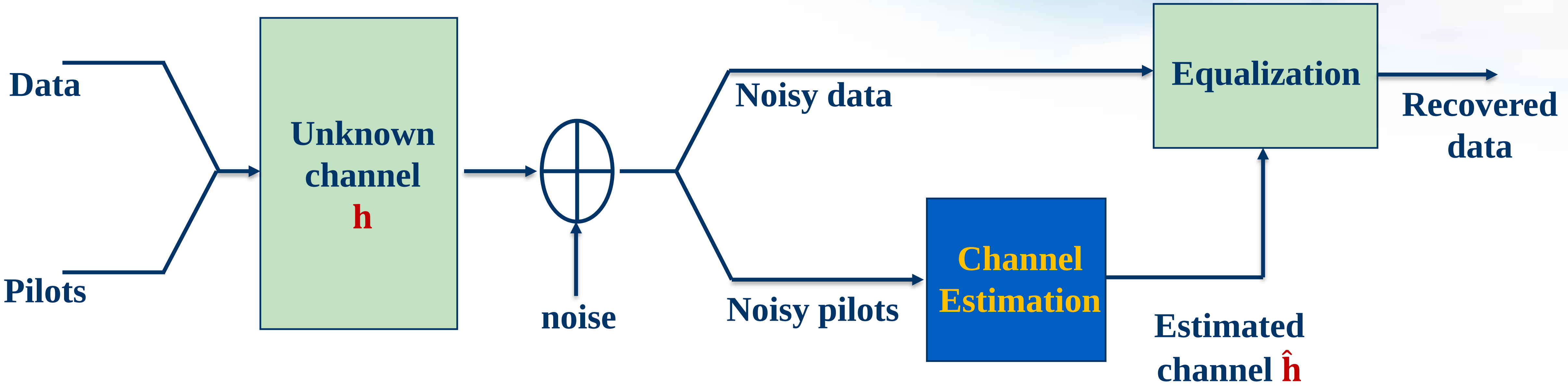

System Model

$$\mathbf{y} = \mathbf{X}\mathbf{h} + \mathbf{n}$$

4.1 Existing Channel Estimators

	Least Square (LS)	Minimum Mean Square Error (MMSE)	Compressed Sensing
Loss Functions	$J(\hat{\mathbf{h}}_{\mathrm{LS}}) = \|\mathbf{y} - \mathbf{X}\hat{\mathbf{h}}_{\mathrm{LS}}\|^2$	$J(\hat{\mathbf{h}}_{\mathrm{MMSE}}) = E\{\|\mathbf{h} - \hat{\mathbf{h}}_{\mathrm{MMSE}}\|^2\}$	$J(\hat{\mathbf{h}}_{\mathrm{CS}}) = \|\mathbf{y} - \mathbf{X}\hat{\mathbf{h}}_{\mathrm{CS}}\|^2 + \beta\|\hat{\mathbf{h}}_{\mathrm{CS}}\|_0$
Closed-form	$\hat{\mathbf{h}}_{\mathrm{LS}} = (\mathbf{X}^H\mathbf{X})^{-1}\mathbf{X}^H\mathbf{y}$	$\hat{\mathbf{h}}_{\mathrm{MMSE}} = \mathbf{R}_{\mathbf{h}}\left(\mathbf{R}_{\mathbf{h}} + \frac{1}{\gamma}\mathbf{I}\right)^{-1}\mathbf{X}^{-1}\mathbf{y}$	No closed-form solution
Need noise statistics	No	Yes	No
Need channel statistics	No	Yes	No
Advantages	Low-complexity and applicable to any channels	High estimation accuracy with strong denoising capability	Low pilot overhead with some denoising capability
Disadvantages	Sensitive to noise	Need extra statistical information of channel and noise, high complexity	Only applicable to sparse channels

MMSE estimators are widely applied in real-world systems, but it requires channel statistics

4.1 When EIT Meets Channel Estimation

- **Traditional MMSE needs channel statistics**
  - **In classical MMSE, $\mathbf{R}_{\mathbf{h}}$ represents mathematical second-order statistics**
  - **In EIT-MMSE, $\mathbf{R}_{\mathbf{h}}$ represents EM statistics calculated from EIT analysis**

Classical statistics

$$\hat{\mathbf{R}}_{\mathbf{h}} = \frac{1}{T}\sum_t \mathbf{h}_t \mathbf{h}_t^{\mathsf{H}}$$

$\mathbf{R}_{\mathbf{h}}$

$\mathbf{y} = \mathbf{X}\mathbf{h} + \mathbf{n}$

Pilot observation $\mathbf{y}_{\text{obs}}$

MMSE Estimator

Channel estimates

$$\hat{\mathbf{h}}^{\text{MMSE}} = \mathbf{R}_{\mathbf{h}} \left(\mathbf{R}_{\mathbf{h}} + \frac{1}{\gamma}\mathbf{I} \right)^{-1} \mathbf{X}^{-1}\mathbf{y}$$

$\mathbf{R}_{\mathbf{h}}$

EM statistics

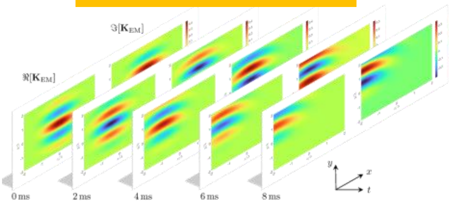

J. Zhu, Z. Wan, **L. Dai**, and T. J. Cui, "Electromagnetic information theory-based statistical channel model for improved channel estimation," submitted to *IEEE Trans. Inf. Theory*, major revision, Feb. 2024.

4.1 Construct EM Correlation Function (EMCF)

- **Apply stochastic integral to Green's function and get EM correlation function (EMCF)**
- **Parameter $\mu \in \mathbb{R}^3$ represents concentration, reflecting the direction of EM incidence**

Green's function

$$\mathbf{G}(\mathbf{x},\mathbf{x}') = \frac{e^{ik_0\|\mathbf{x}-\mathbf{x}'\|}}{4\pi\|\mathbf{x}-\mathbf{x}'\|}\left(\mathbf{I}-\hat{\boldsymbol{\kappa}}\hat{\boldsymbol{\kappa}}^{\mathsf{T}}\right)$$

Stochastic integral

$$\mathbf{E}(\mathbf{x}) = \int_{S^2} \nu^{1/2}(\hat{\boldsymbol{\kappa}}) e^{ik_0\hat{\boldsymbol{\kappa}}\cdot\mathbf{x}}\left(\mathbf{I}-\hat{\boldsymbol{\kappa}}\hat{\boldsymbol{\kappa}}^{\mathsf{T}}\right)\cdot \mathrm{d}\mathbf{W}(\hat{\boldsymbol{\kappa}})$$

EMCF **EM Polarization** **EM Phase**

$$K_{\mathrm{EM}}(\mathbf{x},\mathbf{x}'|\boldsymbol{\mu}) \propto \int_{S^2}\left(\mathbf{I}-\widehat{\boldsymbol{\kappa}}\widehat{\boldsymbol{\kappa}}^{\mathrm{T}}\right)e^{ik_0\widehat{\boldsymbol{\kappa}}\cdot(\mathbf{x}-\mathbf{x}')}\nu(\widehat{\boldsymbol{\kappa}})\mathrm{d}S,$$

Angular weight

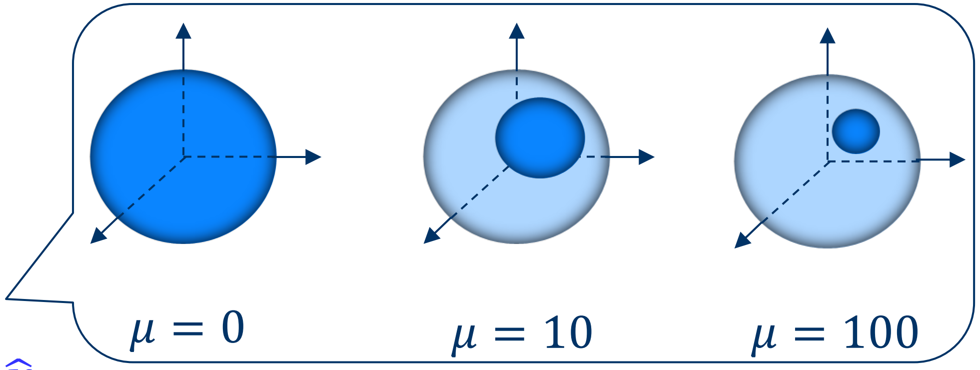

$\nu(\widehat{\boldsymbol{\kappa}}) = e^{\boldsymbol{\mu}\cdot\widehat{\boldsymbol{\kappa}}}$ **: Spherical von Mises-Fisher distribution**

EM propagation law is encapsulated in EMCF

4.1 Closed-form EMCF and Its Properties

- **EMCF encapsulates EM propagation law and enjoys nice analytical properties**
  - **EMCF includes propagation properties like concentration μ, polarization, phase, Doppler effects**
  - **EMCF is complex analytic w.r.t. μ, which facilitates further theoretical analysis**

EMCF Definition

$$\mathbf{K}_{\mathrm{EM}} \propto \frac{1}{\int_{S^2} \nu(\hat{\boldsymbol{\kappa}})\mathrm{d}S} \int_{\hat{\boldsymbol{\kappa}}\in S^2} (\mathbf{I} - \hat{\boldsymbol{\kappa}}\hat{\boldsymbol{\kappa}}^{\mathsf{T}}) e^{\mathrm{i}k_0\hat{\boldsymbol{\kappa}}\cdot(\mathbf{x}-\mathbf{x}')} \nu(\hat{\boldsymbol{\kappa}})\mathrm{d}S$$

EMCF Space-time Distribution:

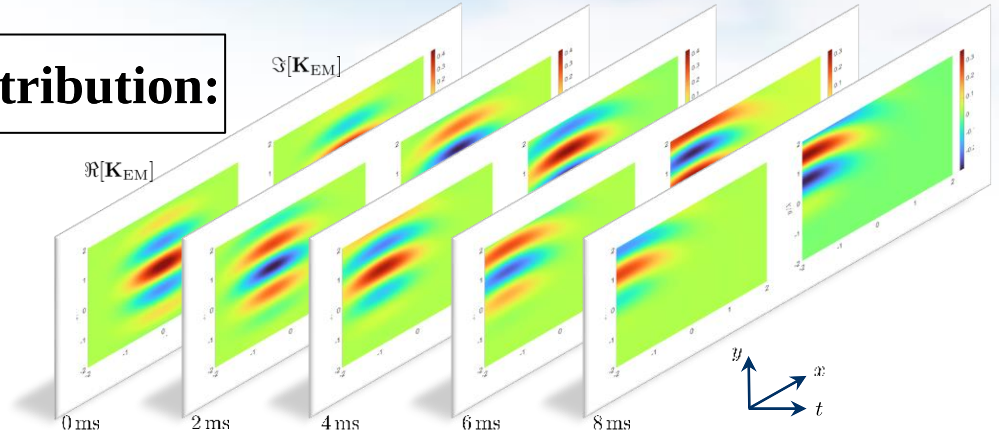

Thm 4.1.1 Assume that the incident EM wave is distributed in the angular domain according to the von Mises-Fisher distribution $f(\hat{\boldsymbol{\kappa}}|\boldsymbol{\mu}) = e^{\hat{\boldsymbol{\kappa}}\cdot\boldsymbol{\mu}}/C(\|\boldsymbol{\mu}\|)$. Then the receiver correlation function is expressed as

$$\mathbf{K}_{\mathrm{EM}}(\mathbf{x},\mathbf{x}'|\boldsymbol{\mu},\sigma^2) := \mathbb{E}\left\{\mathbf{E}(\mathbf{x})\mathbf{E}(\mathbf{x}')^{\mathsf{H}}\right\} = \frac{\sigma^2}{C(\|\boldsymbol{\mu}\|)}\boldsymbol{\Sigma}(k_0\mathbf{z}) \in \mathbb{C}^{3\times 3},$$

where $\boldsymbol{\Sigma}(\mathbf{w}) := \frac{1}{8}(f_0+f_2)\mathbf{I}_3 + \frac{1}{8}(f_0-3f_2)\hat{\mathbf{w}}\hat{\mathbf{w}}^{\mathsf{T}}$, $\mathbf{w} := k_0\mathbf{z} = k_0(\mathbf{x}-\mathbf{x}') - \mathrm{i}\boldsymbol{\mu} \in \mathbb{C}^3,\ f_n(\beta) = \int_{-1}^{1} x^n e^{\mathrm{i}\beta x}\mathrm{d}x.$

4.1 Parameter Learning

- **How to determine the EMCF parameter μ? Learn from the observed data**
  - **EMCF parameter learning: Tune the concentration parameter μ to fit the actual communication environment**

Propagation environment fitting

$$\text{find best} \quad \boldsymbol{\mu}$$
$$\text{s.t.} \quad \mathbf{K}_{\mathrm{EM}}(\mathbf{x};\mathbf{x}'|\boldsymbol{\mu}) \ \text{fits} \ \mathbf{y}_{\mathrm{obs}}$$

Maximum Likelihood

Optimization problem

$$\begin{aligned}\hat{\boldsymbol{\mu}} &= \underset{\boldsymbol{\mu}\in\mathsf{F}}{\operatorname{argmax}}\ \ell(\boldsymbol{\mu}|\mathbf{y}_{\mathrm{obs}}) \\ &= \underset{\boldsymbol{\mu}\in\mathsf{F}}{\operatorname{argmax}}\ \big(\underbrace{-\mathbf{y}_{\mathrm{obs}}^{\mathsf{H}}\mathbf{K}_{\mathbf{y}}^{-1}(\boldsymbol{\mu})\mathbf{y}_{\mathrm{obs}}}_{\text{Data fitness}} \underbrace{-\log\det \mathbf{K}_{\mathbf{y}}(\boldsymbol{\mu})}_{\text{Model Complexity}}\big)\end{aligned}$$

Thm 4.1.2 The derivatives of EMCF $\mathbf{K}_{\mathrm{EM}}(\mathbf{x},\mathbf{x}'|\boldsymbol{\mu},\sigma^2)$ w.r.t. $\boldsymbol{\mu}$ and σ^2 are

$$\frac{\partial \mathbf{K}_{\mathrm{EM}}}{\partial \boldsymbol{\mu}(k)} = -\frac{\sigma^2}{C(\mu)}\left[\mathrm{i}\frac{\partial \boldsymbol{\Sigma}(\mathbf{w})}{\partial \mathbf{w}(k)} + \frac{C'(\mu)\boldsymbol{\mu}(k)}{C(\mu)\mu}\boldsymbol{\Sigma}(\mathbf{w})\right] \ \text{and} \ \frac{\partial \mathbf{K}_{\mathrm{EM}}}{\partial(\sigma^2)} = \frac{1}{C(\mu)}\boldsymbol{\Sigma}(\mathbf{w}),$$

where $$\frac{\partial \boldsymbol{\Sigma}(\mathbf{w})}{\partial \mathbf{w}(k)} = \frac{1}{8}\left[\mathrm{i}(f_1+f_3)\hat{\mathbf{w}}(k)\mathbf{I}_3 + \mathrm{i}(f_1-3f_3)\hat{\mathbf{w}}(k)\hat{\mathbf{w}}\hat{\mathbf{w}}^{\mathsf{T}} + (f_0-3f_2)(\partial_k\hat{\mathbf{w}}\cdot\hat{\mathbf{w}}^{\mathsf{T}} + \hat{\mathbf{w}}\cdot\partial_k\hat{\mathbf{w}}^{\mathsf{T}})\right].$$

Apply gradient ascent to the EMCF likelihood function for parameter learning

4.1 EIT-Inspired Channel Estimator

- **Extract EM statistical information from EMCF, improving the performance of classical LMMSE channel estimator**

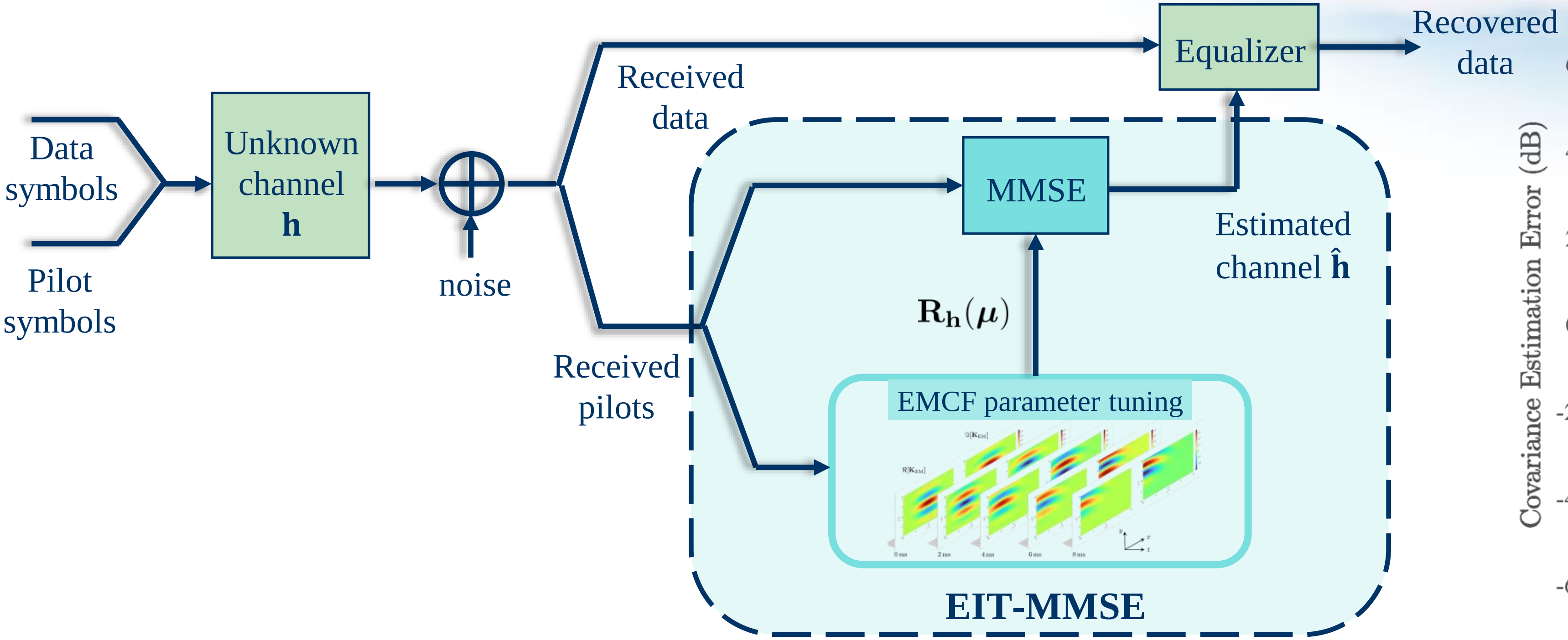

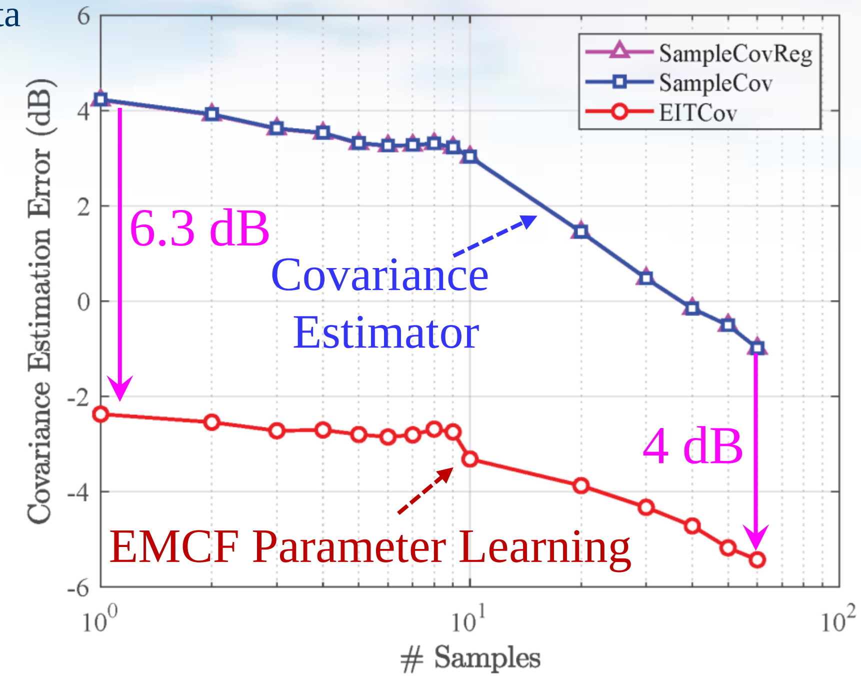

EIT-MMSE utilizes EM prior to compute more accurate channel correlation

J. Zhu, Z. Wan, **L. Dai**, and T. J. Cui, "Electromagnetic information theory-based statistical channel model for improved channel estimation," submitted to *IEEE Trans. Inf. Theory*, major revision, Feb. 2024.

4.1 Simulation Results

- **Derive EMCF from EIT to obtain the EIT-MMSE channel estimator**
- **EIT-MMSE channel estimator achieves better NMSE performance**

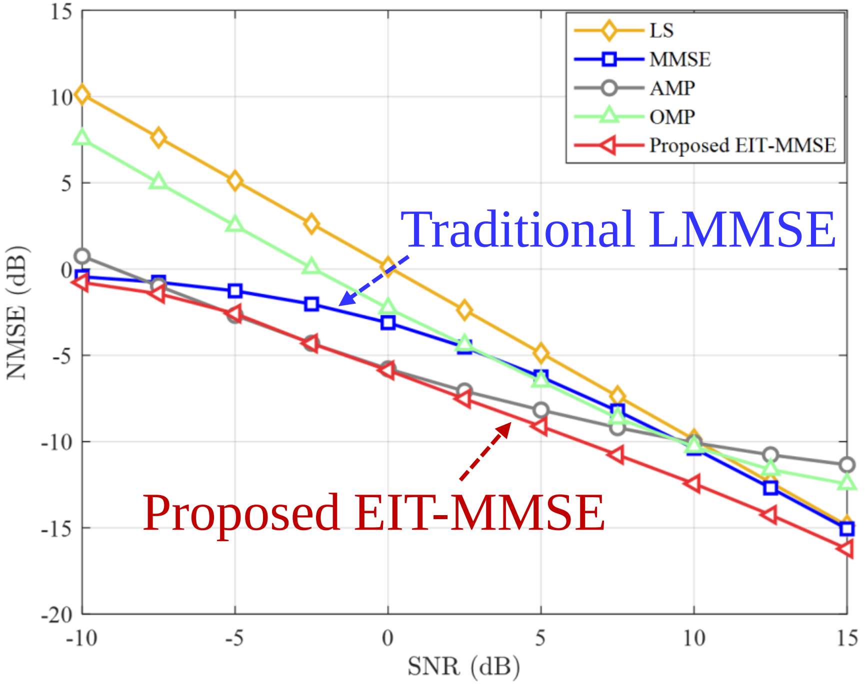

SCM channel model (7 paths)

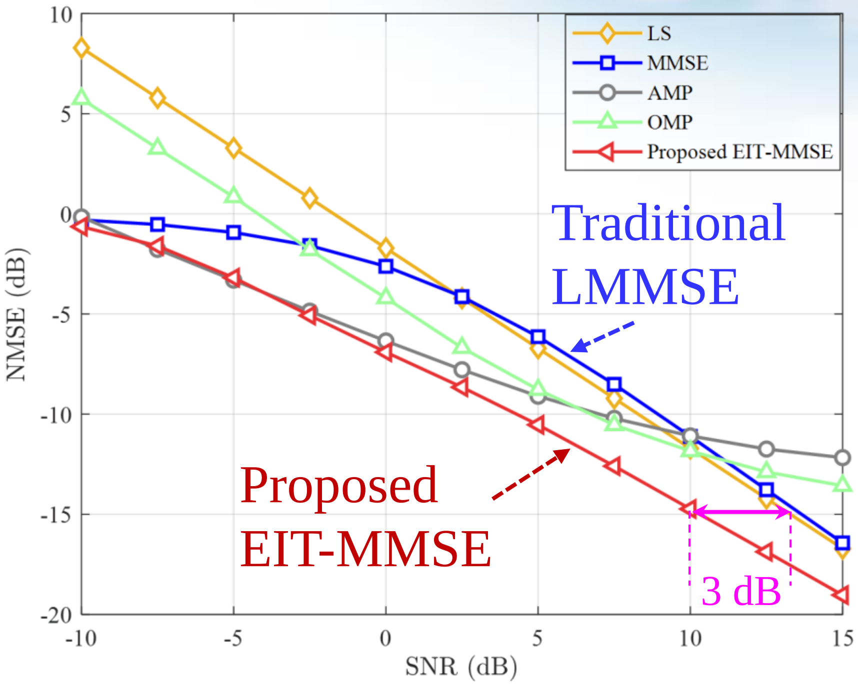

3GPP CDL-A channel model (21 paths)

Simulation Parameter	Value
BS Antenna	32
Array	Half-wavelength
Polarization	Y direction
Carrier	3.5 GHz
Rician factor	10 dB

EIT is able to improve the channel estimation accuracy

J. Zhu, Z. Wan, **L. Dai**, and T. J. Cui, "Electromagnetic information theory-based statistical channel model for improved channel estimation," submitted to *IEEE Trans. Inf. Theory*, major revision, Feb. 2024.

Contents

4.2 Channel Aging Problem

- **User mobility leads to channel aging**
  - **Channel estimation is performed periodically**
  - **Significant channel changes may occur within a single period, leading to outdated CSI in high mobility scenarios**

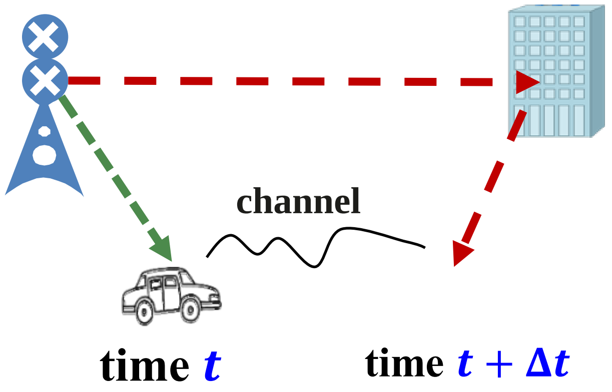

User mobility ➡ **Channel aging**

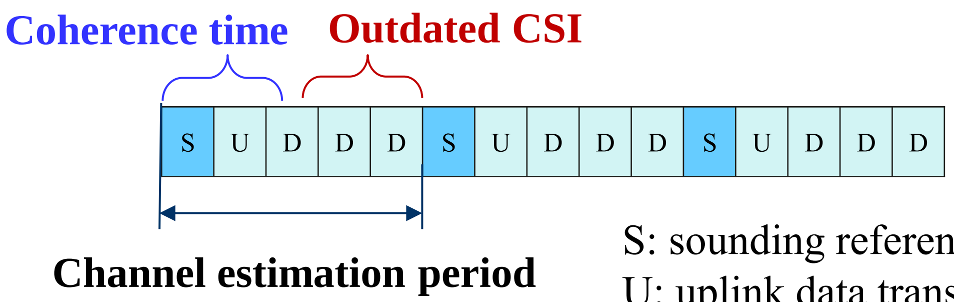

S: sounding reference signal (SRS)
U: uplink data transmission
D: downlink data transmission

Frame structure of communication system

Channel prediction technology is needed in mobile scenarios to alleviate channel aging

C. Wu, X. Yi, Y. Zhu, W. Wang, L. You, and X. Gao, "Channel prediction in high-mobility massive MIMO: From spatio-temporal autoregression to deep learning," *IEEE J. Sel. Areas Commun*., vol. 39, no. 7, pp. 1915–1930, Jul. 2021.

4.2 Discrete v.s. Continuous Channel Model

- **Existing channel predictors**
  - **Represent channel process as time-domain discrete model**
  - **Mismatch the continuous time-varying real EM channel**

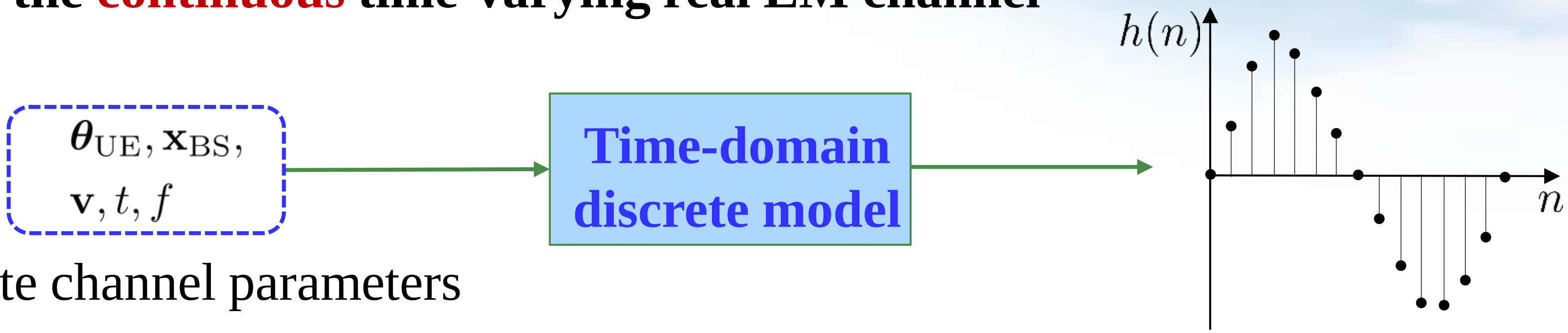

- **Problem: How to design a channel predictor that can accurately capture the continuous time-varying characteristics of EM channels in high-mobility scenarios?**

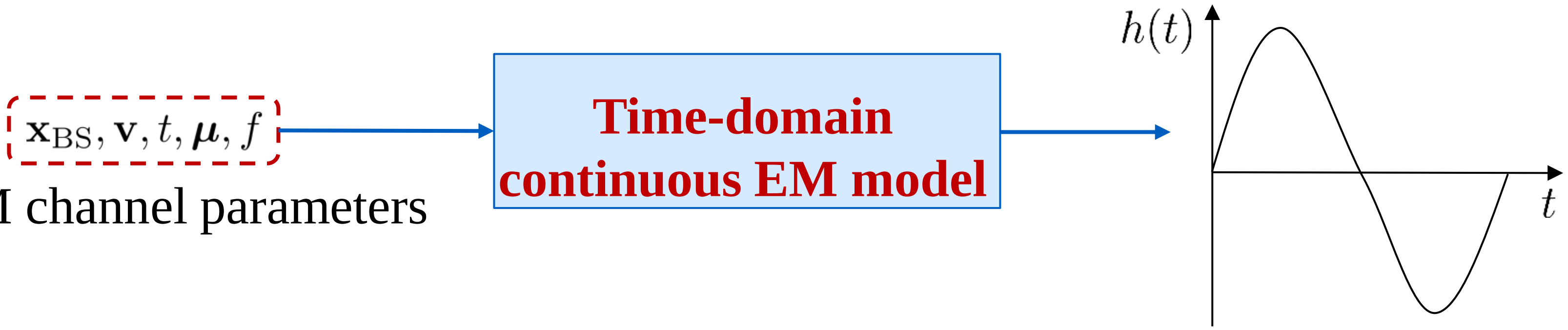

4.2 STEM-CF Based Channel Predictor

- **Spatial-temporal EM correlation function (STEM-CF)**
  - **Channel correlation is contained in the STEM-CF**
  - **Parameter $\boldsymbol{\mu}$ represents concentration, reflecting the direction of EM incidence**
  - **Parameter $\mathbf{v}$ represents user velocity, reflecting the time-varying characteristics of the channel**

$$\mathbf{K}_{\mathrm{STEM}}(\mathbf{x},\mathbf{x}',t,t'|\boldsymbol{\mu},\mathbf{v}) \propto \frac{1}{\int_{S^2}\nu(\hat{\boldsymbol{\kappa}})\mathrm{d}S}\int_{\hat{\boldsymbol{\kappa}}\in S^2}(\mathbf{I}-\hat{\boldsymbol{\kappa}}\hat{\boldsymbol{\kappa}}^{\mathsf{T}})e^{ik_0\hat{\boldsymbol{\kappa}}\cdot((\mathbf{x}-\mathbf{x}')+\mathbf{v}(t-t'))}\nu(\hat{\boldsymbol{\kappa}})\mathrm{d}S, \quad \nu(\hat{\boldsymbol{\kappa}}) = e^{\boldsymbol{\mu}\cdot\hat{\boldsymbol{\kappa}}}$$

- **Continuous channel predictor based on STEM-CF**
  - **According to the MMSE criterion, channel prediction can be achieved by utilizing the spatial-temporal correlation between past and future channels**

$$\mathbf{h}_{\mathcal{F}} = \mathbf{K}_{\mathcal{P}\mathcal{F}}^{\mathsf{H}}(\mathbf{K}_{\mathcal{P}} + \sigma^2\mathbf{I})^{-1}\mathbf{y}$$

STEM correlation between past and future channels

STEM correlation between past channels

STEM-CF utilizes EM spatial-temporal correlation to achieve channel prediction

J. Li, J. Zhu and **L. Dai**, "Accurate channel prediction based on spatial-temporal electromagnetic kernel learning," submitted to *IEEE Int. Conf. Commun. (IEEE ICC'25)*, Nov. 2024.

4.2 STEM-CF Parameter Learning

- **Using ML criterion, concentration $\boldsymbol{\mu}$ and velocity v that are most suitable for the current communication environment can be solved through alternating iterations**

Propagation environment fitting	**STEM parameter learning**

find best $\boldsymbol{\mu}, \mathbf{v}$

s.t. $\mathrm{K}_{\mathrm{STEM}}(\mathbf{x}, \mathbf{x}', t, t' | \boldsymbol{\mu}, \mathbf{v})$ fits $\mathbf{y}_{\mathrm{obs}}$

$$
\begin{aligned}
(\hat{\boldsymbol{\mu}}, \hat{\mathbf{v}}) &= \underset{(\boldsymbol{\mu},\mathbf{v})\in\Omega}{\arg\max}\, l(\boldsymbol{\mu}, \mathbf{v} | \mathbf{y}_{\mathrm{obs}}) \\
&= \underset{(\boldsymbol{\mu},\mathbf{v})\in\Omega}{\arg\max} \big(\underbrace{- \ln \det \mathbf{K}_{\mathbf{y}}(\boldsymbol{\mu}, \mathbf{v})}_{\text{Model Complexity}} \underbrace{- \mathbf{y}_{\mathrm{obs}}^{\mathsf{H}} \mathbf{K}_{\mathbf{y}}^{-1}(\boldsymbol{\mu}, \mathbf{v}) \mathbf{y}_{\mathrm{obs}}}_{\text{Data fitness}} \big)
\end{aligned}
$$

Thm 4.2.1 The derivatives of EMCF $\mathrm{K}_{\mathrm{STEM}}(\mathbf{x}, \mathbf{x}', t, t' | \boldsymbol{\mu}, \mathbf{v})$ w.r.t. $\boldsymbol{\mu}$ and $\mathbf{v}$ are

$$
\frac{\partial \mathbf{K}_{\mathrm{STEM}}}{\partial \boldsymbol{\mu}(k)} = -\frac{\sigma^2}{C(\mu)} \left[\frac{C'(\mu)\boldsymbol{\mu}(k)}{C(\mu)\mu} \boldsymbol{\Sigma}(\mathbf{w}) + \mathrm{i} \frac{\partial \boldsymbol{\Sigma}(\mathbf{w})}{\partial \mathbf{w}(k)} \right] \text{ and } \frac{\partial \mathbf{K}_{\mathrm{STEM}}}{\partial \mathbf{v}(k)} = \frac{\sigma^2 k_0 (t - t')}{C(\mu)} \frac{\partial \boldsymbol{\Sigma}(\mathbf{w})}{\partial \mathbf{w}(k)}, \quad k = 1, 2, 3,
$$

where $$\frac{\partial \boldsymbol{\Sigma}(\mathbf{w})}{\partial \mathbf{w}(k)} = \frac{1}{8} \left[\mathrm{i}(f_1 + f_3) \hat{\mathbf{w}}(k) \mathbf{I}_3 + \mathrm{i}(f_1 - 3f_3) \hat{\mathbf{w}}(k) \hat{\mathbf{w}} \hat{\mathbf{w}}^{\mathsf{T}} + (f_0 - 3f_2)(\partial_k \hat{\mathbf{w}} \cdot \hat{\mathbf{w}}^{\mathsf{T}} + \hat{\mathbf{w}} \cdot \partial_k \hat{\mathbf{w}}^{\mathsf{T}}) \right].$$

Apply gradient ascent to optimize STEM parameters to fit time-varying channels

J. Li, J. Zhu and **L. Dai**, "Accurate channel prediction based on spatial-temporal electromagnetic kernel learning," submitted to *IEEE Int. Conf. Commun. (IEEE ICC'25)*, Nov. 2024.

4.2 Simulation Results

- Based on STEM kernel learning, the EIT channel predictor is obtained
- The proposed channel predictors outperforms other schemes

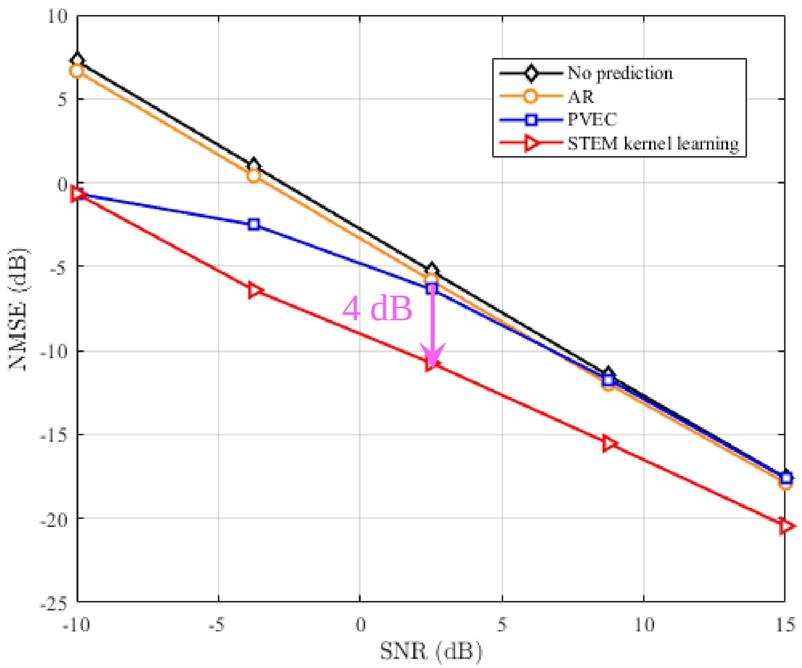

NMSE versus SNR

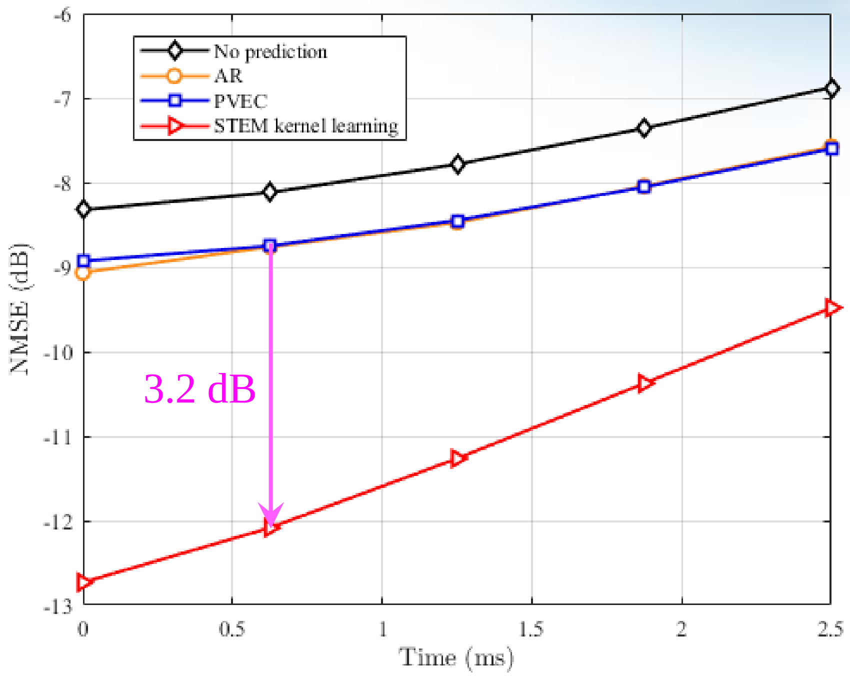

NMSE versus time

Simulation parameters	Value
Number of BS antennas	256
Array form	Half wave length ULA
Antenna polarization	Y-axis direction
User speed	72 km/h

EIT can improve channel prediction accuracy

J. Li, J. Zhu and **L. Dai**, "Accurate channel prediction based on spatial-temporal electromagnetic kernel learning," submitted to *IEEE Int. Conf. Commun. (IEEE ICC'25)*, Nov. 2024.

Contents

4.3 Information Metamaterials

- **Reconfigurable intelligent surface (RIS)**
- **Method 1: Use RIS to replace the RF components of transceivers**
- **Method 2: Use RIS to reconfigure the EM environments**

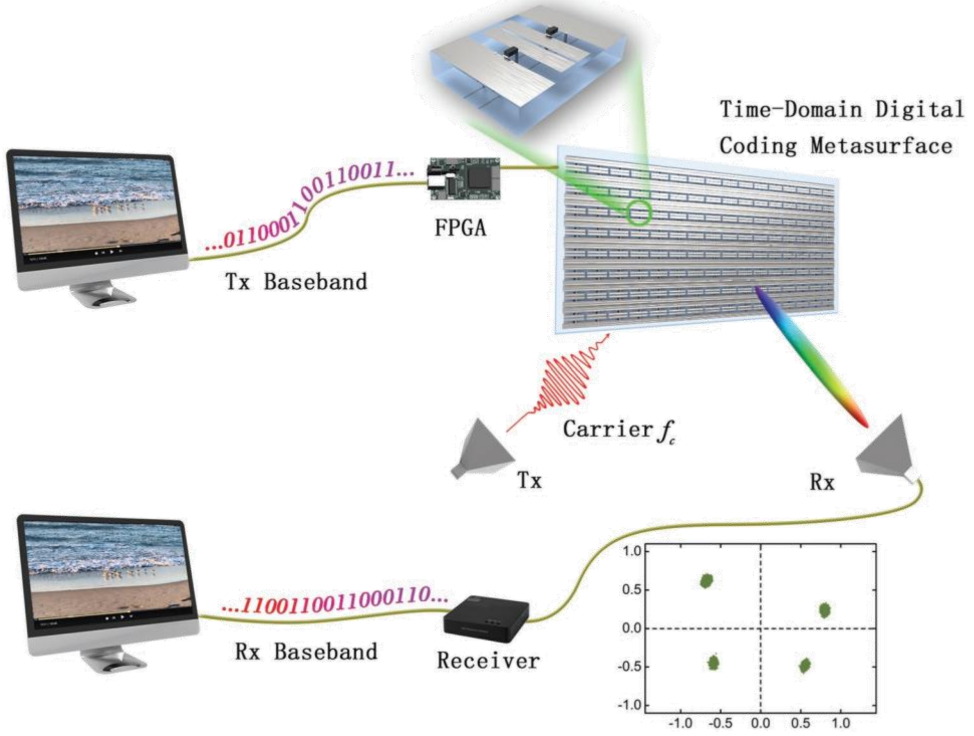

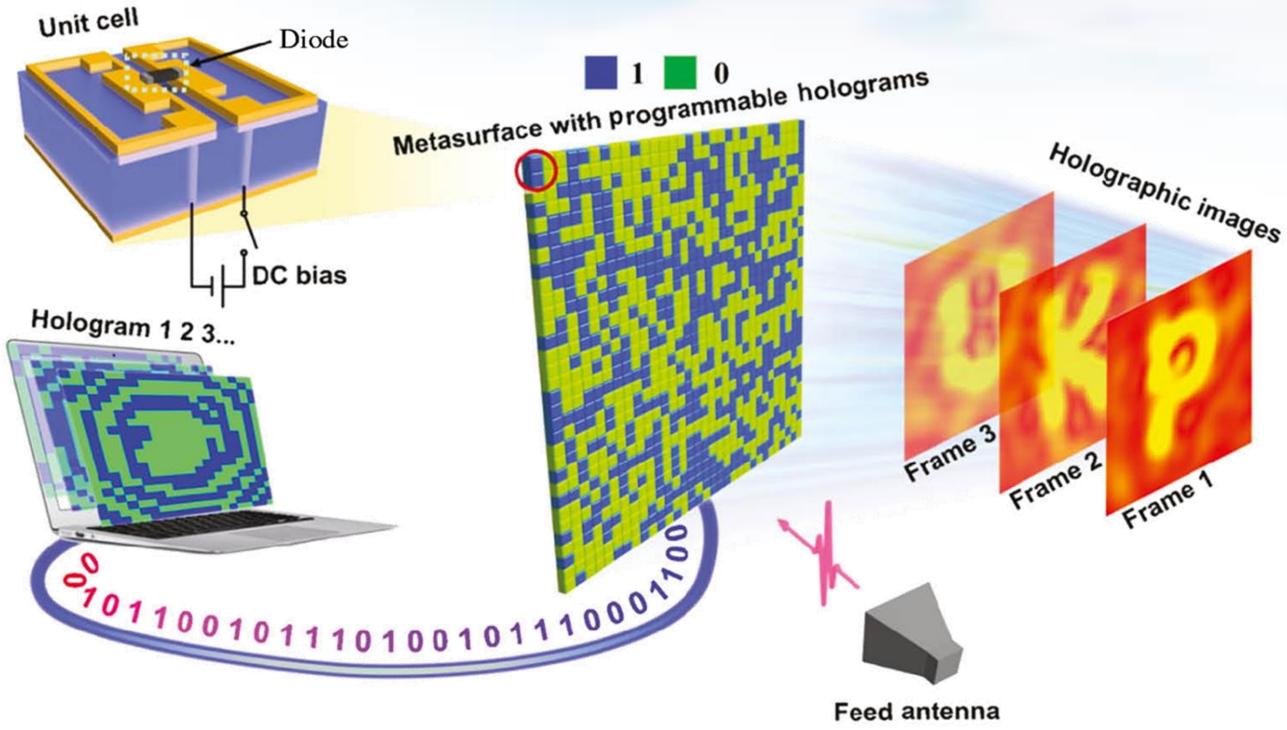

[1] T. -J. Cui, and S. Liu, "An information science view of metamaterials," *Optics and Photonics News*, vol. 27, no. 12, pp. 59-59, 2016.
[2] L. Li and T. -J. Cui, "Information metamaterials–from effective media to real-time information processing systems," *Nanophotonics*, vol. 8, no. 5, pp. 703-724, 2019.

4.3 Hardware Implementations of RISs

- **Metamaterial**: Artificial material with a **structure** that exhibits unnatural properties
- **Metasurface**: Two-dimensional (2D) structure composed of individual elements to manipulate signals
- **Four typical realizations: Electric/magnetic/thermal/light-sensitive**

Capasso, 2011

Cui, 2014

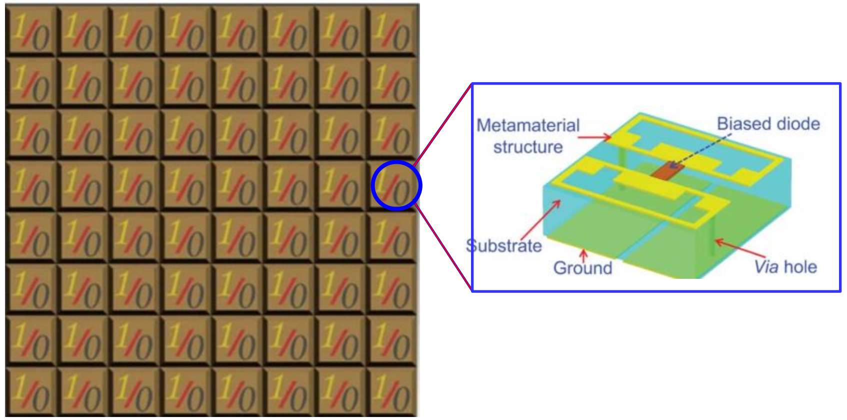

Yang, 2016

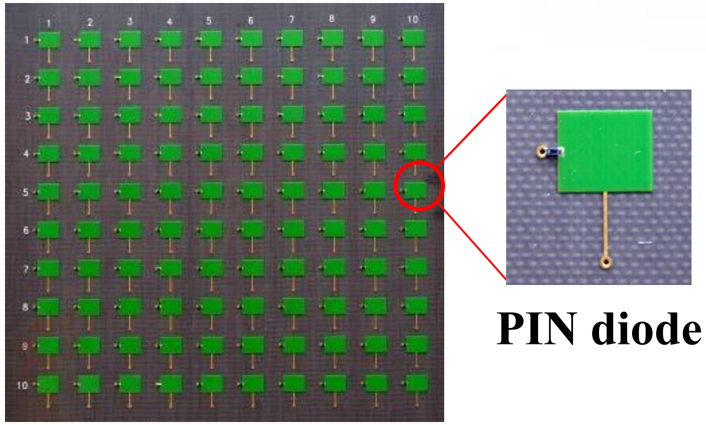

PIN diode

[1] N. F. Yu, P. Genevet, M. A. Kats, F. Aieta, J.-P. Tetienne, F. Capasso, and Z. Gaburro, "Light propagation with phase discontinuities: Generalized laws of reflection and refraction," *Science*, vol. 334, pp. 333–337, Oct. 2011.
[2] T. Cui, M. Qi, X. Wan, J. Zhao, and Q. Cheng, "Coding metamaterials, digital metamaterials and programmable metamaterials," *Light: Science & Applications*, vol. 3, p. 218, Oct. 2014.
[3] H. Yang, X. Cao, F. Yang, J. Gao, S. Xu, M. Li, X. Chen, Y. Zhao, Y. Zheng, and S. Li, "A programmable metasurface with dynamic polarization, scattering and focusing control," *Scientific Reports*, vol. 6, p. 35692 EP, Oct. 2016.

4.3 RIS-Aided Wireless Communications

- Overcome the blockage
- Provide communication links
- Enhance the signal quality
- Increase spectrum efficiency
- Save the power consumption
- Increase the energy efficiency

……

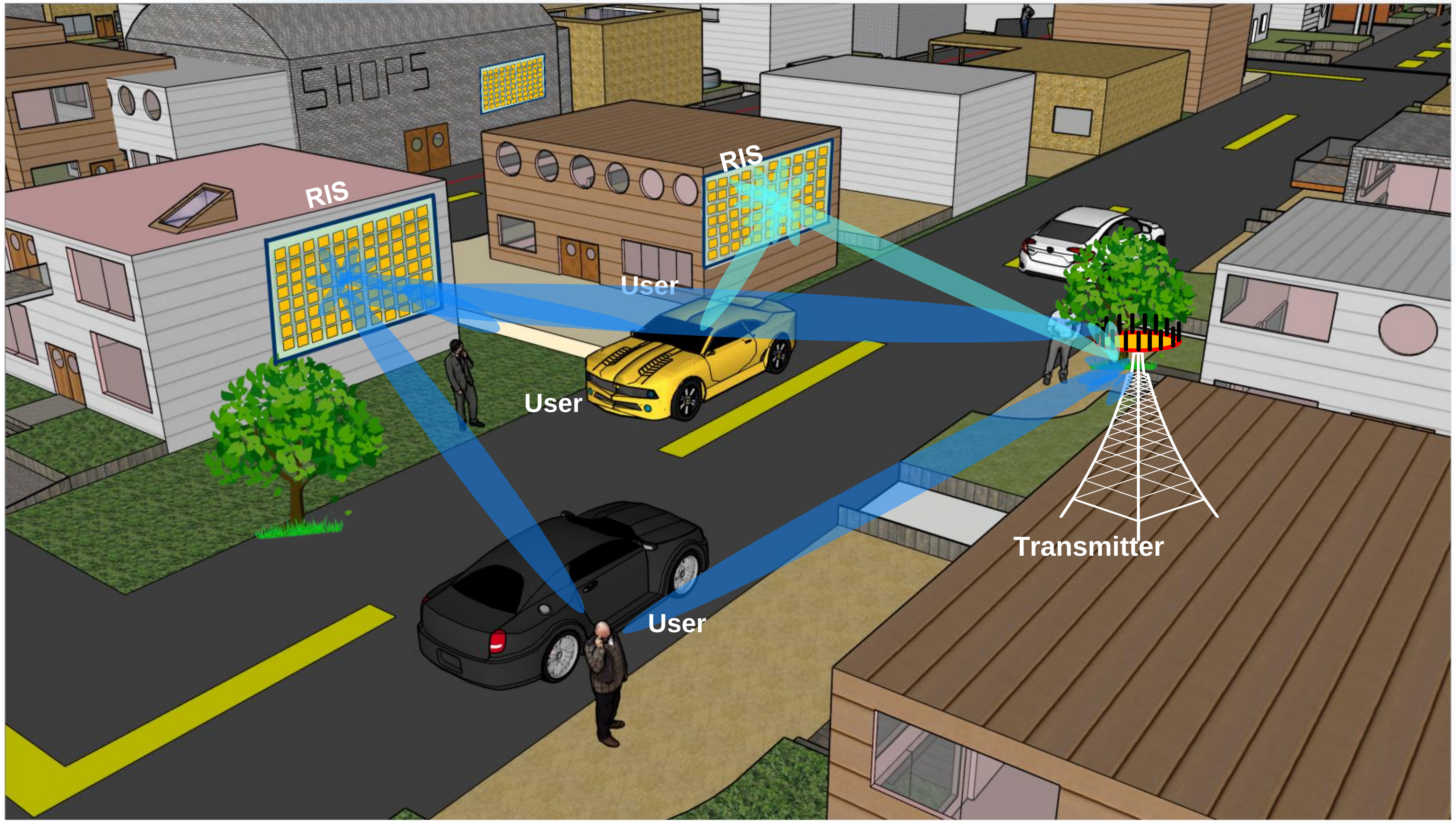

Z. Zhang and **L. Dai**, "Reconfigurable intelligent surfaces for 6G: Nine fundamental issues and one critical problem," *Tsinghua Sci. Technol.*, vol. 28, no. 5, pp. 929-939, Oct. 2023.

4.3 Challenge: Complex Control Process

- **RIS is usually controlled by the base station**
  - **Complex control process: Channel estimation → Precoding → Control signal for RIS**
  - **Wired control: High cost on laying out cables**
  - **Wireless control: Extra receiver on RIS**

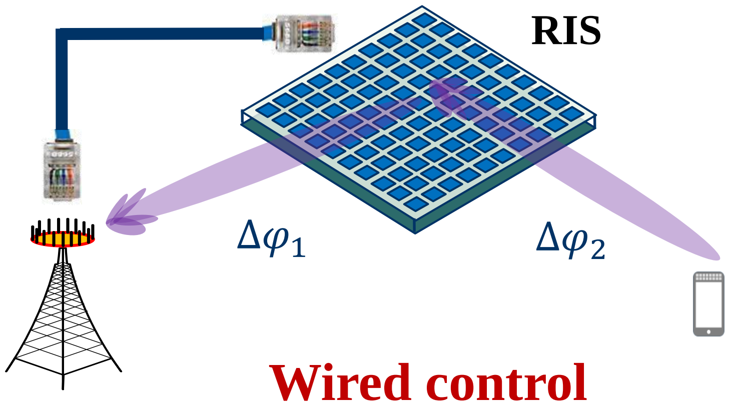

Wired control

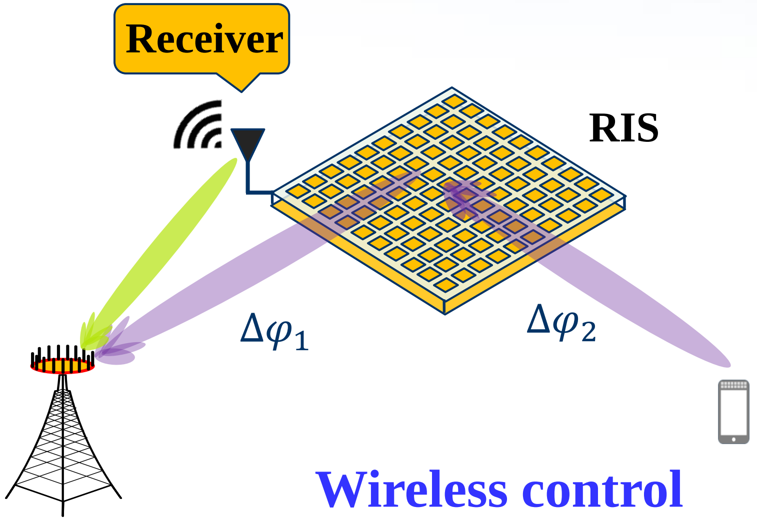

Wireless control

RIS controlled by the BS is difficult to be massively deployed

4.3 The Idea of Holography

- **Holographic imaging**
  - **The physical principle of holographic imaging is optical interference**
  - **Restoring 3D information of objects through algorithms**

Dennis Gabor
Nobel Prize in Physics (1971)

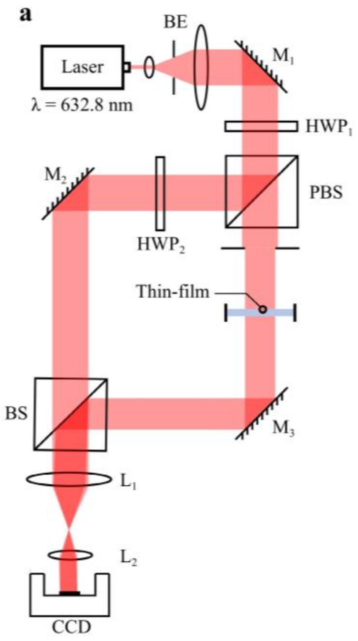

Basic principle of holography

4.3 EIT-Inspired Self-Controlled RIS

Optical Inference: Fringes created when lights meet

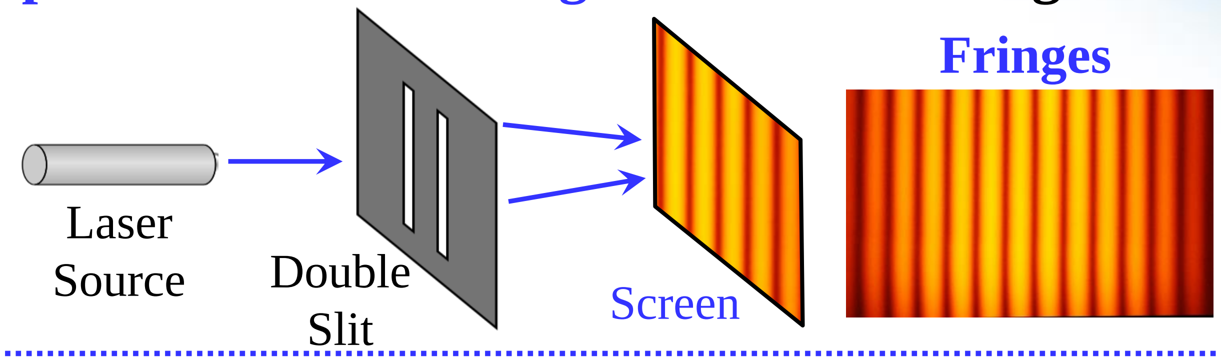

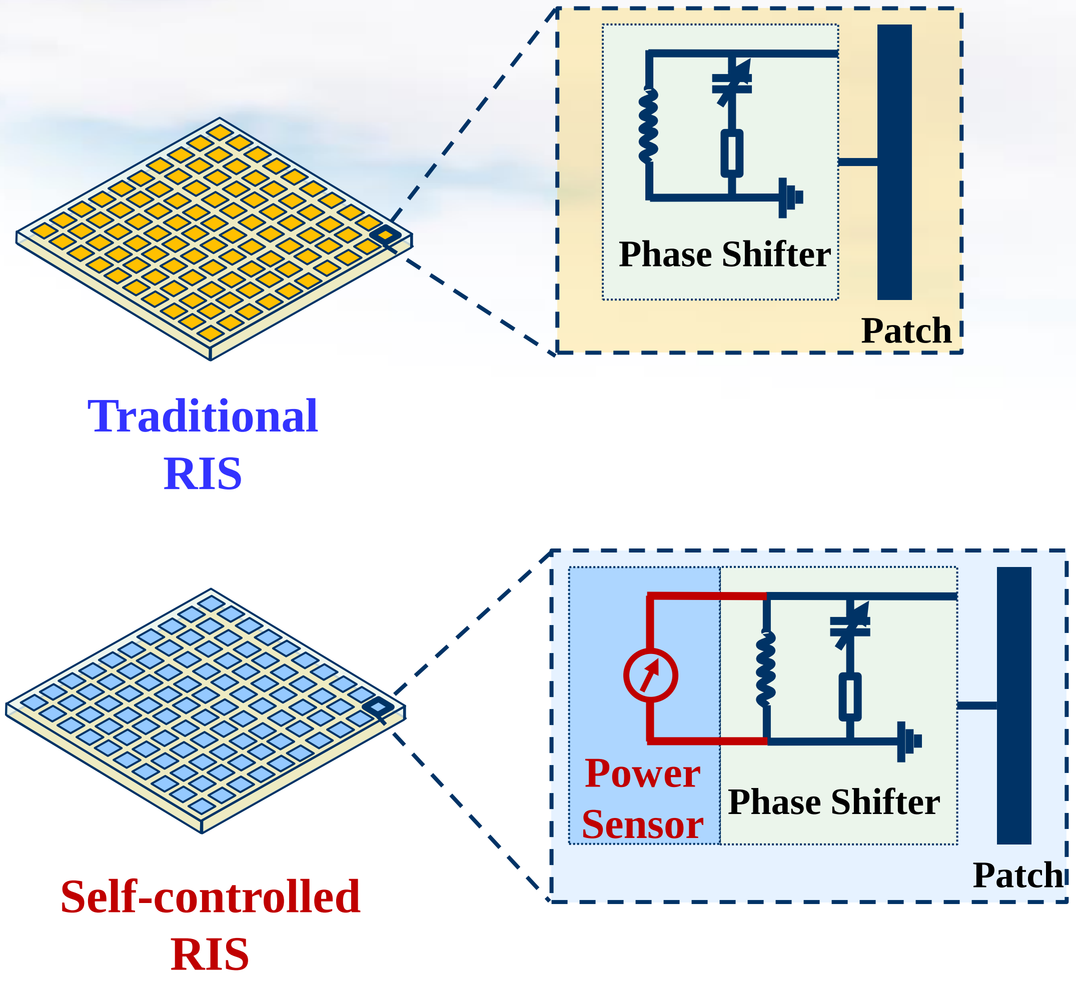

EM Interference: Intensity pattern created when EM waves meet

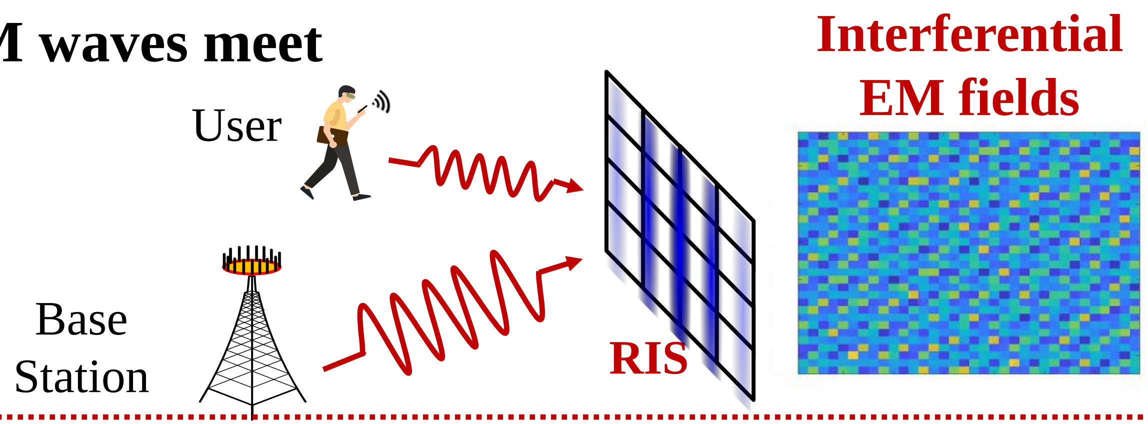

J. Zhu, K. Liu, Z. Wan, **L. Dai**, T. J. Cui, and H. V. Poor, "Sensing RISs: Enabling dimension-independent CSI acquisition for beamforming," *IEEE Trans. Inf. Theory*, vol. 69, no. 6, pp. 3795-3813, Jun. 2023.

4.3 Self-Controlled RIS: Phase Estimation Algorithms

- **Signal: Cosine signal $P(t)$ with initial phase φ**
- **Algorithm: FFT + iterative expectation-maximization (EM)**

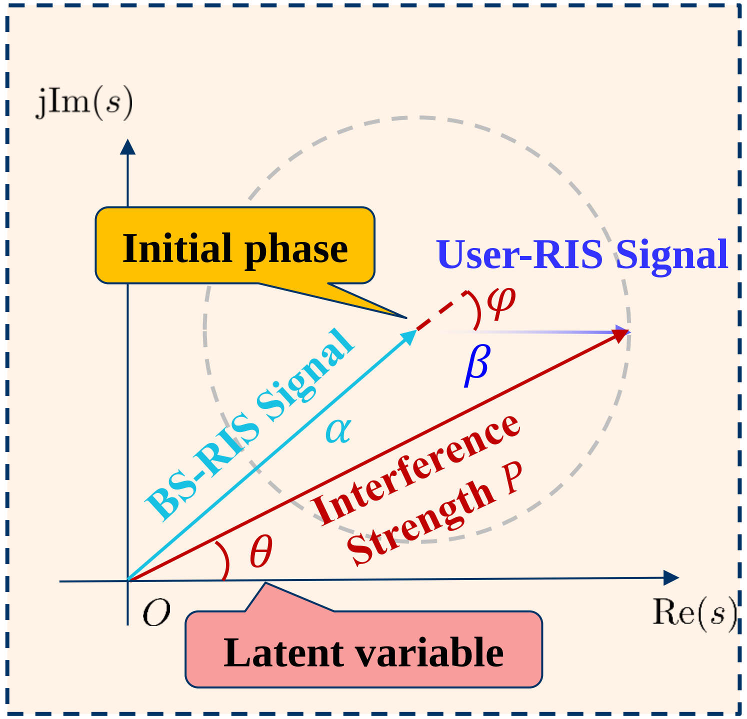

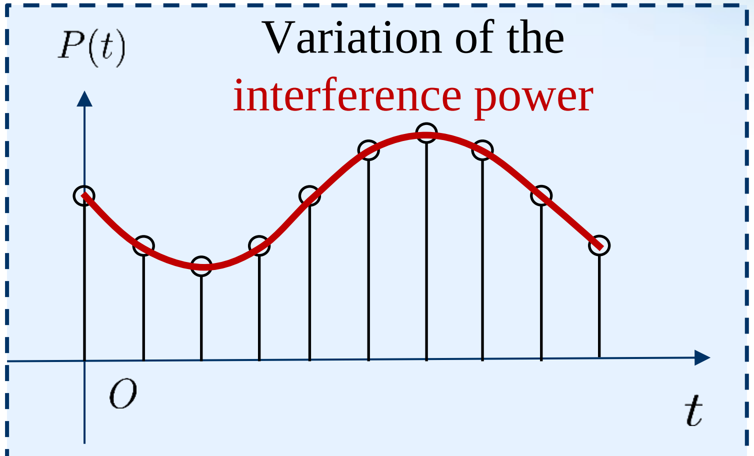

$$P = \alpha^2 + \beta^2 + 2\alpha\beta\cos(\varphi)$$

$$P(t) = \alpha^2 + \beta^2 + 2\alpha\beta\cos(\varphi + \omega t)$$

Algorithm 2 von Mises-EM phase estimation (VM-EM algorithm)

Input: Incident wave intensity α, β; sensor data $P[l]$; amplification factor σ_v^2; predefined phase shifts $\psi_l = \omega t_l$.

Output: $\hat{\varphi}$

$s_l \leftarrow \sqrt{P[l]/A}, \quad \forall l \in \{L\}$

$\hat{\varphi} \leftarrow \arg\{\mathrm{FFT}(P)[1]\}$ — **Obtain initial phase φ via FFT**

$\kappa \leftarrow 1$

while $\hat{\varphi}$ not convergence **do**

$\mu_l \leftarrow \alpha + \beta e^{\mathrm{j}(\hat{\varphi}+\psi_l)}, \quad \forall l \in \{L\}$

$w_l \leftarrow s_l e^{\mathrm{j}\arg(\mu_l)} - \alpha, \quad \forall l \in \{L\}$

$z_\varphi \leftarrow \kappa e^{\mathrm{j}\hat{\varphi}} + \beta \left(\sum_{l=0}^{L-1} w_l e^{-\mathrm{j}\psi_l}\right) / (\sigma_v^2/2)$

$\hat{\varphi} \leftarrow \arg(z_\varphi)$

$\kappa \leftarrow |z_\varphi|$

end while

return $\hat{\varphi}$

Iterative update by EM algorithm

Phase estimation algorithm: Extract channel phase information from dynamic interference signals

J. Zhu, K. Liu, Z. Wan, **L. Dai**, T. J. Cui, and H. V. Poor, "Sensing RISs: Enabling dimension-independent CSI acquisition for beamforming," *IEEE Trans. Inf. Theory*, vol. 69, no. 6, pp. 3795-3813, Jun. 2023.

4.3 Simulation Results

- MSE of phase estimation approach CRLB
- The average capacity approaches traditional RIS system with known CSI

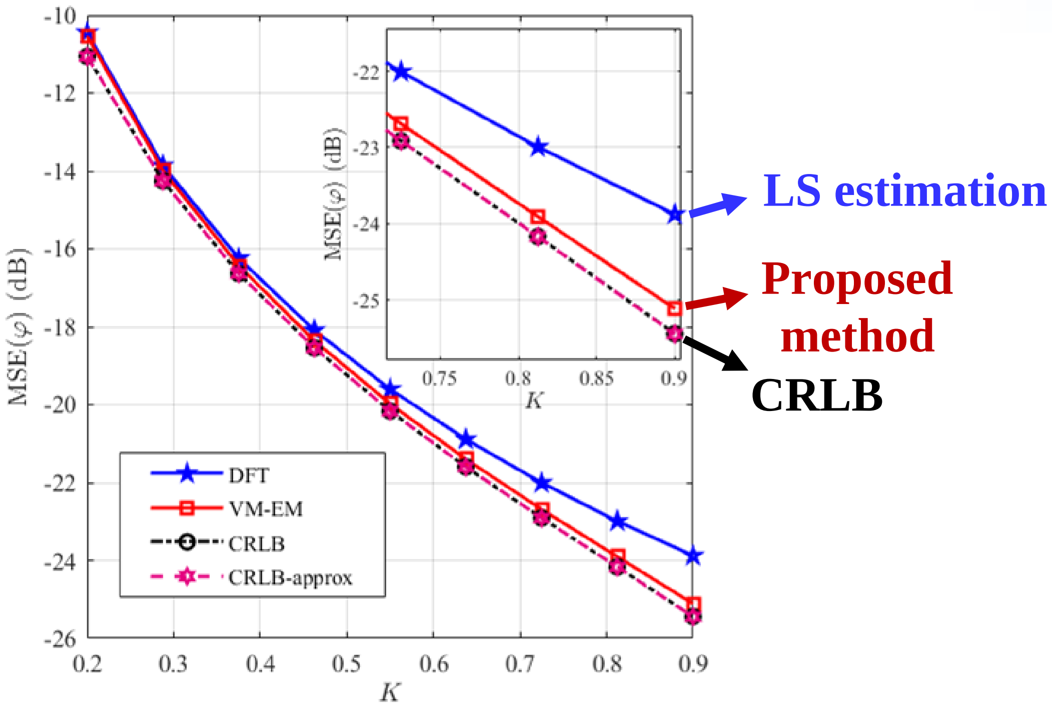

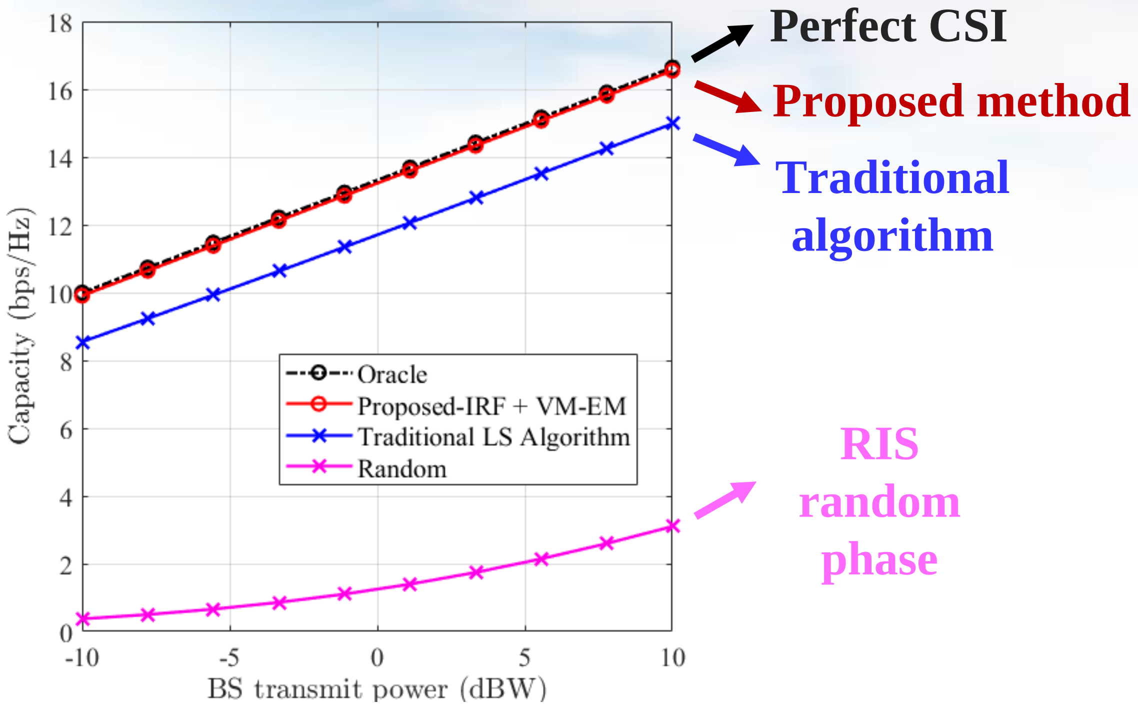

Self-controlled RIS can automatically sense the channel and perform beamforming

J. Zhu, K. Liu, Z. Wan, **L. Dai**, T. J. Cui, and H. V. Poor, "Sensing RISs: Enabling dimension-independent CSI acquisition for beamforming," *IEEE Trans. Inf. Theory*, vol. 69, no. 6, pp. 3795-3813, Jun. 2023.

4.3 Hardware Design and Test

- **Design 32×32 self-controlled RIS and observe the effect of electromagnetic interference**
- **Estimate the location of user with proposed algorithm**

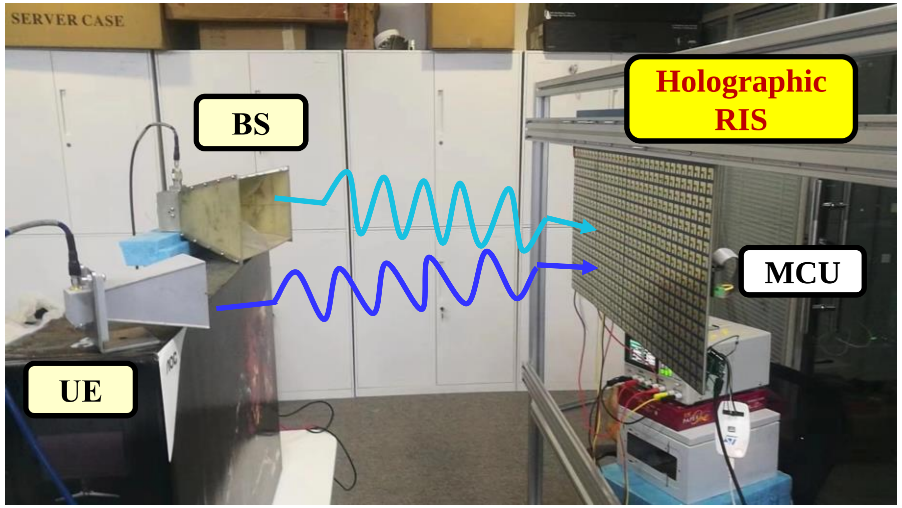

Self-controlled RIS hardware system

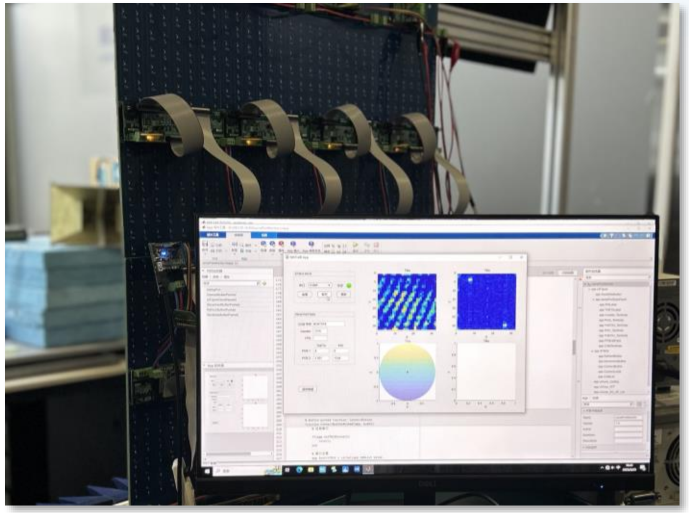

Visual electromagnetic interference

Autonomous closed-loop tracking of mobile users

Verified the software and hardware joint design for self-controlled RIS

Contents

Conclusions

- **Introduction to EIT**
  - EIT for 6G advanced MIMO architectures
  - EIT: Combining Shannon and Maxwell theory
  - EIT v.s. MIMO theory
  - EIT: History and recent achievements
- **Fundamentals of EIT**
  - EIT channel models with near-field correlation
  - EIT DoF/capacity bounds by EM dual-bandlimited property
  - EIT mutual information by F-determinants
- **EIT-Enabled Technologies**
  - Holographic MIMO fully exploits EM DoF
  - Near-field LDMA for EM multiple access
  - Mutual coupling leads to superdirectivity
  - Orbital angular momentum brings infinite DoFs
  - 3D Antenna Arrays explore the third spatial dimension
- **EIT-Inspired Technologies**
  - EIT statistical information improves channel estimation
  - EIT statistical information improves channel prediction
  - EM interference enables self-controlled RIS

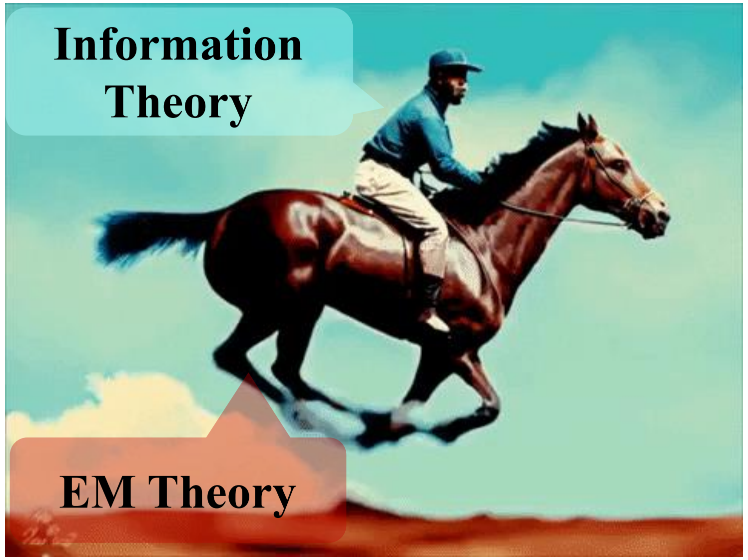

EIT for Future Wireless

- **The Iceberg Effect**
  - **Above the water: Mathematical description of classical communication theory**
  - **Below the water: Physical EM mechanism inspiring new paradigm shift in communication theory and technologies**

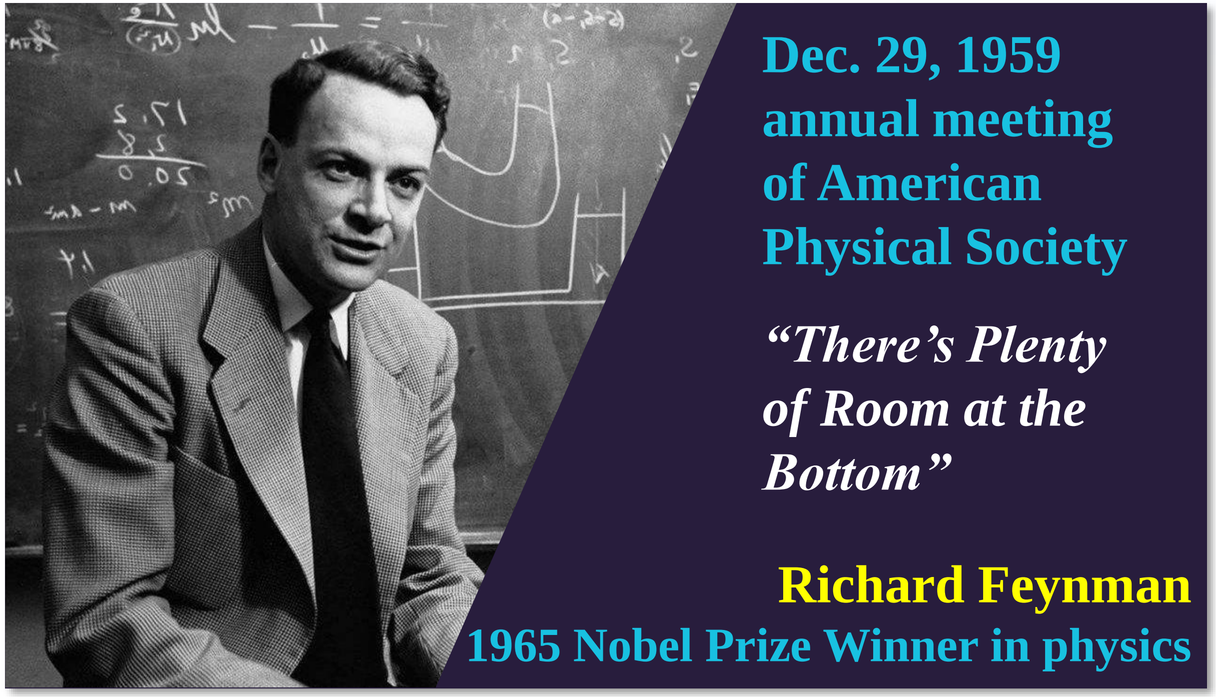

- Application Layer
- Representation Layer
- Session Layer
- Transmission Layer
- Network Layer
- MAC Layer
- **EM Physical Layer [1]**

[1] J. Zhu, Z. Wan, **L. Dai**, M. Debbah, and H. V. Poor, "Electromagnetic information theory: Fundamentals, modeling, applications, and open problems," *IEEE Wireless Commun.*, vol. 31, no. 3, pp. 156-162, Jun. 2023.

IEEE ComSoc ETI on ESIT

Approved by IEEE ComSoc in Nov. 2024

IEEE Communications Society
Emerging Technology Initiative (ETI) on
Electromagnetic Signal and Information Theory

- The aim is to bring together both the industry and academic peers likewise the amalgamation of electromagnetic wave principles with information theory and signal processing tools.
- It provides platform to the researchers seeking to explore key enabling solutions and system designs in realizing ESIT, enhance the performance in terms of energy and spectral efficiencies using the principles of ESIT, near-field communications and reconfigurable antennas, etc.
- It provides insights with "**ComSoc Best Readings on ESIT**" as part of the initiative into latest research trends, challenges and future prospects which align with the latest industry activities, standardization efforts and research on the important topic of ESIT for 6G and beyond.
- We are also establishing a list of **active contributors** so do join us by contacting the Chairs

Website: https://sites.google.com/view/ieee-comsoc-eti-on-esit/home
Linkedin: https://www.linkedin.com/company/ieee-comsoc-eti-on-esit

Chairs:

Aryan Kaushik
Manchester Met
UK

Marco Di Renzo
Paris-Saclay University
France

Linglong Dai
Tsinghua University
China

Industry Co-Chairs:

Wen Tong
Huawei Technologies
Canada

Miguel Dajer
Futurewei Technologies
USA

Doohwan Lee
NTT Corporation
Japan

Call for Papers: IEEE JSAIT Special Issue on EIT

- ***IEEE Journal on Selected Areas in Information Theory* *Special Issue* on Electromagnetic Information Theory (EIT)**
- **Guest Editors**

Prof. Massimo Franceschetti
University of California San Diego
USA

Prof. Linglong Dai
Tsinghua University
China

Prof. Marco D. Migliore
University of Cassino
Italy

Prof. Thomas Marzetta
New York University
USA

- **Important Dates**
  - **Manuscript Submission Deadline: 15 August, 2024**
  - **Expected Publication Date: April, 2025**

https://www.itsoc.org/jsait/calls-for-papers

IEEE JOURNAL ON
SELECTED AREAS IN INFORMATION THEORY

Call for Papers: IEEE ICC 2025 Workshop on ESIT

- *IEEE ICC 2025 7th International Workshop on* **Electromagnetic Signal and Information Theory**
- **General Chairs**

Dr. Tengjiao Wang
Huawei Technologies
China

Prof. Aryan Kaushik
Manchester Met
UK

Prof. Linglong Dai
Tsinghua University
China

Dr. Doohwan Lee
NTT Network Innovation Laboratories
Japan

- **Important Dates**
  - **Workshop Paper Submission: 20 January 2025**
  - **Paper Acceptance Notification: 10 March 2025**
  - **Camera Ready: 31 March 2025**

https://icc2025.ieee-icc.org/call-workshop-papers

Electromagnetic Science
CALL FOR PAPERS

- **Electromagnetic Science Special Issue on Electromagnetic Information Theory (EIT)**

- **Guest Editors**

Prof. Er-Ping Li
Zhejiang University

Assoc. Prof. Wei E.I. Sha
Zhejiang University

Assoc. Prof. Chau Yuen
Nanyang Technological University

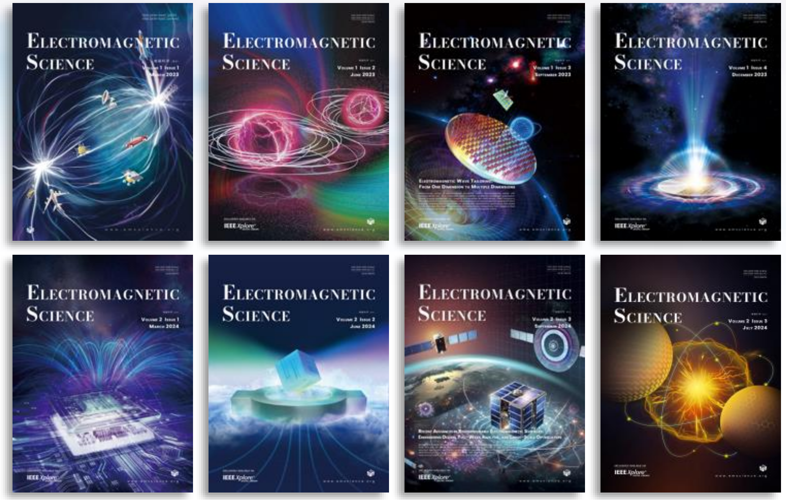

www.emscience.org

- **Important Dates**
  - Submission of papers: **15 May, 2025**
  - Review of papers and revisions: **31 July, 2025**
  - Expected Publication Date: **30 September, 2025**

Electromagnetic Science

EXCLUSIVELY AVAILABLE VIA IEEE Xplore® DIGITAL LIBRARY

https://mc03.manuscriptcentral.com/emscience

Call for Contributions: White Paper on NFC

- The **world's first white paper** on near-field technologies was published at **2024 Global 6G Conference** (contributed by **200+** people, **40+** global entities of **12** countries)

Released at the Global 6G Conference, 2024

The first white paper

Consultants

Tiejun Cui (tjcui@seu.edu.cn), Southeast University

Ping Zhang (pzhang@bupt.edu.cn), Beijing University of Posts and Telecommunications

Xiaohu You (xhyu@seu.edu.cn), Southeast University

Yonina Eldar (yonina.eldar@weizmann.ac.il), Weizmann Institute of Science

Editors in Chief

Yajun Zhao (zhao.yajun1@zte.com.cn), ZTE Corporation

Linglong Dai (daill@tsinghua.edu.cn), Tsinghua University

Jianhua Zhang (jhzhang@bupt.edu.cn), Beijing University of Posts and Telecommunications

QR code for download

Y. Zhao, L. Dai, J. Zhang, *et al*. "6G near-field technologies white paper," FuTURE Forum, Nanjing, China, Apr. 2024.

Thanks for your attention!

Linglong Dai (IEEE Fellow)
Tsinghua University,
Beijing, China
daill@tsinghua.edu.cn

Merouane Debbah (IEEE Fellow)
Khalifa University of Science and Technology,
Abu Dhabi, United Arab Emirates
merouane.debbah@ku.ac.ae

Slides download: https://oa.ee.tsinghua.edu.cn/dailinglong/resources/resources.html